Application of HVDC transmission within Nigerian transmission system: technical and economic evaluation

By
Omowumi Grace Olasunkanmi

Submitted to Swansea University in fulfilment of the requirement for the Degree of Doctor of Philosophy

Department of Electronic and Electrical Engineering
Swansea University

(December 2023)

Abstract

High Voltage Direct Current (HVDC) technology has recently emerged as a significant option in current power networks to address power transmission challenges. Therefore, this research project examines the potential impact of HVDC technology on the Nigerian transmission system. Based on the information provided by the Nigerian Electricity System Operator (NESO), a model of the 330 kV transmission network in Nigeria was created using DIgSILENT PowerFactory. Summer and winter load flow scenarios were examined to enhance the model's precision and consistency. The system performance was evaluated through stability and reliability studies, which helped identify suitable locations for HVDC links. The load point indices (LPIs) and system indices were used for the reliability evaluation, while the PV and QV analyses were used for the stability evaluation. An HVDC model was created and connected to the transmission network at two locations identified by the studies, Gombe and Yola buses. A comparison was conducted using two separate HVDC connections (Case 1: Azura-Gombe and Case 2: Azura-Yola) to identify the critical impact of HVDC on the system reliability and stability. The reliability and stability simulation showed that HVDC technology significantly boosts the reliability and stability of the transmission network and reduces energy losses. However, adding an HVDC link between Azura and Yola, Case 2, significantly improved overall performance, as evidenced by improving the system and load point indices and a better voltage profile and reactive power margin. The system indices, SAIDI improved by 0.07 h/yr, SAIFI by 0.19 interruption/yr, and ASAI enhanced by 0.11%, while the LPIs improved effectively by zeroing the Load Point Interruption Frequency (LPIF) and Load Point Interruption Time (LPIT). During the stability analysis, the loadability increased by 119% while the critical point improved by 0.061 pu/ -394 MVAR. Economically, the cost incurred in Case 1 is 79.17% lower than the base case even though new equipment (HVDC) is installed; this also applies to Case 2, which is 85% lower than the base case. Integrating HVDC technology could improve financial gain, considering improved energy supply, increased production, and general economic growth. This research has contributed significantly to revealed improvements in system and load indices, increased loadability, increased stability, and boosted financial gain with the HVDC connected.

Declarations

This work has not previously been accepted in substance for any degree and is not being concurrently submitted as a candidature for any degree.

Signed: [redacted]
Date: 06/12/2023

This thesis is the result of my investigations, except where otherwise stated. Other sources are acknowledged by footnotes giving explicit references. A bibliography is appended.

Signed: [redacted]
Date: 06/12/2023

I hereby give consent for my thesis, if accepted, to be available for electronic sharing.

Signed: [redacted]
Date: 06/12/2023

The University's ethical procedures have been followed, and ethical approval has been granted where appropriate.

Signed: [redacted]
Date: 06/12/2023

Table of Contents

List of Figures

List of Tables

Acronyms

ACIT	Average Customer Interruption Time
AIT	Average Interruption Time
ASAI	Average Service Availability Index
CAIDI	Customer Average Interruption Duration Index
CfL	Cost for Losses
CREG	Commission for Electricity and Gas Regulation
CSc	Substation cost
DCF	Discounted cash flow
DG	Distributed Generation
EIC	Expected interruption cost
ENS	Energy Not Supplied
ET	Energy tariff
FD	Fault Duration
FF	Failure Frequency
HVAC	High voltage alternate current
HVDC	High voltage direct current
IC	Investment cost
IGBT	Insulated gate bipolar transistor
IPP	Independent Power Providers
IRR	Internal Rate of Return
LPI	Load point interruption
LPIF	Load point interruption frequency
LPIT	Load point interruption time
MTTR	Mean Time to Repair
NESO	Nigerian Electricity system operator
NDHC	Niger Delta Holding Company
NO	Number of outages
N_{occ}	Number of connected customers
OTSc	Overhead transmission system

NPV	Net Present Value
PHCN	Power Holding Company of Nigeria
DAC	Discounted annual cost
DSPF	DigSILENT PowerFactory
PV	Power-Voltage
QV	Reactive-Voltage
RD	Repair Duration
RPC	Reactive Power Compensation
RPM	Reactive power margin
SAIFI	System Average Interruption Frequency Index
SAIDI	System Average Interruption Duration Index
SARI	System Average Restoration Duration Index
SISI	System Average Interruption Severity Index
SV	Salvage Value
SVC	Static Var Compensator
TFD	Total Fault Duration
TCN	Transmission Company of Nigeria
TIC	Total investment cost
TEIC	Total expected interruption cost
TLPENS	Total load point energy not supplied
TNO	Total Number of Outages
UNMIK	United Nations Interim Administration Mission in Kosovo
UHV	Ultra High Voltage
VSC	Voltage Source Converter

Acknowledgements

I want to thank my supervisor, Professor Andrew R. Barron, for his invaluable guidance and support throughout my PhD journey. I appreciate Dr. Alvin Orbaek White's support and editing of my manuscript during my second year. I want to express my sincere gratitude to Dr. Shirin Alexander, my supervisor during the last year of my PhD, for her insightful suggestions.

I am deeply grateful to Dr. Grazia Todeschini, who was my supervisor in the first year of my PhD and at any time did not leave me on the PhD journey alone. Her wealth of technical knowledge, unwavering support, invaluable guidance, and endless patience are appreciated. She has been a great mentor and a source of inspiration for me to grow personally and professionally.

I would also like to thank the faculty and staff from the Electronic and Electrical Engineering Department, whose knowledge and resources helped complete the research. The university's academic atmosphere has supported my intellectual and personal growth.

Many thanks to the Federal Government of Nigeria and the Management of Olabisi Onabanjo University for the opportunity availed me to undergo my research program at Swansea University, UK.

I thank especially Olasunakanmi and Lara Onanuga, Seye and Dipo Olomo, Lekan and Yetunde Apena, Theophilus, Ifedayo, and Festus for all the support they have given to me throughout my period of studying in the UK. I thank all my friends and siblings (Jide, Odun, Tayo, Yemi, Bola, Niyi, and Tola) for your pleasant and encouraging words during the research. I am very thankful to Lawrence Akintokun and Dapo Afolabi and their family in the USA and the Koleola's in Canada for their encouragement during the most challenging moments.

My thanks also go to my parents, Mr. and Mrs. Olusegun Olomo, who supported me morally and spiritually, and my in-laws for their encouragement. To my children, Oluwaseyi Mary, Oluwamolade Joseph, and Olajuwon Michael, their belief in my abilities has been a constant source of motivation, a big thank you for your sacrifices without complaint and for keeping the flags flying during the period of my research. I want to thank my husband, Olasunkanmi; he has always been a blessing and a strong pillar of support.

I sincerely thank everyone listed above, whose name I may have accidentally forgotten, for their encouragement and support. You have been a massive help to me academically, and I sincerely appreciate your presence.

1 Introduction

1.1 Overview of Nigeria's power system

The Federal Republic of Nigeria is situated in the sub-region of West Africa, between latitudes 40°16' and 130°53' North and longitudes 20°40' and 140°41' East. It is surrounded by Benin Republic (Cotonou) to the West, Cameroon to the East, Chad to the Northeast, and Niger to the North. It is the fourteenth largest nation in Africa, having a total land area of around 923,768 square kilometres [1], [2]. The country's population is about 220 million in 2023 [3].

The rainy (summer) season (April to October) and the dry (winter) season (November to March) are the two primary climatic seasons in Nigeria [4]. Maximum average temperatures of more than 40°C have been reported in the country's far north [5]. In contrast, the average temperatures in most other areas of the nation, particularly in the south, are generally stable at around 32 °C [6].

Generally, access to electricity is one of the significant determinants of the economic prosperity of any country, as regular and reliable access to energy is critical to the foundations of a stable and growing economy [7]. However, this directly impacts economic development, such as infrastructure development, healthcare, education life expectancy, child mortality, investment in research and innovation, and contributes to income generation and employment [8]. Nigeria has been producing commercial electricity for over a century. Still, the population of about 220 million cannot access a dependable power supply because of the slow speed at which its energy infrastructure is being developed and maintained [9]. The current increase in electrical energy demand due to modern lifestyles has forced the world, including Nigeria, to rely heavily on electrical power systems to propel industrial and economic growth [10]. The Nigerian transmission network produces more power than it consumes. Still, due to unplanned outages caused by open circuit faults, earth faults, and failure of protective relays such as directional earth faults and distance protection relays, customers are frequently left without power for many hours throughout the year. Over half (about 56%) of Nigerians linked to the national grid experience erratic, inconsistent, and weak power supplies. In comparison, the

remaining population (about 44%) has no connection to the national power system at all [9], [11].

Nigeria has 12,522 MW of installed generation capacity [12] but can only dispatch around 4000 MW of the installed capacity daily [13]. The generators consist of 3 hydro stations with an installed capacity of 1890 MW (15.09% of installed capacity) and 20 gas stations with an installed capacity of 10632 MW (84.91% of installed generation) [14].

In general, gas generation is the main form of power generation in Nigeria [14]. Yet, the combined contribution of gas and hydro sources is insufficient to meet the expected demand for energy. The power system is characterised by a vast gap between supply and demand [15]. According to the Nigeria electricity sector report, the estimated demand as of 2016 was 28360 MW [14]; however, the world's demand for electricity grew by 2.2% [16]. Therefore, the estimated power demand in 2023 would be around 32727 MW. Figure 1.1 shows the grid mix where the generated power is about 8.88%, dispatch power is approximately 8.61%, and the estimated demand power is around 59.34%. It shows that all generated power is not effectively transmitted and distributed to consumers, which is attributed to transmission losses. It suggests that to close the gap between supply and demand and guarantee that the public has reliable access to electricity, there is a need for increased energy efficiency.

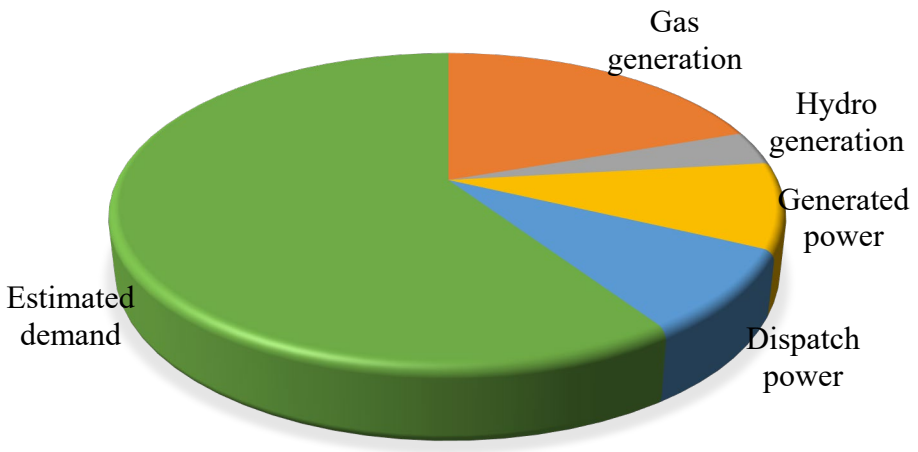

Figure 1.1: Nigeria grid mix.

The Nigerian Electricity Regulatory Commission (NERC) reports that approximately 7.4% of the 4000 MW generated power is lost in transmission across the network [17]. At the distribution stage, up to 27.7% of the electricity load is rejected, leaving about 2519 MW of supply [18] for a growing population of about 220 million people, who are expanding.

Therefore, the power grid is inadequate to meet the increasing power demand. Due to both lack of generation and deficiencies in maintenance and infrastructure, long hours of outages, and a low voltage profile, many of the basic comforts provided by the availability of electricity are not dependably available in the country [7], [19], [20], [21].

Furthermore, the demand for power in Nigeria is continuously increasing. In contrast, the existing power grid has consistently demonstrated its ineffectiveness in keeping up with this growth as the average amount of generated power lingers between 3,000 MW and 4,000 MW [22]. The power supply has consistently lagged the load demand, as shown in Figure 1.2. For example, in 2022 and 2023, the generated power was 28163 MW and 29072 MW, lower than the estimated demand of 32104 MW and 32727 MW, respectively.

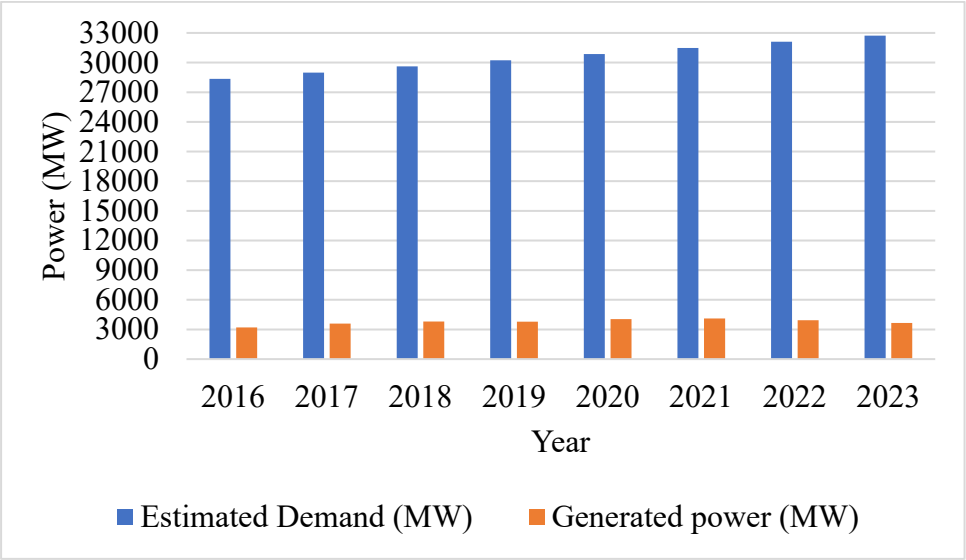

Figure 1.2: Growth in generation/energy demand.

The transmission system does not cover the entire country; therefore, providing a consistent and high-quality energy supply is challenging for the current Nigerian transmission network [23]. It currently has a maximum transmission capacity of around 4,000 MW and is technically weak, making it vulnerable to significant disturbances and challenges [24]; however, the transmission network is crucial to the whole system's performance [25], and it is the foundation upon which any present-day or future infrastructure stands. The transmission stands out as the weakest link in the entire chain of Nigeria's electricity network. Inadequate transmission infrastructure has been highlighted as responsible for stranded capacity, a characteristic of the electricity grid [20], [26]. The Nigerian transmission system currently

experiences numerous issues regarding the drop in voltage profile, reduced reliability, voltage collapse, and high-power losses [9], [27].

The voltage profile is the distribution of voltage levels throughout the transmission network. A voltage profile is essential to ensure system security, as system security is crucial for the efficient and reliable operation of electrical devices and equipment connected to the network [28].

Also, a reliable power system is essential because when a power system delivers electricity with the quality and characteristics specified in the appropriate standards, the reliability of the power will increase [29]. Hence, reliability analysis is essential in the planning, designing, and operating electric power systems.

Furthermore, voltage collapse occurs because of power system voltage instability. It is a condition where voltage decreases to a deficient level because of several events. Voltage collapse may happen due to sudden changes in load or failure to coordinate control parameters with the protective system [30].

Moreover, the high-power losses caused by the resistance of the conductor against the current flow generate heat within the conductor, increasing its temperature. The rise in temperature of the cable increases its resistance, which increases power losses [31]. Skin effects and corona losses also contribute to transmission losses. The country is currently experiencing under-capacity and poor transmission due to massive losses on the transmission lines [32]. It significantly contributes to poor performance and lower power supply efficiency in Nigeria.

An additional challenge with new transmission lines is the time required to obtain planning permissions and the identification of available rights-of-way. The Nigerian power grid is a crucial infrastructure for socioeconomic growth. Nigeria, Africa's most populous nation in Africa, has a rapidly expanding economy, which is driving up the power demand. Inadequate generation capacity, ineffective transmission and distribution networks, and frequent supply outages are just a few of the issues the Nigerian power sector has faced. These problems have made it more difficult for the nation to supply reliable and adequate electricity to meet the needs of its citizens and economy [33].

The electric utility’s objective is to provide electricity to satisfy its customers’ needs and expectations to a better level within the resources under operational and economic viability [19], [34], [35]. One of the critical activities that must be carried out effectively to ensure that

Nigeria is among the industrialised nations is to ensure that power is effectively transmitted to all parts of the country [8].

The power sector reform emphasised the need for a 30% expansion in the transmission capacity of the country's 330 kV network to meet an anticipated increase in generating capacity. Based on the findings, new lines were planned to be added to the existing 330 kV network [36]. As a result, considerable investment is necessary to enhance the transmission infrastructure to keep up with the expected rise in generation capacity and customers' expectations of an improved power supply [20], [26]. Thus, to meet the growing demand and access improved electricity, interconnecting an overhead high voltage direct current (HVDC) link is considered an alternative solution.

High voltage direct current (HVDC) technology is one of the technical options that can be considered for future transmission system development [37] to meet the growing electricity demand. The advantages of HVAC include easy voltage transformation and current interruptions. However, this has limitations in situations of long transmission lines due to factors such as voltage instability and increasing transmission losses [38]. Furthermore, the limitations in current carrying capacity, the need for reactive power compensation at various locations along the transmission lines, losses due to the skin effect (non-uniform current distribution in conductors), and the Ferranti effect (received voltage exceeding transmitted voltage) are characterised by HVAC [39]. Thus, in recent years, the utilisation of HVAC systems has fallen due to the enormous losses involved with employing AC transmission across long distances and has been considered as one feasible plan to increase power grid delivery capability [40], [41].

To solve these limitations of HVAC, using HVDC for long-distance power transmission is a solution [42], [43]. This offers numerous advantages over high voltage alternate current (HVAC), which include the transmission of bulk power from one point to another point over long distances greater than 500 km efficiently for overhead lines, cheaper for bulk power transmission, and more energy transmitted with lower operational losses [44], HVDC lines have less corona effect and power flow can actively control [45].

About 39 HVDC systems have been commissioned worldwide almost two decades after the first project began commercial operation in 1999 [41]. Countries using the HVDC link include China, the USA, Brazil, Italy, Germany, India, Canada, France, and Belgium; Estonia and Finland; the Netherlands and Norway; Sweden and Lithuania. The United Kingdom has

been connected to countries like Norway, France, Belgium, and the Netherlands [46], [47]. Similarly, in Africa, there are HVDC links such as the Caprivi Link HVDC Scheme connecting Namibia and Zambia [48], Inga- Kolwezi (formerly known as Inga-Shaba) HVDC overhead link in the Democratic Republic of the Congo [49], and the HVDC link between Mozambique near the Cahora Bassa and South Africa [50].

1.2 Nigeria transmission network description

The transmission system comprises a network of substations and transmission lines that connect generation sources to load centres, allowing the wholesale power system to transport power from generation resources to bulk consumers [10]. The Nigerian power system is functionally and technically composed of three sub-systems. The generation system (power stations) is managed by the Generating Companies (GENCOs), Independent Power Providers (IPP), and Niger Delta Holding Company (NDHC) with a total installed capacity of 14034 MW [13], [51].

The generators in the Nigerian network are connected to the transmission system via step-up transformers [36]. The Nigerian generators produce either 11 kV or 16 kV, which are subsequently stepped up to 330 kV for transmission. From 330 kV, the voltage is stepped down to 132 kV, then to 33 kV, known as the primary distribution voltage, and then to 11 kV, utilized as the secondary distribution voltage. The 11 kV is further stepped down to 230 V for a line to neutral and 0.415 kV for a line to line [52]. The bulk of the power transmitted through the primary grid is fed through 330/132/33 kV transformers [53].

Figure 1.3 shows Nigeria's transmission system comprising high-voltage lines and switching stations with a transmission voltage level of 330 kV and a sub-transmission voltage rating of 132 kV. The Transmission Company of Nigeria (TCN) manages the transmission system. The role of the system operator is to keep the transmission system and the connected installed generation safely and reliably [54].

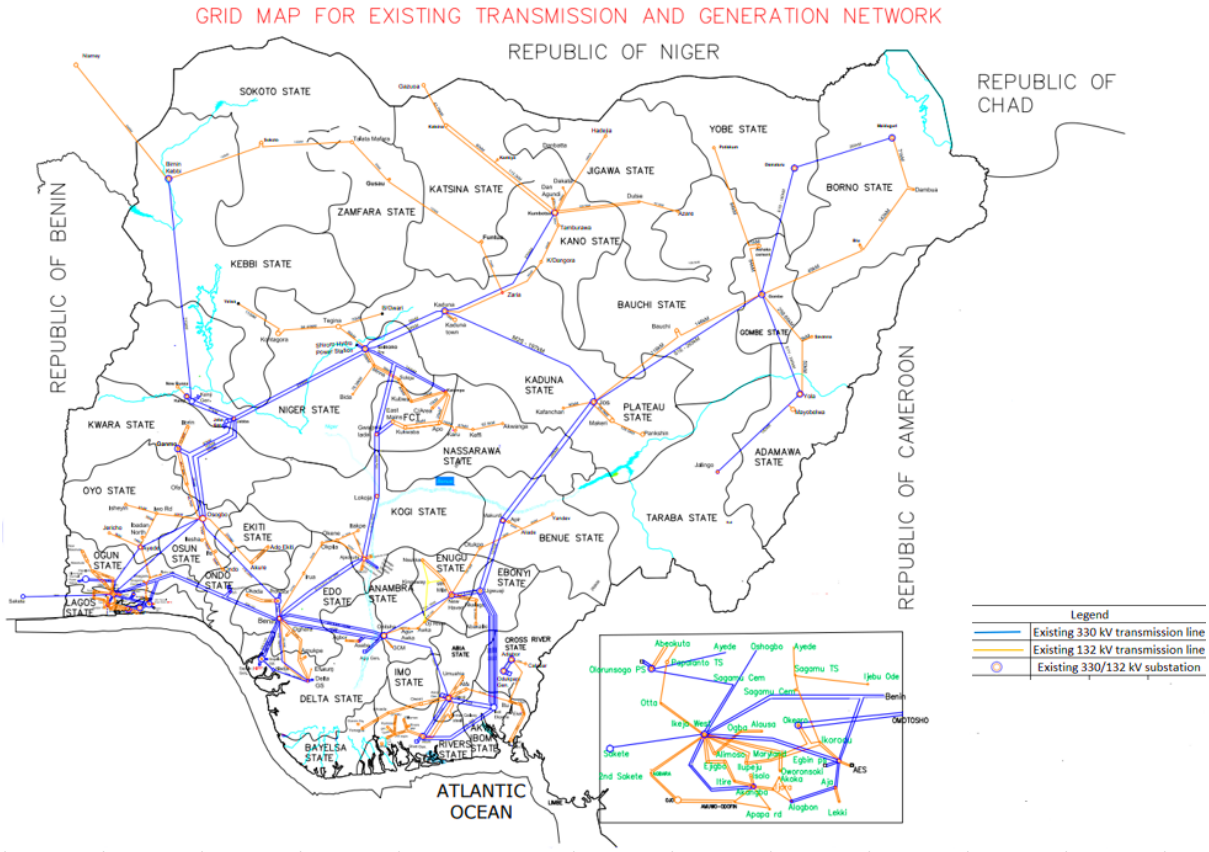

Figure 1.3: High Voltage grid map [53].

The Distribution Companies (DISCOs) manage the sub-transmission with medium voltage and lower voltage of 33 kV and 11 kV lines [55]. There are six GENCOs, one TCN, and eleven DISCOs. The system's nominal frequency is 50 Hz and should be maintained within ±0.5% under normal operating conditions, while it is acceptable to vary within ±2.5% under stressed operating conditions [56]. The 330 kV voltage level limit is between 280.5 kV (0.85 pu) and 346.5 kV (1.05 pu) [57]. Nigeria currently supplies electricity to three neighbouring countries, and these are the Republic of Benin, Togo, and Niger [12].

The Nigerian 330 kV transmission system model used in this study consists of 64 transmission lines totaling 6546.47 km, 52 busbars, 20 generators, and 23 loads. The network was modelled with DIgSILENT (DIgital SImuLation and Electrical NeTwork) PowerFactory (DSPF) 2020 using data provided by the Nigerian Electricity System Operator (NESO). DSPF is a commercial package for power system analysis, offering comprehensive modelling capabilities and advanced algorithms. Its user-friendly interface, compatibility with Windows, and unique database concept enhance efficiency and accuracy. Its flexibility makes it ideal for automated solutions in business applications, making it a preferred choice for this research

[58], [59]. Also, it offers a full suite of functions for studying sizeable interconnected power systems [36].

Two scenarios were considered in this study: summer (June), which is known as the rainy season, and winter (December), which is known as the dry season [1]. The peak total loads are 4804.33 MW -314.84 MVAR and 4396.34 MW -122.46 MVAR, respectively. The single-line diagram of the transmission network used in this research is shown in Figure 2.1. It is worth noting that this model is based on data provided in 2019; nevertheless, it is still actual because the transmission system has not changed substantially since then.

1.3 General overview of HVDC technology

High Voltage Direct Current (HVDC) transmission consists of two types of technology, named based on the type of converter used. These are the Line-commutated Current Source Converters (LCCs) and Voltage Source Converters (VSCs) [44], [60]. LCC technology is based on a semiconductor-based switch called thyristor. This switch can hold AC voltage in either polarity, but current can only flow in one direction. On the other hand, VSC is based on an Insulated Gate Bipolar Transistor (IGBT). The IGBT is a fully controllable switch, and power can flow in both directions, which is a benefit over the LCC technology.

Due to the bi-directional flow capability in the VSC, it is not necessary to reverse the DC voltage polarity of the converters to change the direction of power flow between them. The VSC-HVDC technology allows for the independent regulation of both active and reactive power flow [44], [61], [62]. Given the above advantages, all new HVDC interconnections are based on VSC.

This research project, therefore, aims to provide valuable insights that can guide investment plans and future expansion in the nation's energy infrastructure by examining the deployment of HVDC within the context of the Nigerian power system. The conclusions will help readers better understand the technical and financial consequences of using HVDC technology in Nigeria. However, regardless of the choice of future electricity transmission, the transmission network must function well for overall system security and dependability. Therefore, it is necessary to analyse the use of high voltage direct current (HVDC) transmission within Nigeria's transmission system. Currently, HVDC is not in service, but there is an interest in exploring the benefit of this technology on the Nigerian HVAC transmission system [36].

1.4 Research objectives

The research will study the feasibility of using HVDC transmission to mitigate some of the issues described in Section 1.1 (voltage profile, reliability, and stability problems) and will consist of the following objectives:

1. Modelling the current Nigerian transmission system configuration using the Nigerian Energy System Operator (NESO) data and load flow analysis.
2. Evaluation of network reliability (network indices and load indices)
3. Evaluation of network stability
4. Identification of areas that require building new HVDC lines.
5. Economic evaluation of the HVDC project.

1.5 Thesis original contributions

1. The 330 kV transmission network model was successfully built. Two load flow studies were executed (summer and winter scenarios). The power flow study highlighted the importance of accurate data in power system studies. Some alterations were made to improve the model and ensure it was fit for additional research.
2. The reliability study allowed the identification of the loads with lower reliability. These loads are more prone to failures than others in the system. Two buses (Gombe and Yola) were chosen to investigate the effects of HVDC connections on system reliability. Adding an HVDC line between Azura and Gombe was the best improvement in reliability indices.
3. The stability study revealed the amount of reactive power absorption needed to improve the voltage profile for the weak buses (Gombe and Yola). The HVDC link between Azura and Yola increased the system's stability.
4. The financial advantages of employing HVDC connections on the weak buses were studied using net present value (NPV). The efficiency of the HVDC link between the two buses (Gome and Yola) was highlighted, and the economic implication of having the HVDC between Azura and Yola was considered more beneficial. These studies offer information on the benefits and financial impacts of implementing HVDC technology in power systems, assisting in establishing power transmission policies and well-informed decision-making.

1.6 Thesis outline

The thesis is structured in six chapters, including this introduction. The subsequent chapters are organised as follows.

Chapter 2 describes the building and validating of a computer model of the Nigerian transmission system using the commercial software DigSILENT PowerFactory. This model will be used for more detailed power system studies in the next steps of this research work. In addition, the assumptions that were made to improve the solution and results are discussed. The last part of the chapter describes the results of the load flow study and its conclusions. Both summer and winter scenarios are described.

In Chapter 3, the reliability analysis is carried out. The reliability indices are introduced first to provide common terminology, and values for different countries are listed based on the literature review. The results for both network indices and load indices for the existing system configuration identify the points in the network with low reliability and suitability for HVDC connection. Finally, two HVDC interconnections are described (Case 1 and Case 2), and the impact of HVDCs on system reliability is introduced.

Chapter 4 studies the stability analysis of the network to determine the weakest buses using static voltage stability analysis. The P-V and Q-V analyses were used to carry out this study. The implication of the HVDC interconnections on both the PV and QV analysis was described. The study also investigated the impact of HVDC control modes, converter ratings, and reactor(s) on static voltage stability.

Chapter 5 presents the economic analysis of having an HVDC link to the network based on the Net Present Value (NPV), the loss cost, and expected interruption cost parameters across 40 years.

Conclusions and recommendations are presented in Chapter 6.

1.7 List of publications and conference

Conference contribution:

1. O. G. Olasunkanmi, Z. Deng, and G. Todeschini, “Load flow analysis of the Nigerian transmission grid using DIgSILENT PowerFactory,” in 2021 56th International Universities Power Engineering Conference: Powering Net Zero Emissions, UPEC 2021- Proceedings, 2021, pp. 8–13, https://doi.org/10.1109/UPEC50034.2021.9548253

Journal Articles:

1. O. G. Olasunkanmi, W. O. Apena, A. R. Barron, A. O. White, and G. Todeschini, “Impact of a HVDC Link on the Reliability of the Bulk Nigerian Transmission Network,” Energies, vol. 15, no. 24, pp. 9631, Dec. 2022, https://doi.org/10.3390/en15249631.

2. O. G. Olasunkanmi, A. R Barron, A.O.White, and G. Todeschini, ‘’Evaluation of a HVDC interconnected to improve the voltage stability of the Nigerian transmission network’’, Journal of Electronics and Electrical Engineering, Vol. 3 Issue 1 pp 84-100, Jan.2024, https://doi.org/10.37256/jeee.3120243799**.**

2 Load Flow Analysis of the Existing Transmission Network

2.1 Introduction

The study of a power system in a standard and steady-state operation is known as load flow analysis [63]. More specifically, a load flow study can be defined as the flow of active and reactive power from generating stations to the loads through different branches of the network and gives steady-state solutions of the voltages at all the buses for a particular load condition [64]. Steady-state operation is a condition where all the variables and parameters are constant during observation [65].

According to [66], [67], [68], load flow analysis is mainly used to examine the normal operation state. Its purpose is to check whether the system can operate safely if equipment overloads, or some node voltages are too low or too high. Generally, a load flow is carried out to determine where additional transmission lines, substations, and other infrastructure are required to meet rising energy demand and identify network voltage drop issues. The studies are performed using digital computer simulation which addresses the operation, planning, running, and development of control strategies [66], [67], [69], [70], [71], [72].

The first step in resolving load flow studies is to identify known and unknown variables in the system. Based on these variables, buses are classified into three types: slack buses, generation buses, and load buses. The Slack bus must provide a mismatch between scheduled generation and overall system load, including losses and total generation. Since both voltage magnitude and angles are specified, the slack bus is usually referred to as the reference bus or swing bus [73].

Specific input data are required to calculate load flow analysis:

- Bus data: each bus in the power system is characterized by factors such as voltage magnitude, voltage angle, and type (e.g., slack bus, generator bus, load bus). The slack bus is a reference bus with a known voltage magnitude and angle.

Part of the work presented in this chapter has been published in [36].

- Load data contains information on the different loads connected to the system, such as the active power demand (P), the reactive power demand (Q), and the power factor.

Line parameters such as resistance and reactance are required for transmission line modelling. These characteristics define the impedance of the line and its effect on power flow [72], [74].

Using suitable mathematical techniques, calculating the load flows in all system elements is possible. The commonly used techniques are Gauss-Seidel, Newton-Raphson, and the fast-decoupled power flow methods. The Gauss-Seidel method is simple but converges slower, the Newton-Raphson method is iterative, and because of the quadratic convergence, the method is mathematically superior to the Gauss-Seidel method. In the fast decoupled method, the convergence is geometric, and the technique requires more iterations to converge compared to the Newton-Raphson power flow formulation [73], [75], [76]. Given the complexity of the calculation, a solution using digital computers is a standard practice for planning. At each bus, there are four quantities of interest to be known for further analysis: load or generator real power (P), load or generator reactive power (Q), voltage magnitude /V/, and voltage phase angle (δ) [77].

Nigeria has continued to experience insufficient power supply from the national grid, which has limited the country's potential economic growth. The transmission system is characterized by poor voltage profile networks, especially in the North, with insufficient dispatch and control infrastructure, radial and fragile grid structure, frequent system collapse, and exceedingly high transmission losses [21], [78]. Hence, the grid is highly stressed and weak, which makes it prone to voltage instability and, eventually, voltage collapse. In this chapter, the load flow of the Nigerian transmission network will be assessed to evaluate the bus voltage profiles, real and reactive power flow, and power system losses. Therefore, running the load flow for the Nigerian transmission network using the commercial software PowerFactory will provide detailed information on the present state of the power system, that is, the power injected at every bus from the generators, the voltage, and losses on the transmission lines. It uses the Newton-Rapson method, which converges fast and is more accurate, so it is advantageous for large power systems [64], [72]. This information will provide the data for further analysis and evaluation in the reliability and stability studies of the Nigerian transmission network.

2.2 Literature review

Several researchers have used various methods for analysis, simulation, and modelling in power systems. A few load flow solution techniques exist in the literature, such as Gauss-Seidel, Newton-Raphson, Fast Decoupled Load Flow, and backward/forward sweep method. Some published papers and literature reviews can be found in this section.

The Nigerian power sector planned to increase the generation capacity; however, the transmission link remains weak in the system. Therefore, [79] studied the 330 kV transmission network and introduced new lines and power stations. The analysis was carried out using the Newton-Raphson algorithm in ETAP. The result revealed that the network increased its capacity to support larger loads, with a maximum loadability of 238.4%. Other authors [80] and [81] studied the 330 kV network facing challenges in reactive power management and voltage control and used the Newton-Raphson algorithm to analyse the network. From [80], the result revealed that Jos, Gombe, Abuja, Maiduguri, Kano, Kaduna, and Makurdi buses (seven buses) are facing voltage profile violations; however, this author recommends adding more substations and additional lines to strengthen the network, especially in the critical buses like Kano, Kaduna, and Maiduguri.

Moreover, in [81], the analysis also revealed that the same seven buses as found by [80] are out of the statutory voltage limit (voltage below 0.95 pu) but found out that additional two buses, which include Birni-Kebbi and Okapi bus voltage are also outside the statutory limit. Total active power losses of 135.219 MW were also revealed. The use of shunt capacitive compensation and dynamic static var compensator (SVC) to improve the voltage profile was suggested respectively [79], [80], [81].

Further study by [82] performs load flow analysis on the existing electricity system in the Solapur District of Maharashtra State, India, using the Newton-Raphson method. The model was developed using MATLAB and actual data supplied by Maharashtra State Electricity Transmission Co. Ltd. The analysis was performed on the 220 kV lines. The study identified overloaded buses and used static capacitor banks for reactive power compensation to improve the voltage profile. Similarly, the work in [67] also identifies the weak voltage points in some buses on the Myanmar Power System Network in Asia. Then, it compensates for the weak bus voltages with series and shunt capacitors to improve the transient and steady-state stability of the network. In the research, line compensations were applied to improve transmission line performance. However, the first line loading at the receiving end resulted in

10.85 % high voltage regulation, which was considered undesirable. Therefore, capacitor banks were used to compensate and improve line performance. Including shunt and series capacitors were employed, and the best results were obtained with a voltage regulation of 0.3005 % and 93 % efficiency of the transmission line.

Furthermore, the Tehran Metro's distributed power system in Iran was studied by [83] using ETAP for modelling, simulation, and load flow analysis. This study presents a comparison of three widely used load flow techniques: Newton-Raphson (NR), Fast Decoupled (FD), and Gauss-Seidel (GS). The results of these three load flow methods are almost the same. Total generation and power losses were acquired and examined as the outcomes of the load flow evaluation. The results of these three load flow methods are almost the same (NR- 1354.6 kW, FD- 1354.7 kW, and GS- 1354.6 kW). It provides insightful information about applying various load flow approaches in distributed power systems, focusing attention on their effectiveness. A load flow-based simulation was also used to determine where the distribution system unit (distributed generation) should be placed to optimise the load profile and reduce power losses in the test distribution system [83].

Another author [84] observed that iterative approaches such as Newton-Raphson and Gauss-Seidel used in transmission networks are unsuitable for distribution network and load flow analysis. Alternatively, a new load-flow method, a backward/forward sweep iterative method, was used for load-flow studies, where the branch current is calculated using the backward propagation, and bus voltages are computed using the forward propagation. Simulations are performed for scenarios with and without distribution generators (DGs). The simulation results of the load flow study with and without DGs were compared, and the researchers determined how these distributed energy resources affected the functionality of the microgrid. The method was found to be easy to implement, accurate, and straightforward when carried out with MATLAB software, and the results were verified, and fast convergence characteristics were obtained. IEEE standard 33 buses were analysed using with and without distributed generators installed as a case study [84].

Table 2.1: key results summarising the literature review.

Author	Objective	Method	Result	Recommendation	Conclusion
[79]	Investigate generated power on the network and where the network experiences high voltages.	Newton Raphson's method in ETAP	Power before network expansion 4948.78 MW	Building more generators and transmission lines and upgrading single lines to double circuit lines	More power was evacuated, and a maximum loadability of 238.4% was achieved.
[80] & [81]	Investigated the management of reactive power and voltage control	Newton-Raphson's method is used, and MATLAB software is utilized for simulation analysis.	Identifies buses with voltage levels outside the statutory limit	More substations, additional lines, and shunt capacitor compensation	More power was transmitted, and the voltage profile improved
[82]	Power system model for optimal operation and plan for future expansions.	MATLAB software was used to model and NR for load flow analysis	Overload buses were identified.	static capacitor banks for reactive power compensation	Effective improvement in the voltage profile.
[83]	Compare load flow techniques, NR, FD, and GS, in terms of their numerical methods.	ETAP software	Total generation and power losses were acquired.	-	The location of distributed generation for load profile improvement was revealed, and power losses were minimised.
[84]	NR, FD, and GS iterative were compared with backward/forward sweep iterative techniques.	Simulations were carried out in MATLAB software.	Poor convergence in NR and GS iterative techniques for distribution power flow analysis	Recommending Backward/Forward Sweep iterative equations for faster convergence.	Improving system performance, stability, and efficiency in the presence of DGs using backward/forward iterative.
[67]	Focusing on voltage profile maintenance and compensating strategies.	Newton-Raphson method using MATLAB software	Weak voltage points were identified.	Compensated with shunt, series, & series and shunt capacitors	Among the three compensations, shunt capacitive compensation is the best to enhance the efficiency of the line

The literature review explores load flow analysis methods, including the Newton-Raphson method, which is widely used for solving nonlinear power flow equations in complex systems. The literature emphasises the need for load flow analysis and voltage regulation to ensure the dependability and stability of power systems. Infrastructure growth is critical for fixing power network issues and providing efficient power generation, transmission, and distribution. Overall, by integrating current knowledge with findings from the literature, the review can guide the current studies and give information about state-of-the-art load flow analysis.

2.3 Load flow analysis methodology

2.3.1 Modelling of Nigeria transmission network

The Nigerian transmission network was modelled on DigSILENT PowerFactory using data from the Nigerian Electricity System Operator (NESO). The single-line diagram of the network is shown in Figure 2.1. Two scenarios were considered for power flow studies: summer, the rainy season (June), and winter – the dry season (December). The studies of these two scenarios (summer and winter) allow for verifying and confirming the accuracy and dependability of load flow analysis techniques and models. By comparing the outcomes of the two scenarios, it is feasible to confirm that the analytic procedures are functioning appropriately. This is significant for power system operation and planning and also allows researchers to investigate the impact of various scenarios on system voltages, currents, and power flows.

Data used includes shunt reactors, capacitance, generators, and load data. Shunt reactors with a rated power of 765 MVAR were added to thirteen buses in the summer, and 975 MVAR was added to twelve in the winter. The apparent power (S) and reactive power (Q) for each load and generator were not provided, but this was calculated by assuming a power factor between 0.7 and 1. Appendix A.0.1 and Appendix A.0.2 show the active, reactive, and apparent power for the loads and generators, while some buses have no reading (NR), and Table 2.2 shows the transmission line length. After the modelling using the actual data from NESO, the load flow was executed; after that, some modifications were made to make the model close to the data given by NESO.

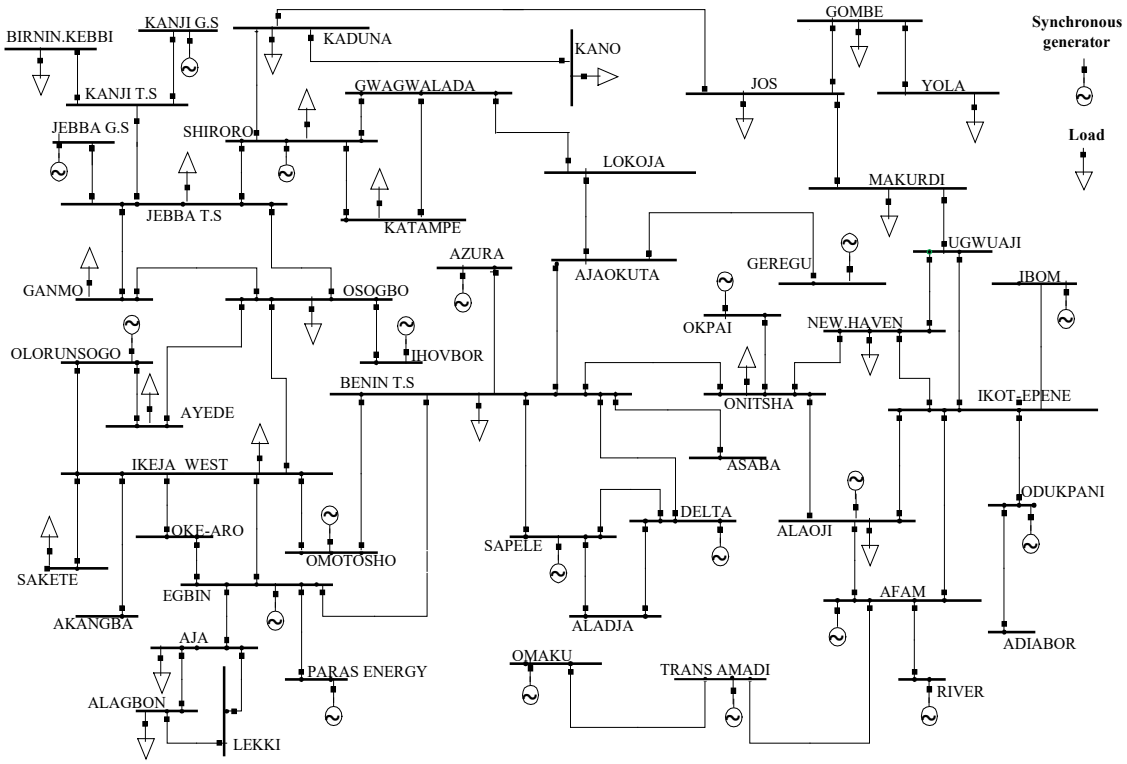

Figure 2.1: Single-line diagram of the existing transmission network.

Table 2.2: Nigeria 330kV transmission line length.

	Transmission line		
S/N	**From**	**To**	**Length (km)**
1	Afam	River	45
2	Aja	Lekki	11
3	Aja	Alagbon	26
4	Aja	Egbin	14
5	Ajaokuta	Geregu	11
6	Ajaokuta	Lokoja	50
7	Alagbon	Lekki	32
8	Alaoji	Afam	25
9	Ayede	Osogbo	119
10	Azura	Benin	20
11	Benin T.S	Asaba	58
12	Benin T.S	Sapele	50
13	Benin T.S	Ajaokuta	195
14	Benin T.S	Delta	107
15	Benin T.S	Onitsha	137
16	Delta	Aladja	32
17	Egbin	Benin T.S	218
18	Egbin	Paras Energy	28
19	Gwagwalada	Katampe	60
20	Gwagwalada	Lokoja	140

21	Ganmo	Jebba T.S	173
22	Ganmo	Osogbo	87
23	Gombe	Damaturu	160
24	Gombe	Yola	240
25	Ibom	Ikot Epe	75
26	Ikeja West	Oke Aro	32
27	Ikeja West	Akangba	18
28	Ikeja West	Egbin	62
29	Ikeja West	Osogbo	235
30	Ikot Epene	Alaoji	38
31	Ikot Epene	Afam	90
32	Ikot Epene	Odukpani	72
33	Jebba G.S	Jebba T.S	8
34	Jebba T.S	Osogbo	157
35	Jos	Makurdi	285
36	Jos	Gombe	265
37	Kaduna	Jos	197
38	Kaduna	Kano	230
39	Kaduna	Shiroro	96
40	Kainji T.S	B.Kebbi	310
41	Kainji T.S	Kanji G.S	0.47
42	Kainji T.S	Jebba T.S	81
43	Makurdi	Ugwuaji	50
44	New-Haven	Epene	143
45	New -Haven	Onitsha	96
46	Odukpani	Adiabor	18
47	Oke Aro	Egbin	30
48	Okpai	Onitsha	56
49	Olorunsogo	Ayede	60
50	Olorunsogo	Ikeja West	30
51	Omaku	Egbema	86
52	Omotosho	Benin	120
53	Omotoso	Ikeja W	160
54	Onitsha	Alaoji	138
55	Osogbo	Ihovbor	251
56	Sakete	Ikeja West	70
57	Sapele	Aladja	63
58	Sapele	Delta	93
59	Shiroro	Gwagwalada	60
60	Shiroro	Katampe	144
61	Shirro	Jebba T.S	244
62	Trans Amadi	Afam	45
63	Uguwaji	New Haven	165
64	Ugwuaji	Ikot Epene	143

2.3.2 Load flow formulation

The remaining generator buses are regulated or PV buses because the net real power (P) is specified, and the voltage magnitude (V) is controlled. Most buses in practical power systems are load buses. Load buses are PQ buses since they specify net real (P) and reactive power (Q) loads. Voltage magnitudes and angles (δ_i) are unknown for PQ buses, but only the voltage angle is known for PV buses. There are no variables to solve on the slack bus because both voltage magnitudes and angles (δ_i) are specified [73].

The input and output variables of the power flow problem are:

- the real and reactive power (voltage magnitude and phase) at each load bus (PQ buses);
- the actual power generated and the voltage magnitude (reactive power generated and voltage phase) at each generation bus (PV buses).
- the voltage magnitude and phase (the real and reactive power generated) at the slack bus.

The equations adopted to solve the power flow problem are the real power balance equations at the generation/load buses and the reactive power balance at the load buses:

$$P_i = V_i \sum_{j=1}^{N} V_j Y_{ij} \cos\left(\delta_i - \delta_j - \gamma_{ij}\right) = P_i^{sp} \quad i \in n_p \tag{2.1}$$

$$Q_i = V_j \sum_{k=1}^{N} V_k Y_{kj} \cos\left(\delta_j - \delta_k - \gamma_{jk}\right) = Q_i^{sp} \quad i \in n_Q \tag{2.2}$$

where

N is the total bus number.

n_Q is the list of the buses for which the reactive power is specified.

n_p is the list of buses for which the active power is specified.

P_i and Q_i are the real and reactive power injections calculated at the *i*th and *j*th bus; P_i^{sp} and Q_i^{sp} are the real and reactive power injections specified at *i*th and *j*th bus; $V_i = V_i \angle \delta_i$ is the *i*th bus voltage.

$Y_{ij} = Y_{ij} \angle \gamma_{ij}$ is the $[i, j]$ th element of the bus admittance matrix [85].

2.4 Load flow results

2.4.1 Summer result with initial network model

A first attempt was made to calculate the load flow based on the data provided. Although the load flow converged, the voltage profile obtained from PowerFactory did not match the data. Additionally, the generator's slack bus Egbin output power was 120 MW instead of 626 MW. The total generated power dropped to 4298 MW, while the expected value was 4804 MW. After some investigations and checks of the network, it was discovered that the shortage of load data totalling 520.83 MW was the reason for the drop in the slack bus output power. Therefore, three loads with 486.66 MW active power were added at the Aja, Alagbon, and Makurdi buses to balance the network, with a reactor capacity of 761 MVAR installed on 13 buses.

2.4.2 Winter result with the original network model

Similar to the findings of the summer scenario, the reference generator at Egbin produced 161 MW of active power instead of 705 MW. As a result, the total power generated was 3850 MW instead of 4395 MW, as given in the original data. From the investigation and checks of the network, it was concluded that the lack of data for some loads caused the drop in power. Hence, for the winter scenario, three loads with a total power of 523.95 MW were added at Aja, Alagbon, Lekki, and Markurdi buses to match the generation data provided by the NESO. The reactors were installed on 12 buses with a total capacity of 971 MVAR.

2.4.3 Network modification

Based on a discussion with the Nigerian Electricity system operator (NESO), network inspection, and practical considerations, other modifications were implemented to match the voltage profiles:

i. It was observed that for summer, the voltage drops between Aja and Egbin were equal to 0.1 kV in simulation, whereas the original voltage drop data was 16 kV. This applied to the two scenarios (summer and winter scenarios). The line resistance was increased from 0.0394 Ω/km (resistance of 330 kV double circuit line) to 2 Ω/km on the Aja to Egbin line. The increase in the line resistance only affects the Aja to Egbin line to match this voltage drop (16 kV). The value of 2 Ω/km was selected as a suitable one after a few tests of 0.1 Ω/km to 3 Ω/km were

carried out. As a result, the network losses increased from 131 MW to 150 MW, while the voltage difference between Aja and Egbin was the same as in the original data.

ii. The voltage magnitudes at Molai and Damaturu were above 5% of the nominal value (366 kV and 352 kV, respectively) because they were connected to the main grid through long lines (160 km and 260 km, respectively) with high shunt capacitance. However, no loads were attached to them; therefore, disconnecting the Molai and Damaturu busbar in the DIgSILENT model was decided. It was applied to the two scenarios. By doing so, the voltage levels at Gombe and Yola improved.

iii. Due to the disconnection of the Molai and Damaturu busbars, the capacitance provided by the long transmission line was removed. Therefore, the shunt reactors connected at (Gombe) were used to compensate for the transmission lines (used to connect the Molai and Damaturu) and were adjusted accordingly to maintain the system voltage level (particularly at Yola).

iv. Furthermore, to make the voltage profile of the summer scenario close to the original data, the settings of the shunt reactor model in the simulation were modified. The following reactors were added: 15 MVAR shunts connected in parallel with three steps at Gombe, while at Jos and Markurdi, five 15 MVAR shunts connected in parallel with three steps were set up. At Yola, there was no connection to the bus. For the winter scenario, a shunt bank with five steps on the Yola bus was modelled, where five 5 MVAR shunts were connected in parallel as a shunt bank reactor. A summary of the shunt reactor's parameters is shown in Table 2.3. The above modifications were also made for the winter scenario to make the network model close to the original data.

Table 2.3: Reactors parameters.

		Rated parameters				Summer			Winter	
Bus No	**Bus Name**	**Rated power (MVAR)**	**Reactive power at each step**	**Max No. of step**	**Actual No. of step**	**Shunt connected (MVAR)**	**Output MVAR**	**Actual No. of step**	**Shunt connected (MVAR)**	**Output MVAR**
8	Alaoji	75	75	1	0	75	0	1	75	75
13	Benin T.S	150	75	2	2	75	155	1	75	78
19	Gombe	150	15	10	3	15	11	1	15	5
23	IkejaWest	0	0	1	1	0	0		Out of service	
26	Jebba T.S	75	75	1	1	75	75	1	75	77
27	Jos	75	15	5	3	15	51	1	15	74
28	Kaduna	250	25	10	5	25	210	1	25	66
31	Kano	45	15	3		Out of service			45	43
32	Katampe	65	65	1	1	65			Out of service	
35	Makurdi	70	7	10	1	7	5	2	7	36
39	Oke-Aro	75	15	5	2	15	45	4	15	288
44	Onitsha	75	15	5	5	15	76	1	15	77
45	Osogbo	150	75	2	1	75	72	2	75	147
53	Yola	5	5	1		Out of service		5	5	5
	Total	1260					761			971

2.4.4 Summer results after modifications

After the above modifications were made, the load flow simulation corresponded with the original data; the total reactor output power was 761 MVAR, as shown in Table 2.3. The actual generated power was 4804 MW, while the sum of demand was 4654.46 MW, and active power losses were 150 MW on the network. Table 2.4 shows the summary of the load flow after modifications. Load added includes Aja (162.70 MW), Alagbon (162.00 MW), and Makurdi (161.96 MW) for the summer scenario modification. The voltage levels of the modelled network were within the statutory voltage limit (0.85 pu to 1.05 pu) (load flow result), and the voltage percentage difference ranged from -1.02% to +1.03%) as shown in Table *2.5*. The voltage difference between load flow results and data provided was 0% at Aja, Gombe, Jos, Makurdi, and Yola and 0.01% at Alagbon. Most buses operate in the range of the desired voltage level as the voltages are close to 1.00 pu. The results of the load flow with HVDC will be presented in Chapter 4.

Table 2.4: Summary of load flow results (summer).

	NESO data			Load flow result		
	P (MW)	Q (MVAR)	S (MVA)	P (MW)	Q (MVAR)	S (MVA)
Generator	4298	-602	4340	4804	-298	4814
Load	4168	955	4276	4654	1281	4828
Losses	130			150		
Compensation		765			761	

Table 2.5: Summer voltage profile.

		NESO Data		Load flow result		
Bus No.	**Bus**	**Volt (kV)**	**pu**	**Volt (kV)**	**pu**	**% Diff**
1	Adiabor	330	1.00	330	1.00	0
2	Afam	NR	-	335	1.02	-1.02
3	Aja	316	0.96	316	0.96	0
4	Ajaokuta	328	0.99	330	1.00	0.01
5	Akangba	313	0.95	316	0.96	0.01
6	Aladja	NR	-	341	`1.03	-1.03
7	Alagbon	315	0.95	315	0.96	0.01
8	Alaoji	335	1.02	334	1.01	0.01
9	Asaba	NR		336	1.02	-1.02
10	Ayede	320	0.97	320	0.97	0
11	Azura	NR	-	333	1.01	-1.01

12	Birnin-Kebbi	338	1.02	337	1.02	0
13	Benin T. S	337	1.02	335	1.02	0
14	Damaturu	NR	-	-	-	-
15	Delta	344	1.04	343	1.04	0
16	Egbin	332	1.01	332	1.01	0
17	Ganmo	330	1.00	328	0.99	0.01
18	Geregu	NR	-	330	1.00	-1.00
19	Gombe	300	0.91	299	0.91	0
20	Gwagwalada	324	0.98	326	0.99	0.01
21	Ibom	NR	-	330	1.00	-1.00
22	Ihovbor	NR	-	330	1.00	-1.00
23	Ikeja West	317	0.96	316	0.96	0
24	Ikot-Epene	333	1.01	333	1.01	0
25	Jebba G. S	330	1.00	330	1.00	0
26	Jebba-T. S	331	1.00	330	1.00	0
27	Jos	303	0.92	302	0.92	0
28	Kaduna	314	0.95	318	0.96	0.01
29	Kanji G. S	332	1.01	332	1.01	0
30	Kanji T. S	NR	-	332	1.01	-1.01
31	Kano	318	0.96	312	0.95	0.01
32	Katampe	317	0.96	318	0.96	0
33	Lekki	315	0.95	316	0.96	0.01
34	Lokoja	327	0.99	330	1.00	0.01
35	Makurdi	316	0.96	316	0.96	0
36	Molai	NR	-	-	-	-
37	New.Haven	330	1.00	329	1.00	0
38	Odukpani	NR	0	330	1.00	-1.00
39	Oke-Aro	315	0.95	314	0.95	0
40	Okpai	NR	0	0	0	0
41	Olorunsogo	319	0.97	319	0.97	0
42	Omaku	NR	0	337	1.02	-1.02
43	Omotosho	341	1.03	340	1.03	0
44	Onitsha	332	1.01	332	1.00	0.01
45	Osogbo	322	0.98	324	0.98	0
46	ParaEnergy	NR	0	332	1.01	-1.01
47	River	NR	0	336	1.02	-1.02
48	Sakete	313	0.95	312	0.95	0
49	Sapele	339	1.03	337	1.02	0.01
50	Shiroro	322	0.98	332	1.01	0.03
51	TransAmadi	NR	-	337	1.02	-1.02
52	Ugwuaji	329	1.00	328	0.99	0.01
53	Yola	300	0.91	300	0.91	0.0

2.4.5 Winter results after modifications

Similarly to the summer scenario, the load flow results matched closely with the original load flow result of total generated power of 4395 MW with a total load demand of 4299 MW, and the losses on the network was 95.97 MW, with a reactor output power of 971 MVAR as seen in Table 2.6. The modelled voltage magnitudes were within the statutory voltage limit of 0.85 pu to 1.05 pu, as shown in Table 2.7. The percentage voltage difference ranges from -0.01% to +1.00 %, and the voltage difference was reduced at Aja (0.01%), Alagbon (0%), Gombe (0%), and Lekki (0%), compared to the original load flow. The loads that were added to the winter scenario were Aja (122.95 MW), Alagbon (134 MW), Lekki (133.50 MW), and Makurdi (133.50 MW). The summary of the winter load flow is given in Table 2.6.

Table 2.6: Summary of load flow results (Winter).

	NESO Data			**Load Flow Data**		
	P (MW)	Q (MVAR)	S (MVA)	P (MW)	Q (MVAR)	S (MVA)
Generator	3850	-206	3856	4395	-149	4397
Load	3775	1741	4157	4299	1785	4654
Losses	75.65			95.97		
Compensation		975			971	

Table 2.7: Winter voltage profile.

		NESO Data		**Load flow result**		
Bus No	**Bus**	**Volt (kV)**	**pu**	**Volt (kV)**	**pu**	**% Diff**
1	Adiabor	333	1.01	333	1.01	0.00
2	Afam	NR	-	331	1.00	-1.00
3	Aja	316	0.96	315	0.95	0.01
4	Ajaokuta	339	1.03	341	1.03	0.00
5	Akangba	314	0.95	316	0.96	0.01
6	Aladja	NR		343	1.04	-1.04
7	Alagbon	314	0.95	314	0.95	0.00
8	Alaoji	330	1.00	329	1.00	0.00
9	Asaba	NR	-	334	1.04	-
10	Ayede	320	0.97	320	0.97	0.00
11	Azura	NR	-	330	1.00	-1.00
12	Birnin-kebbi	319	0.97	319	0.97	0.00
13	Benin	337	1.02	337	1.02	0.00
14	Damaturu	NR	-	-	-	-
15	Delta	344	1.04	343	1.04	0.00
16	Egbin	332	1.01	332	1.01	0.00
17	Ganmo	331	1.00	330	1.00	0.00

18	Geregu	NR	0.00	340	1.03	-1.03
19	Gombe	318	0.96	317	0.96	0.00
20	Gwagwalada	338	1.02	337	1.02	0.00
21	Ibom	NR	-	335	1.01	-1.01
22	Ihovbor	NR	-	338	1.02	-1.02
23	Ikeja West	319	0.97	316	0.96	0.01
24	Ikot-Epene	333	1.01	334	1.01	0.00
25	Jebba G. S	332	1.01	333	1.01	0.00
26	Jebba T. S	335	1.02	333	1.01	0.01
27	Jos	328	0.99	328	0.99	0
28	Kaduna	332	1.01	332	1.01	0
29	Kanji G. S	336	1.02	336	1.02	0
30	Kanji T. S	NR	-	330	1.00	1.00
31	Kano	320	0.97	321	0.97	0
32	Katampe	334	1.01	334	1.01	0
33	Lekki	315	0.95	314	0.95	0
34	Lokoja	342	1.04	342	1.04	0
35	Markurdi	332	1.01	333	1.01	0
36	Molai	NR	-	0	0.00	0
37	New.Haven	334	1.01	333	1.01	0
38	Odukpani	NR	-	333	1.01	-1.01
39	Oke-Aro	320	0.97	323	0.97	0
40	Okpai	335	1.02	337	1.02	0
41	Olorunsogo	319	0.97	320	0.97	0
42	Omaku	NR	-	330	1.00	-1.00
43	Omotosho	339	1.03	339	1.03	0
44	Onitsha	334	1.01	334	1.01	0
45	Osogbo	326	0.99	326	0.99	0
46	ParasEnergy	NR	-	332	1.01	-1.01
47	River	NR	-	330	1.00	-1.00
48	Sakete	318	0.96	317	0.95	0.01
49	Sapele	342	1.04	340	1.03	0.01
50	Shiroro	335	1.02	335	1.01	0.01
51	Trans Amadi	NR	-	330	1.00	-1.00
52	Ugwuaji	330	1.00	333	1.01	-0.01
53	Yola	316	0.96	317	0.96	0

2.5 Conclusion

Based on system data provided by the Nigerian Electricity system operator (NESO), a PowerFactory model of the Nigerian 330 kV transmission system was created, and two load flow scenarios were examined. The first iteration of these studies contained some discrepancies with the available data and some load flow violations. Therefore, assumptions and modifications were made to improve the results and to make the system model more accurate and reliable. From the load flow results, the power generated in the summer is higher than that generated in the winter because of the higher summer demand, driven mainly by air conditioners. Moreover, during the winter, the weather is stormy; this is when the distribution companies demand a low load due to the tripping of the weak feeders.

The model presented in this chapter will be used to carry out specialist studies to address the impact of HVDC technology on the Nigerian transmission system. More specifically, research on system reliability and stability studies will be conducted, and the best locations for HVDC links will be identified.

3 Reliability Analysis

3.1 Introduction

Reliability is the ability of a system to perform its required functions under stated conditions for a specified period. [86]. A power system works to satisfaction if it does not fail during its service life; nonetheless, failures and repairs are common during a system's useful life. Therefore, the electric utility's objective is to provide electricity to satisfy its customers' needs and expectations, which is expected to be achieved at a reasonable level of reliability and as economically as possible [19], [34], [35], [87], [88].

When the total system failure is minimized, the reliability of the power network is expected to improve, and system operation is optimised and enhanced [89]. Facilities within the system to satisfy the consumer demand are adequate if all the system requirements (Load, voltage, var, etc.) are fully satisfied, and they are inadequate if any of the system constraints are violated. Moreover, power system reliability evaluation is essential for studying the current system, identifying weak points, and determining what enforcement is needed to meet future demand [35], [90].

In practice, reliability is assessed through various indices; the most used are the System Average Interruption Frequency Index (SAIFI), System Average Interruption Duration Index (SAIDI), Customer Average Interruption Duration Index (CAIDI), and Average Service Availability Index ASAI [91]. SAIDI measures the length of power outages during a particular year, while SAIFI records the frequency. The average amount of time needed to provide service to the typical customer after a sustained interruption was measured by CAIDI [90], [92]. These typical values will be used in this research for each index provided by the IEEE Standards 1366-2012, where the Nigerian transmission network will be evaluated using DigSILENT PowerFactory to provide qualitative analysis for system operation and planning [89], [91]. The value obtained will be used as a guide to verify if the system meets standard requirements or not, and the reliability index will be used to identify the low-reliability load point on the transmission network. This study will evaluate the best location of high voltage direct current

The majority of the work presented in this chapter has been published in [9].

(HVDC) links in Nigeria's transmission network to improve the voltage profile and reduce losses.

This research will offer important information about implementing HVDC technology in Nigeria's transmission system by carefully analysing variables, including load points and system indices. The overall goal is to assist in constructing a more stable and reliable power system that can satisfy the country's expanding demand for energy while assuring a steady and adequate supply of electricity.

3.2. Reliability performance in various countries

The reliability indices for some countries are discussed briefly in this section, based on results from the literature review. These results provide a reference and illustrate the different performances of power systems in various world regions.

In Algeria, the Commission for Electricity and Gas Regulation CREG uses SAIFI, SAIDI, and AIT to describe the state of operation of the electrical power supply system and consumer equipment. Table 3.1 gives an overview of the transmission grid achievements for the reliability indices for 2011-2014 [93].

Table 3.1: Values of reliability indices in Algeria.

Indices	2011	2012	2013	2014
SAIFI (number/yr/customer)	1.82	2.3	1.8	1.4
SAIDI (min/yr/customer)	81	77	59	45
AIT (min/yr)	47	77	45	39

Table 3.2 shows the value of the indices obtained in the transmission system in some European countries from 2007 to 2010. The United Nations Interim Administration Mission in Kosovo (UNMIK) has the highest Energy Not Supply (ENS), and Croatia has the highest Average Interruption Time (AIT). According to the Council of European Energy Regulators (CEER), ‘‘ENS provides a better indication of an interruption on EHV/HV than the indices SAIFI or SAIDI’’ [94].

Table 3.2: AIT and ENS indices for transmission system.

AIT (h/yr) (Transmission)				
Country/year	2007	2008	2009	2010
Croatia	18.8	19.5	54.6	25.4
Serbia	-	-	3.89	24.73
UNMIK	714	690	771	230
ENS (MWh/a) (Transmission)				
Croatia	630	666	1840	-
Serbia	-	-	2508	-
UNMIK	11470	11166	11462	-

In Australia, the National Electricity looked at the performance relative to a target set for 2004/05, and the average reliability achieved over the previous five years is given in Table 3.3. From the table, overall performance in Australia during 2004/2005 was similar to or better than the targets established for interruption frequency and duration. However, some regions may have somewhat exceeded their targets.

Table 3.3: Australia target and actual indices for 2004/2005 [95]**.**

Energy Australia	**SAIDI (hrs) Target**	**SAIDI (hrs) Actual**	**SAIFI Target**	**SAIFI Actual**
Central Coast	4.38	3.8	3	2.7
Maitland	4	4.1	4	2.7
Muswellbrook	4.03	3.65	4	2.6
Newcastle	1.67	1.97	2	1.3
Sydney East	0.48	0.57	1	0.4
Sydney North	2.07	2.85	2	1.9
Sydney South	0.83	0.93	1	0.8

A reliability simulation was carried out on Electrical Transient Analyzer Program (ETAP 16.0.0) software on Maharashtra 400 kV and 765 kV transmission systems in India, and the SAIFI and SAIDI for some of the lines are presented in Table 3.4 [56]. This index created a reliability assessment framework during transmission planning to ensure system security, robustness, and reliability [96].

Table 3.4: SAID and SAIFI in India.

Name of Line	**SAIDI (hrs/month)**	**SAIFI (interruption/month)**
Aurangabad-Boisar 1	78.767	1.500
Aurangabad-Boisar 2	94.613	1.167
Bhableshwar-Aurangabad	0.272	0.167
Bhableshwar- Padghel 1	0.402	0.500
Bhableshwar- Padghel 2	0.572	0.330
Bhableshwar- ParaliPG1	16.298	1.500

In Oman (Western Asia), the calculated system reliability indices SAIFI, SAID, AIT, and ENS were used to measure future targets to improve the transmission system performance. The results obtained for three years are shown in Table 3.5 [97].

Table 3.5: ENS, AIT, SAIFI, and SAIDI for Oman.

Indices	2006	2007	2008
ENS(MWh/yr)	1995	2028	2080
AIT (min/yr)	96.91	93.66	79
SAIFI (interruption/month)	-	0.02	0.094
SAIDI (hrs/month)	-	2.12	19.98

The reliability indices of Nairobi are given in Table 3.6. They were measured over a year following IEEE Standard 1366-2003 [98] and compared to Nairobi South and Nairobi West; Nairobi North Country had the highest SAIDI and SAIFI values, indicating longer and more frequent power outages. Nairobi South had the lowest SAIDI and SAIFI values of the three regions, indicating more reliability regarding interruption duration and frequency.

Table 3.6: Nairobi County power reliability indices for the year 2020.

Country	SAIDI	SAIFI	CAIDI
Nairobi North Country	13.1	5.1	2.6
Nairobi South Country	10.7	3.6	3
Nairobi West Country	10.7	4.8	2.2

In the United Kingdom, National Grid Electricity Transmission (NGET) measured the transmission system reliability and the reliability of supply between 2017 and 2020, and the system performance report is given in Table 3.7 [99], [100]. The national electricity transmission system remained steady during these periods despite variance in the stated reliability numbers. This consistency indicates that the system's high level of reliability has been maintained throughout time due to the lack of significant performance changes. In 2018/2019 and 2019/2020, the 99.999967% reliability percentage remains constant.

Table 3.7: Reliability of supply for the national electricity transmission system.

Year	Reliability
2017/2018	99.999975%
2018/2019	99.999967%
2019/2020	99.999967%

Table 3.8: Egypt reliability indices for transmission system and sub-transmission networks.

Index	2002/2003	2003/2004	2004/2005	2005/2006
SAIFI (interruption/month)	0.09	0.12	0.09	0.06
SAIDI (hrs/month)	1.85	1.44	0.62	0.53
SARI (minutes)	21	12.3	7	9.50
SISI (minutes)	16.84	10.1	-	12.31

The reliability of the electricity supplied by the Egyptian Transmission Company through a list of predetermined delivery points to the transmission system and sub-transmission networks was assessed in terms of SAIFI, SAIDI, System Average Restoration Duration Index (SARI), and System Average Interruption Severity Index (SISI). The results are given in Table 3.8. These values were utilised to pinpoint the network's weak points and provide pertinent advice for reinforcement and extension plans [101].

On the other hand, a distribution system reliability study was conducted on Nigeria's distribution network to create a system planning strategy as one of the primary mitigation techniques for increased distribution network protection and reliability. The reliability assessment of a 33 kV feeder that supplies power to Kaura-Namoda, Zamfara State, Nigeria, was examined using the reliability index SAIFI, SAIDI, CAIDI, and ASAI as tools.

The results are 18.699 interruptions per year, 30.13 hours per year, 1.61 hours, and 99.66%, respectively [102]. The results of this research are expected to be different since the transmission network's reliability was only assessed.

Overall, [103] provides reference values for the network reliability indices, shown in Table 3.9 to provide a reference, although this standard may not be applied in all countries under consideration.

Table 3.9: Reliability indices compared with the IEEE standard 1366 [103].

Index	SAIDI (h/yr)	SAIFI (interruption/yr)	CAIDI (h)	ASAI %
IEEE Standard 1366	1.5	1.1	1.36	99.9999
India	0.27	0.17	1.62	-
Algeria	45	1.4	-	-
Egypt	1.27	0.09	14.11	-
Kenya	11.5	4.5	2.6	-
USA	4.08	1.49	2.05	99.91
UK	1.5	0.8	1.67	99.96
Australia	0.93	0.8	1.16	-

Table 3.9 summarizes the reliability results from the literature. Reliability indices for the USA, UK, and Australia are also included [103] to provide a reference with Western countries. It is worth observing that Egypt's reliability is close to that of other Western countries. In contrast, for different regions in the African continent, reliability is generally much lower.

According to these countries, the literature review shows that reliability is essential in power system planning, and the countries use different indices to measure their reliability, which is independent. However, it is challenging to study because a lot of data is required, and fault data could be one of the most difficult tasks to obtain.

3.3. Evaluation techniques

Reliability evaluation of a complete power system, including generation, transmission, and distribution, is often not conducted due to the system size. Therefore, the reliability of transmission systems and distribution network segments is assessed independently [25].
A single reliability technique does not exist, but the approach and resulting formulae depend upon the problem and the assumptions made [104].

Reliability models can be divided into two categories, namely deterministic (absence of randomness) and stochastic (random) models. Deterministic models are usually expressed in terms of differential equations, together with the initial and boundary conditions, which precisely predict the development of a system. In contrast, stochastic models are given by random variables whose outcomes are uncertain and can only compute the probability distribution of possible outcomes [105].

Stochastic modelling is a mathematical technique that considers random variables and probabilistic events. Unlike deterministic models with predetermined outcomes, stochastic models use random variables to simulate various scenarios. These models are essential for determining systems' behavior, evaluating risk, and making valuable decisions. Stochastic models provide probability distributions that characterise the likelihood of various outcomes, which help to inform decision-making. This modeling technique is beneficial when evaluating the probability of system reliability under multiple circumstances. Random variables are used as inputs in a stochastic simulation model, producing random outputs. The outputs can only be regarded as estimations of the genuine features of a model due to their randomness. Therefore, in a stochastic simulation, output measures must be treated as statistical estimates of the actual characteristics of the system. By making assumptions about the random

component of a model, stochastic models allow the validity of the hypotheses to be tested statistically [106], [107], [108], [109]

This method is thought to be more suitable due to the higher accuracy of the results that can be obtained. As a result, a reliability assessment based on statistical analysis methods will be more appropriate for this research [110]. Based on the data provided by the Nigerian transmission system operator, a stochastic model will be used, and the statistical analysis method will be adopted.

3.4 Reliability indices

The results of the reliability evaluation are referred to as "reliability indices" [111]. These indices produce load point and system indices (frequency and energy indices). The load point indices measure the expected number of outages and their duration for individual customers. In contrast, the system indices measure the system's reliability as a whole and can be used to compare the effects of different design and maintenance strategies on the system's reliability [65], [112]. These indices work better together than separately. The load-point indices reveal the reliability of specific buses, while the system indices evaluate the overall sufficiency [35].

Reliability indices typically consider aspects such as the number of customers, the connected load, the duration of the interruptions or faults measured in seconds, minutes, hours, or days, the amount of power (kVA) interrupted, and the frequency of interruptions or faults [92]. The main reliability indices will be defined in the next sections.

3.4.1 Load point indices

The load point indices measure the expected number of outages and the duration of these outages for individual customers on each bus bar. The load indices are the areas of the system that are inadequate and prone to interruptions. The load point indices considered in this research are Load Point Interruption Frequency (LPIF) and Load Point Interruption Time (LPIT). These load point indices can be used to identify weak points in a system and are helpful for a system designer [65], [113] and they are defined as follows:

$$\text{LPIF} = \sum_{k} Fr_k \qquad \text{Unit: } 1/\text{yr} \tag{3.1}$$

$$\text{LPIT} = \sum_{k} 8760 * Pr_k \qquad \text{Unit: h/yr} \tag{3.2}$$

where Fr_k is the frequency of occurrence of contingency k and

Pr_k is the probability of occurrence of contingency *k*.

3.4.2 System indices

These provide a measure of global adequacy that can be used to compare the performance of one system to that of another and are used to track the performance of a region or a circuit. These reliability indices are commonly used to quantify the performance of the systems [113], [114]. In this research, SAIFI, SAIDI, CAIDI, and ASAI are used to measure the performance of the network:

- SAIFI: System Average Interruption Frequency Index (interruptions/year). This index measures the number of interruptions customers experience each year with the total number of customers on the network [95], and it is expressed as follows:

$$\text{SAIDI} = \frac{\sum \text{ACIF}_\text{i} * \text{C}_\text{i}}{\sum \text{C}_\text{i}} \qquad \text{Unit: interruption/yr} \tag{3.3}$$

  where ACIF_I is the Average Customer Interruption Frequency, and C_i is the number of customers supplied by load point i (customers on a particular bus bar).
- SAIDI: this stands for System Average Interruption Duration Index (hours per year). This index captures the duration of power outages each year [91] and is measured in time units, often minutes or hours. A high SAIDI value is alarming since it suggests that consumers are experiencing lengthy periods of power interruptions, which is not good news [115]. This is given in equation 3.4 [95]. SAIDI is the average time each customer was without electricity each year.

$$\text{SAIDI} = \frac{\sum \text{ACIT}_\text{i} * \text{C}_\text{i}}{\sum \text{C}_\text{i}} \qquad \text{Unit: h/yr} \tag{3.4}$$

where $ACIT_i$ is the Average Customer Interruption Time.

- CAIDI: Customer Average Interruption Duration Index (h). This index expresses the average time required to restore service, and the expression is given in equation 3.5 [116].

$$\text{CAIDI} = \frac{\text{Sum of customer interruption duration}}{\text{Total number of customer}} = \frac{\text{SAIDI}}{\text{SAIFI}} \quad unit: h \tag{3.5}$$

- ASAI: Average Service Availability Index; this represents the fraction of time that a customer is connected during the defined calculation period, as shown in the expression in equation 3.7. It is often calculated in percentages, and a better value for ASAI is having more than three 9's [91], [116].

$$\text{ASAI} = 1 - \text{ASUI}\ (\%) \tag{3.6}$$

where

$$\text{ASUI} = \frac{\sum \text{ACIT}_i * C_i}{\sum C_i * 8760} \tag{3.7}$$

3.5 Reliability analysis methodology

The reliability of the Nigerian transmission system was carried out in PowerFactory (PF). In this project, forced outage data was obtained from the Nigerian Electricity System Operator (NESO), which consists of the time of occurrence of a fault, duration of fault (hr), and restoration time. The connected load at each bus bar was also provided in MW, but the number of connected customers was not given. Therefore, the number of customers connected at each bus bar was calculated, as shown later. The data was used to compute the reliability indices (SAIDI, SAIFI, CAIDI, and ASAI) using equations 3.1 to 3.7.

3.5.1 Network model and HVDC model

The first step in the reliability assessment was to build a model of the Nigerian transmission network (Figure 2.1), which includes electrical parameters and reliability data provided by the Nigeria Electricity System Operator (NESO). Where data were lacking, assumptions were made to calculate the number of customers connected to each busbar. The load flow results are presented in Chapter 2. Additionally, a generic HVDC model was built separately (Figure 3.1) – this model will then be connected to the network at the locations with lower reliability, as explained in a later section.

Outage data consists of the time of occurrence of a fault, fault duration in hours, and restoration time. The total connected load at each bus bar was also provided in MW, but the number of connected customers was not given. Because this quantity is required for reliability assessment, the number of customers connected at each bus bar was calculated as shown in section 3.5.3.

Initially, the network was modelled using the data provided by the NESO to calculate the reliability, and based on the reliability result, the HVDC location was determined. The HVDC was modelled and then connected to the network to test for reliability improvement.

3.5.2 Repair Duration (RD) and Failure Frequency (FF) computation

The data provided by the NESO for the reliability study include the time of occurrence of faults (including planned and unplanned outages), the restoration time, the number of outages (NO), and the fault duration (FD). This data was provided for each month in 2019 (January to December) and for each line. The FD and the NO, however, could not be applied directly in the study but were used to determine the Mean Time to Repair (MTTR), also known as Repair Duration (RD), and the Failure Frequency (FF), as required by PF to run the reliability analysis.

It was necessary to calculate two intermediate quantities: the Total Fault Duration, TFD (i.e., the cumulative fault duration across the entire year), and the Total Number of Outages, TNO (i.e., the cumulative number of outages in the whole year). Once TFD and TNO were known, each line's MTTR and FF were obtained according to the equations below [65], [88]. These were determined using the following equations:

$$\text{Repair duration(RD)} = \frac{\text{Total fault duration (TFD)}}{\text{Total no of outages (TNO)}} \quad \text{unit: hr} \tag{3.8}$$

$$\text{Failure frequency(FF)} = \frac{\text{Total no of outages(TNO)}}{\text{Line length}} \quad \text{unit: } 1/(\text{yr. km}) \tag{3.9}$$

3.5.3 Number of customers' computation

The reliability indices SAIFI and CAIDI are evaluated based on the number of customers interrupted. Since NESO did not provide the number of customers, some assumptions were made based on the literature review. According to [117], the average number of residential customers connected to an 11/0.415 kV distribution transformer of 500 kVA in Nigeria is 268. In typical operation, the transformer does not always operate at full load conditions. In this study, it is assumed that the transformer is 80% loaded.

Based on the above, the following rating is assigned to each customer:

$$S_{Customer} = \frac{500 \times 0.8}{268} = 1.49 \text{ kVA} \tag{3.10}$$

The number of connected customers (N_{OCC}) on a load bus bar is then calculated using the following equation:

$$N_{OCC} = \frac{\text{Load(MVA)}}{\text{S}_{\text{customer (kVA)}}} \quad (3.11)$$

The NESO only provided the active power demand for each load. The apparent power of each load was calculated in Appendix A.0.1. The number of connected customers for Aja was calculated using equation 3.12, as shown below:

$$N_{OCC} = \frac{202.76 \times 10^6 \text{ VA}}{1.49 \times 10^3 \, VA} = 136082 \quad (3.12)$$

The same approach was applied at all busbars for both scenarios (summer and winter), with the resulting number of connected customers shown in Table 3.10.

Table 3.10: N_{OCC} for the two scenarios.

	Summer			Winter		
Bus	**P (MW)**	**S (MVA)**	N_{OCC}	**P (MW)**	**S (MVA)**	N_{OCC}
Aja	162.70	202.76	136082	123.41	123.41	382826
Alagbon	162.00	178.52	119811	135.03	143.99	96638
Alaoji	414.70	426.69	286372	330.60	403.17	270584
Ayede	208.01	209.47	140581	230.0	237.04	159090
Birnin-kebbi	198.00	198.02	132899	187.0	202.15	135669
Benin T. S	132.92	179.60	120536	170.90	195.43	131164
Ganmo	80.03	80.00	53691	122.0	122.61	82291
Gombe	154.01	156.89	105299	116.0	153.28	102872
Ikeja West	1135.0	1152.56	773529	1102.0	1305.86	876417
Jebba T. S	14.05	14.07	9443	21.00	22.14	14856
Jos	80.02	101.81	68331	54.0	67.18	45089
Kaduna	176.0	176.00	118121	102.0	102.00	68456
Kano	277.0	277.00	185906	199.0	199.00	133557
Katampe	465.0	482.83	324047	381.10	390.90	262352
Makurdi	161.96	208.11	139673	135.23	135.23	90758
New Haven	100.0	101.19	67913	170.00	230.22	154507
Onitsha	141.5	152.13	102104	168.0	196.37	131792
Osogbo	167.0	195.09	130930	162.60	198.04	132915
Sakete	226.0	228.00	153018	54.0	59.68	40055
Sapele	64.14	79.94	53652	74.40	74.91	50278
Shiroro	61.60	61.80	41479	88.0	88.57	59444
Yola	73.05	77.49	52008	42.0	52.50	35233
Lekki	0.00	0.00	0	135.03	135.03	90624
Total	4654.46	4939.98	3315425	4303.30	4838.73	3547467

3.5.4 HVDC model and control

The model of a VSC-HVDC was built in PowerFactory based on typical values found in some literature. The VSC-based technology was chosen because it represents the future of HVDC interconnectors. In the rest of the research, this technology will be called 'HVDC' to simplify the notation. This model will be integrated into the network, depending on the locations informed by the reliability and stability study. The baseline model will be maintained, while other parameters, such as the power set point and the line length, will be adapted for the location(s) under study.

An overview of the model is shown in Figure 3.1. A bipolar configuration was adopted because it is the most common [69], [118]. The bipolar configuration consists of two independent DC circuits, where each circuit can draw half of the rated power. The ground return electrode carries minimal current in this configuration (compared to the monopolar one), which is not shown in Figure 3.1 for simplicity. One advantage of the bipolar configuration, in the context of this study, is that it can operate by delivering part of the rated power in the event of maintenance or outage of one of the two lines, as the other half of the system continues to supply power. A bipolar topology was considered for this model because it is widely used for long-distance HVDC transmission projects, particularly where high power transfer capacity is required [70].

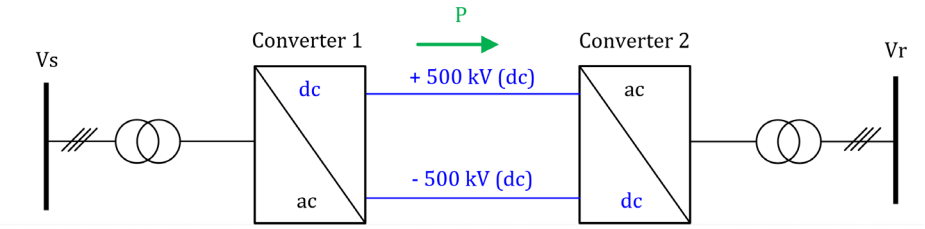

Figure 3.1: VSC-HVDC single-line diagram.

Different HVDC control modes govern and manage the functioning of HVDC transmission networks. These control modes aim to preserve the HVDC system's reliable and effective functioning while achieving specific goals [119]. One of the goals is to keep the voltage and current within acceptable parameters to avoid instability. The objectives also include controlling the power transferred between interconnected grids to maintain a balanced power system and satisfy demand. The control scheme regulates the active power flow from the AC grid to the DC grid and manages the DC voltage to maintain a defined reference level. It also delivers the necessary reactive power to the alternating current mains. This control system

comprises two controllers: one for regulating DC voltage and one for managing current flow [120].

The DC voltage control can be explained with the equations below. The reference currents (I_d, I_q) are achieved by the DC voltage controller from the reference real power and reference DC voltage, as given below.

$$I_d^* = \left(\frac{P^*}{V_s}\right) + K_v\,(V_{dc}^* - V_{dc}) \tag{3.13}$$

$$I_q^* = 0 \tag{3.14}$$

where P^* is the reference real power to be transmitted across the HVDC, V_s is the supply voltage, K_v is the proportional gain constant, and V_{dc}^* is the reference DC voltage. Reference reactive current (I_q) is taken as zero to maintain the unity power factor.

The reference currents (I_d^*, I_q^*) from the DC voltage controller are fed into the AC controller, which provides reference voltages (V_d^*, V_q^*) to the PWM block. The operation of the current controller is expressed as follows in the Laplace domain:

$$V_d^* = V_d - \left(R \cdot I_d + sL \cdot I_q\right) - (K_p + K_i/s)\,(I_d^* - I_d) \tag{3.15}$$

$$V_q^* = V_q - \left(R \cdot I_q + sL \cdot I_q\right) - (K_p + K_i/s)\,(I_q^* - I_q) \tag{3.16}$$

In this work, the sending end converter was set to control the DC voltage (V_{dc}) either with the reactive power (Q) or the phase angle ($\text{Cos}\emptyset_2$) while the receiving end converter was set to control the active power (P) and either the voltage magnitude (V_{ac}) or reactive power (Q). As a result, four different variable combinations can be identified for each converter (V_{dc}-Q, P-V_{ac}, P-Q, and V_{dc}- $\text{Cos}\emptyset_2$). This led to the definition of four HVDC control modes to be used in this project:

I. V_{dc}-Q/P-V_{ac}: the sending end converter controls V_{dc} and Q; the receiving end converter controls P and V_{ac}.
II. V_{dc}- $\text{Cos}\emptyset_2$/P-V_{ac}: the sending end converter controls V_{dc} and $\text{Cos}\emptyset_2$ while the receiving end converter P and V_{ac}.
III. V_{dc}- $\text{Cos}\emptyset_2$//P-Q: the rectifier controls V_{dc} and $\text{Cos}\emptyset_2$ and the inverter controls P and Q.
IV. V_{dc}-Q/P-Q: the rectifier controls V_{dc} and Q, while the inverter reference output is P and Q [121].

The main electrical parameters for the HVDC model are listed in Table 3.11 [122]. The DC voltage level was ±500 kV based on values for other global HVDC systems [123].

Table 3.11: Electrical parameters of the HVDC model in PF.

Parameters	Values
Rated DC voltage	±500 kV
Converter-rated power	500 MVA
Rated AC voltage	330 kV
Topology	Bipolar
Short circuit impedance	10%
Copper losses	25 MW

The model of an HVDC (Figure 3.1) was built separately to be integrated into the Nigeria transmission system. For reliability studies, control mode I (Converter 1 controlled in $V_{dc}-Q$ mode, Converter 2 controlled in $P-V_{ac}$ mode) was used [121]. This fixed control mode is sufficient because the power flow is unidirectional in the system under consideration, as shown in Figure 3.1. When this model is deployed, Converter 1 is connected to the sending end (with voltage *Vs*), while Converter 2 is connected to the receiving end (with voltage *Vr*), where the loads are located [124], [125], [126].

PF does not allow input reliability values for some components, such as the converters. Therefore, the overall HVDC reliability was modelled in the AC line connecting the sending end to the converter transformer. Since this component is modelled in series to the rest of the system, failure of the AC line will result in overall HVDC failures, thus allowing it to represent the intended behaviour correctly. This approach may need to be revised for future and more detailed reliability studies.

The main electrical parameters for the HVDC model are given in Table 3.11, and the primary control and reliability parameters are listed in Table 3.12 [122].

Table 3.12: Control and reliability parameters of the HVDC model in PF.

Parameters	Values
dc voltage setpoint	1 pu
ac voltage setpoint	1 pu
Reactive power setpoint	0 MVAR
Active power setpoint	(to be set based on the location)
Failure frequency	3 (1/yr)
Repair duration	5 hours

3.6 Reliability study results

This section presents the reliability study results, starting with the reliability indices for the overall network and then describing load point indices at various locations.

3.6.1 System indices

SAIDI, SAIFI, CAIDI, and ASAI were used to evaluate the transmission network's reliability. These parameters were calculated according to equations 3.3 - 3.6. The results are summarized in Table 3.13. During the winter, SAIDI is equal to 0.872 hr/yr, thus indicating a better performance than in the summer. This result can be explained by observing that, generally, the faults are cleared earlier in the winter (dry season) than in the summer (rainy season) when the weather is stormy and windy. Also, during the summer, power interruptions are more prolonged due to increased demand and the vulnerability of transformers or overhead lines. High temperatures and sudden peaks in energy demand also contribute to more extended downtime and higher SAIDI values.

The summer has a higher value of SAIFI (0.811 vs 0.404 in the winter), which means that the frequency of interruptions is higher. It can be explained by observing that heavy storms will cause trees to fall and land on transmission lines, posing leakages to the earth. When this occurs, transmission lines will trip and cause a short circuit because transmission lines run for several kilometres, and many of these lines are in forest areas [127]. This situation is aggravated by observing that isolators and fuses fail more often during the summer than winter, thus increasing overall system failure. In summer, electricity demand increases; this stresses the networks and increases the likelihood of interruptions due to weather conditions like thunderstorms and high temperatures.

A CAIDI value of 2.16 implies that there was no supply of electricity for 2.16 hours every day for the whole year; this means that, on average, it takes 2.16 hours to restore the power supply whenever there is an interruption or system failure. This value can be explained by observing that SAIDI and SAIFI are used numerators and denominators for CAIDI calculations. As the number of customers experiencing prolonged outages decreases, the denominator (SAIDI) of the CAIDI index decreases relative to the value of the numerator (SAIFI), and the overall index rises [128]. This result indicates that interruptions last longer in the winter than in summer. They occur less frequently (0.4037 interruptions/yr), increasing the average duration of interruptions per interruption event (CAIDI) in the winter. The value of ASAI was 99.98% for both scenarios. Although this number appears high, it is still below the standard value of 99.9999% [116].

Table 3.13: Base case reliability indices result for the Nigerian transmission system.

Index	SAIDI (h/yr)	SAIFI (interruption/yr)	CAIDI (h)	ASAI %
Summer	1.441	0.811	1.779	99.983
Winter	0.872	0.404	2.160	99.989

3.6.2 Manual calculation

In this section, system reliability indices were calculated manually and compared with the PF results. This process was carried out to confirm the simulation results' validity and demonstrate that, for radial feeders, reliability can be calculated easily by applying the formulae presented in Section 3.3. The summer scenario was used for this validation.

To manually calculate system indices, the following data is required: TNO, TFD, and N_{OCC} . The values used are summarized in Table 3.14, and detailed calculations will be carried out in the following subsections. It was assumed that three radial feeders possess low reliability compared to the rest of the system, which is highly interconnected. The three radial feeders are labelled as A, B, and C in Figure 3.2. As a result, the indices of each radial feeder were calculated, and the results were combined and compared with the results obtained from PF.

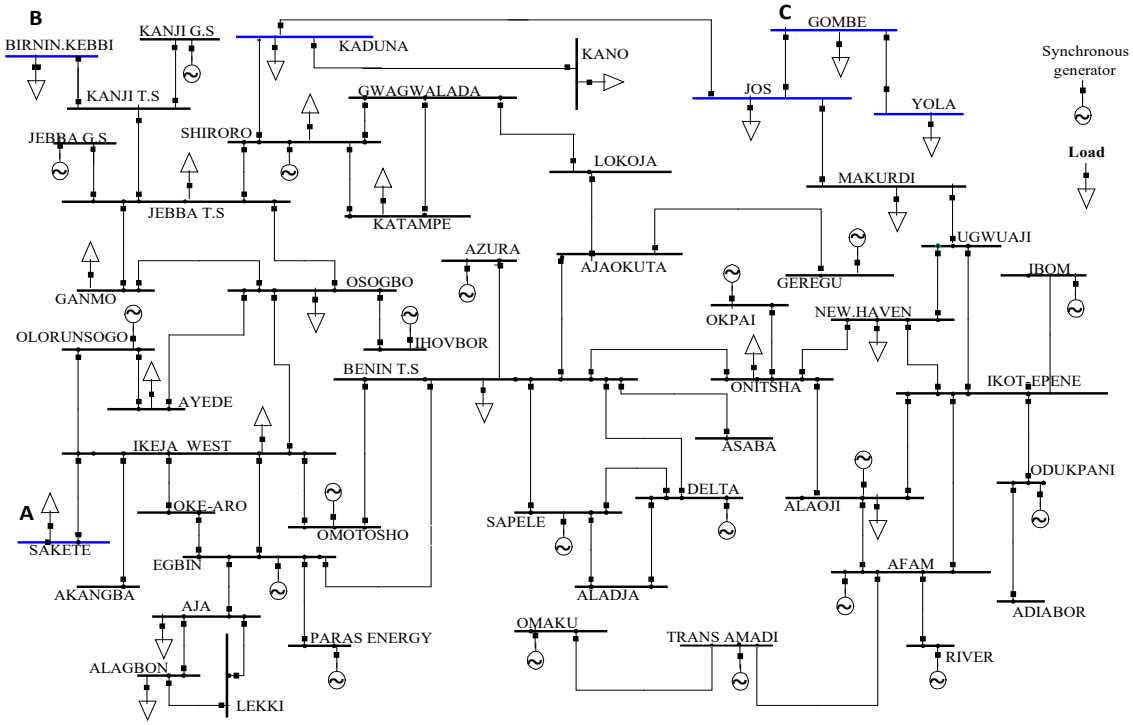

Figure 3.2: Single-line diagram of the Nigerian 330 kV transmission network highlighting the radial feeders (A, B, C).

Table 3.14: Line data for manual reliability (summer scenario).

Line	TNO	TFD (h/a)	N_{OCC}
Jos ↔ Gombe	2	0.50	Gombe: 105299
Gombe ↔ Yola	6	2.99	Yola: 52008
Birnin Kebbi ↔ Kanji	4	17.14	Birnin Kebbi: 132899
Sakete ↔ Ikeja West	10	14.82	Sakete: 153018

- **SAIFI calculation**

The SAIFI calculation for each radial feeder was carried out below, where the symbol '↔' indicates a line. It is worth noticing that for the radial feeder C, the calculation requires considering the total line length of the load from Yola to Jos, and this is why there is an additional term compared to the other two feeders:

$$A_{SAIFI} = N_{OCC,Sakete} \times NO_{Sakete \leftrightarrow Ikeja} \tag{3.17}$$

$$A_{SAIFI} = 153018 \times 10 = 153018 \text{ (interruption/yr)} \tag{3.18}$$

$$B_{SAIFI} = N_{OCC,BirninKebbi} \times NO_{BirninKebbi \leftrightarrow Kanji} \tag{3.19}$$

$$B_{SAIFI} = 132899 \times 4 = 531596 \text{ (interruption/yr)} \tag{3.20}$$

$$C_{SAIFI} = N_{OCC,Gombe} \times NO_{Jos \leftrightarrow Gombe} + N_{OCC,Yola} \times NO_{Jos \leftrightarrow Gombe} + N_{OCC,Yola} \times NO_{Gombe \leftrightarrow Yola} \tag{3.21}$$

$$C_{SAIFI} = 105299 \times 2 + 52008 \times 2 + 52008 \times 6 = 626662 \text{ (interruption/yr)} \tag{3.22}$$

SAIFI is then calculated by adding the terms calculated above (equation 3.18, 3.20, and 3.22) and dividing by the total number of customers (Tc) from Table 3.10:

$$SAIFI = \frac{A_{SAIFI} + B_{SAIFI} + C_{SAIFI}}{T_C} \tag{3.23}$$

$$SAIFI = \frac{(153018 + 531596 + 626662)}{3315425} = 0.811 \text{ interruption/yr} \tag{3.24}$$

- **SAIDI Calculation**

Similarly to the approach described in the previous section, three intermediate quantities are calculated based on the N_{OCC} and the FD:

$$A_{SAIDI} = N_{OCC,Sakete} \times FD_{Sakete \leftrightarrow Ikeja} \tag{3.25}$$

$$A_{SAIDI} = 153018 \times 14.82 = 226773 \text{ (h/yr)} \quad (3.26)$$

$$B_{SAIDI} = N_{OCC,BirninKebbi} \times FD_{BirninKebbi \leftrightarrow Kanji} \quad (3.27)$$

$$B_{SAIDI} = 132899 \times 17.14 = 227789 \text{ (h/yr)} \quad (3.28)$$

$$C_{SAIDI} = N_{OCC,Gombe} \times FD_{Jos \leftrightarrow Gombe} + N_{OCC,Yola} \times FD_{Jos \leftrightarrow Gombe} + N_{OCC,Yola} \times FD_{Gombe \leftrightarrow Yola} \quad (3.29)$$

$$C_{SAIDI} = 105299 \times 0.5 + 520081 \times 0.5 + 520081 \times 2.99 = 234157 \text{ (h/yr)} \quad (3.30)$$

SAIDI is determined by adding all the terms above (equations 3.26, 3.28, and 3.30):

$$SAIDI = \frac{A_{SAIDI} + B_{SAIDI} + C_{SAIDI}}{T_C} \text{ (h/yr)} \quad (3.31)$$

$$SAIDI = \frac{(226773 + 227789 + 234157)}{3315425} = 1.442 \text{ (h/yr)} \quad (3.32)$$

- **CAIDI and ASAI calculation**

Applying equations 5 and 6, respectively, CAIDI and ASAI were determined and are obtained in equations 3.33 and 3.35, respectively:

$$CAIDI = \frac{SAIDI}{SAIFI} = \frac{1.442}{0.811} = 1.778 \text{ (h)} \quad (3.33)$$

$$ASAI = 1 - \frac{SAIDI}{8760} \text{ (\%)} \quad (3.34)$$

$$ASAI = 1 - \frac{1.442}{8760} = 0.999835 = 99.9835\% \quad (3.35)$$

It is worth noticing that the reliability indices are calculated by PF based on RD, FF, and the N_{OCC}, while in the manual calculation, FD, NO and N_{OCC} were used.

A summary of the results and the difference between the PF results and manual calculation is presented in Table 3.15. One can observe that the calculated numbers are very close to the ones obtained in the simulation, thus confirming the hypothesis that the radial feeders mainly contribute to the poor reliability performance of this network and give confidence in the simulation results.

Table 3.15: Comparison of results according to PF and manual calculation.

Index	SAIDI (h/yr)	SAIFI (interruption/yr)	CAIDI (h)	ASAI %
PF results	1.441	0.811	1.779	99.9832
Manual calculation	1.442	0.811	1.778	99.9835
Difference	0.001	0	0.001	0.0003

3.6.3. Load point indices for the radial feeders.

After calculating network reliability indices, LPIs were obtained through PF to identify the weakest load busbars. These loads are located at the end of the radial feeders studied in the previous sections. The LPIs at Gombe, Yola, Birnin Kebbi, and Sakete bus bars were higher than in the rest of the system, such as Ikeja and Kaduna, as shown in Table 3.16. The LPIF (1/yr) at Gombe is very close to 2 – this threshold indicates that a load is subject to frequent interruptions. Thus, the investigation of the LPIF and LPIT results shows differences in the frequency and length of disruptions at the various sites. Compared to Birnin-Kebbi and Sakete, Gombe often has fewer, shorter disruptions, whereas Yola typically sees more frequent, shorter interruptions. The longer duration and higher frequency of interruptions in Birnin-Kebbi and Sakete indicate regions where the reliability of the electrical supply should be improved.

Figure 3.3 – Figure 3.5 shows in detail the LPIs for the feeders under consideration: the loads indicated in red are the ones where LPIs are greater than 2. It is worth observing that nearby loads may sometimes have very different performances. For example, LPIs at Ikeja are close to zero, while at Sakete, they are higher than 10 (Figure 3.3). This is because Ikeja is interconnected to the rest of the system by several lines, as shown in Figure 3.2, while a single line connects the load at Sakete, making it prone to outages. Similar considerations apply to the radial feeder loads shown in Figure 3.4 and Figure 3.5.

Table 3.16: LPI values for the four loads with the lowest performance in the network.

Load point interruption	Gombe	Yola	Birnin-Kebbi	Sakete	Ikeja	Kaduna
LPIF (1/yr)	1.987	7.988	3.999	10.003	0.001	0.001
LPIT (h/yr)	0.497	3.487	17.136	14.824	0.000	0.001

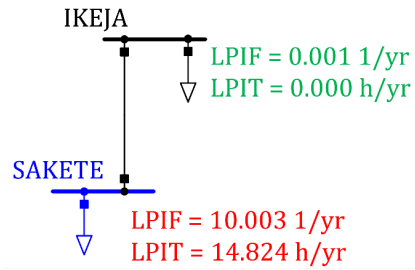

Figure 3.3: LPI results for radial feeder A.

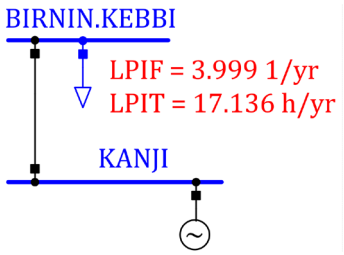

Figure 3.4: LPI results for radial feeder B.

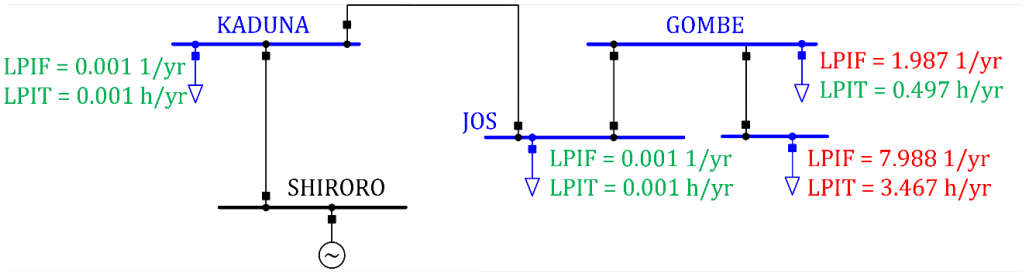

Figure 3.5: LPI results for radial feeder C.

3.6.4. Comparison with other countries

The comparison of the reliability results in Table 3.9 with the Nigerian power transmission reliability, summer scenario of Table 3.13 shows that:

- In terms of SAIDI, the Nigerian transmission system experiences more power outages than India, Egypt, and Australia. On the contrary, the Nigerian transmission system performance appeared more reliable than Algeria's.
- The high SAIFI value indicates more faults than in Algeria, India, Egypt, and Australia. It further produces an overall negative impact on CAIDI, decreasing both reliability and customer supply.

3.7 Impact of HVDC on reliability indices

The reliability results overall indicated that the weakest points of the transmission system are the radial feeders. However, it was determined that the attention should focus on radial feeder C (Figure 3.5) as it is the longest and has two load busbars (Yola and Gombe).

In this section, the impact of HVDC on reliability is presented for two cases: Case 1 is the Azura-Gombe HVDC connection, and Case 2 is the Azura-Yola connection. In both cases, Azura was the sending end busbar, and it was selected because of the presence of a large generator and the distance from the loads. The HVDC length was 1020 km and 1025 km for Cases 1 and 2, respectively. The HVDC parameters shown in Table 3.12 were adopted in both cases: it is worth noticing that a rated power of 500 MVA was used even if the loads are smaller at these busbars, given future system expansion.

Table 3.17 presents the values of system indices for Case 1 and Case 2, together with the results for the original network, referred to as Case 0 (Base Case). For Case 2, there was an improvement of 1.371 h/yr on the average time (SAIDI) when customers were without electricity in the year. Case 2 has the lowest SAIDI, indicating the shortest average interruption time compared to 1.418 h/yr for Case 1 and for Case 0 when there was no HVDC link on the network (1.441 h/yr). Additionally, the frequency of interruption (SAIFI) and the service available to the customers during the year (ASAI) are improved for Case 2 by 0.62 interruption/yr and 99.9843%, respectively, compared to the base case and Case 1. The SAIFI also indicates the lowest interruption frequency. Only the average time to repair (CAIDI) was improved for Case 1, with 1.980 hours, compared to Case 2, with 2.204 hours. To determine CAIDI, SAIDI is divided by SAIFI. In contrast to Cases 0 and 1, SAIDI decreased in Case 2, but SAIFI reduced much more sharply. Considering the decrease, the Case 2 CAIDI result was higher since SAIFI decreased more than SAIDI did. The combined effect of lower SAIFI and SAIDI values is why Case 2's CAIDI is larger than the other cases. However, the best performance was obtained for Case 0 with 1.779 hours.

Table 3.17: Reliability results without HVDC and with HVDC link on the network (Summer scenario).

Index	SAIDI (h/yr)	SAIFI (interruption/yr)	CAIDI (h)	ASAI %
Without HVDC links (Case 0)	1.441	0.811	1.779	99.9832
HVDC between Azura - Gombe (Case 1)	1.418	0.716	1.980	99.9838
HVDC between Azura - Yola (Case 2)	1.371	0.622	2.204	99.9843

Table 3.18: LPI results for Case 1.

Load point interruption Case 1	Gombe	Yola	Birnin- Kebbi	Sakete
LPIF (1/yr)	0	6.000	3.999	10.003
LPIT (h/yr)	0	2.990	17.136	14.824

Table 3.19: LPI results for Case 2.

Load point interruption Case 2	Gombe	Yola	Birnin- Kebbi	Sakete
LPIF (1/yr)	0	0	3.999	10.003
LPIT (h/yr)	0	0	17.136	14.824

In conclusion, the simulation results show that for Case 2, the system has a better SAIDI, SAIFI, and ASAI. The LPIs were calculated and compared with Case 0 for both cases, with results summarised in Table 3.18 and Table 3.19. One can notice that the LPI improves at the busbars close to where the HVDC is connected, and in particular, Case 2 effectively zeroed the LPI for both Gombe and Yola loads, thus confirming its superior performance to Case 1. It is also worth noting that the HVDC does not affect other loads. This is expected from the previous analysis, as it has been demonstrated that the LPIs at the end of each radial feeder are determined by the reliability of the line they are connected to.

The results above indicate the positive influence of HVDC on network reliability and load indices.

3.8 Conclusion

The reliability analysis for the Nigerian transmission system was studied based on data provided by the Nigeria Electricity System Operator (NESO) for both the summer and winter of 2019. Given that the network configuration has not changed substantially since then, the results of this work can still be considered up to date. An HVDC model was developed using data retrieved from the literature, as currently, no HVDCs are used in Nigeria.

The data provided by the NESO were used to build a summer and a winter scenario in PF. Reliability studies were conducted, and system and load indices were obtained. Manual calculations were carried out to demonstrate that the reliability of the radial feeders is not affected by the rest of the system, which is highly meshed. This finding simplifies the analysis for systems with a similar configuration, mainly when not all system data are available.

Based on the results of the reliability data, two locations were identified to test the impact of the HVDC connection on system reliability. The reliability study results indicated improved overall system reliability in both cases. The reliability- study results improved the overall system reliability in both cases. In particular, adding an HVDC line between Azura and

Yola (referred to as Case 2) provided the best results, both in terms of system indices and load indices. The next step of this study is to repeat a similar assessment for system stability and to assess the impact of HVDC interconnections on stability indices.

4 Stability Analysis

4.1 Introduction

Power systems are more unstable than ever due to increased electricity usage and the difficulty and expense of constructing new transmission lines. However, due to the strained working conditions of networks, modern power systems have been compelled to operate close to their stability limits, which results in voltage instability or collapse [129], [130]. The transmission lines had to run close to their load limits to accommodate the demand for electricity in areas with high load densities due to the impossibility of installing new generating units and economic and environmental constraints [131]. This situation is expected to worsen owing to increased forecasted demand [132].

The availability of a stable and reliable electricity grid is a crucial driver of economic growth and societal change, particularly in developing economies such as Nigeria. In this context, power system planning is essential for making informed decisions about energy investment for future grid development [34], [133]. While waiting for such developments, electricity providers in Nigeria must increase the use of existing transmission facilities due to the constantly growing load demand [134]. The northern part of the country is mainly affected by poor voltage profiles due to insufficient dispatch and control infrastructure, radial and fragile system topology, frequent system collapse, and exceedingly high transmission losses. The country's generation stations are spread out, and unacceptable voltage drops on the network are observed with long-distance electricity transmission. As a result, voltage collapse could result from even minor disruptions [26], [36], [135]. Consequently, studying voltage stability is crucial for a safe and dependable power supply.

In general terms, power system stability is the ability of an electric power system to regain a state of operating equilibrium after being subjected to a physical disturbance [136], [137]. Stability analysis allows identifying a power system operation that provides energy to consumers at an acceptable voltage and frequency with the lowest possible cost [138], [139].

This chapter is based on the work published in [133].

Within the broad range of stability studies, this chapter focuses on static voltage stability analysis to evaluate the voltage stability and loadability margins under the current and future demand levels. Static analysis will offer insightful information to determine the voltage magnitude at different points and the increased load demand on the power system. This information is critical for ensuring the voltage levels remain within acceptable limits and preventing voltage collapse. The research aims to evaluate the system's steady-state voltage stability under various operating situations and locate important voltage collapse points. The static voltage stability analysis is conducted to identify the weak areas regarding the system's reactive power shortage and ascertain the crucial contingencies of voltage stability margins [140].

Various approaches are used in static voltage stability analysis, including modal analysis, optimization method, continuation load flow method, Power-Voltage (PV) curves, and Reactive–Voltage curves (QV) method (also known as nose curves). The nose curve, employed in voltage stability analysis, indicates the critical condition in which the system is working at its highest loading point before voltage collapse [141]. A further increase in load beyond the nose point or critical point will result in voltage instability [142].

PV and QV curves are among the most popular static voltage stability analysis methods, and they are adopted in this work [1]. A PV curve graph shows the relationship between active power (P) and voltage magnitude (V) at each busbar. In contrast, the QV curve is a graphic representation of the relationship between the reactive power (Q) injected into or consumed by a power system and the corresponding voltage (V) at each busbar [143]. The ability of PV and QV curves to accurately give information such as power limits, critical voltage, and stable and unstable operation areas has made them become practical tools for static voltage stability analysis [129], [142], [143]. More specifically, these curves allow the identification of weak busses with the tendency to experience voltage instability or a limited ability to maintain a steady voltage level under certain operating conditions. Weak buses are characterized by having low voltage magnitude, often close to the voltage collapse point [144].

A voltage magnitude less than 0.95 pu is considered to have a low voltage magnitude. It should be noted that the maximum statutory voltage limit for operation for assessing the over-voltage degree is 1.05 p.u level. Similarly, the minimum statutory voltage limit for operation has been set at 0.95 p.u [145]. Generally, Power system components are designed to operate at maximum efficiency within a specific voltage tolerance range. To ensure reliable transmission system operation, a per unit (pu) value of 0.95, which is in line with 95%,

represents a balance between efficiency and safety. It ensures conformity to grid codes and conforms to industry requirements [146], [147].

This work aims to conduct a voltage stability analysis on the Nigerian transmission network using a detailed computer model and applying PV and QV analysis. Next, the impact of an HVDC on system stability was assessed. This analysis used data from the Nigeria Electricity System Operator (NESO). PF was chosen for this research due to its versatility and capability to conduct numerous power system studies[148]. The research presented in this paper is part of a larger project to investigate the impact of HVDC connections on various power-system performance measures, which include reliability and voltage profile. Previous work using this model can be found in [9], [36].

4.2 Literature review

Given the continuous growth in demand and the difficulties related to developing new transmission lines, numerous researchers have investigated using power electronic equipment to improve power system stability. Power electronics are gaining popularity due to the improved performance and reduced cost observed in the last decade. In [130], a new line voltage stability index (BVSI) was used to identify weak lines and buses on various loading conditions and network configurations. Different loading conditions using IEEE benchmark models (the 14-bus, 30-bus, 118-bus test systems). An analytical approach was applied to determine the optimal location of reactive power compensation placement, which was used to improve system voltage stability with current and increased demand [130].

PowerFactory software was used by [149] to conduct a case study for the IEEE-14 bus system to identify the weak bus in a system. The FACTS device can be added to the weak bus using two traditional methods, PV and QV curve analysis. Both methods compared the study of Static Var Systems (SVS) at different buses. So, the PV and QV curves detect the weak bus zone and give a better position for SVS placement, preventing the system from collapsing voltage. For stability improvement, SVS is connected to bus 13 and bus 25 MVAR, with 45 MVAR each. Thus, system-critical scalable demand and load margin are improved. For SVS placement, bus 13 and bus 14 are the optimal locations to improve the system stability and transmission power capacity and reduce losses [149].

The work presented in [150] used a Multi-Criteria Decision Making (MCDM) method on IEEE 14-bus, IEEE 30-bus, and IEEE 118-bus test systems to improve the voltage stability of the test system. The method optimises the allocation of the FACTS controller according to

increasing the loading margin, reducing voltage deviation, and reducing active power losses. With this objective, optimal SVC location was presented among the weakest buses. However, it was revealed that in the event of contingencies, SVC on buses does not enhance the state of overloaded lines [150].

The impact of HVDC was further studied, and the research shows that VSC-HVDC stabilizes the AC voltage as AC loads continuously change [144]. Since the AC transmission line creates reactive power while being lightly loaded, the connected VSC-HVDC initially uses it to maintain the AC voltage. VSC-HVDC generates reactive power to support the AC system as the connected loads increase. Continuous reactive power support from VSC-HVDC improves the voltage stability margin. The reactive power of VSC-HVDC supports capability and then maximizes the reactive power when the transmission network voltage is low. The VSC-HVDC stabilizes AC voltage as the AC loads continuously change but keeps active power transmission constant [144].

Another paper studies the effect of an HVDC link on the transient stability of an interconnected power system. This study applied a three-phase ground fault to the network at a different location [151]. The faults were cleared by opening the respective transmission lines, and the critical clearing time for each fault in a particular operating condition of the power system was observed. Without HVDC, the clearing time is longer than with HVDC, and the system loses synchronism. The study was repeated, and the system's behavior was studied by observing the rotor angles of the synchronous machines. The results show that after the inception of the HVDC link, the system did not lose synchronism when the fault was cleared, and the clearing time was improved significantly [151].

The study by [152] further examines how changing the active power flow through VSC-HVDC improves voltage stability for power systems with VSC-HVDC links [152]. Different load scenarios were researched, and a comparison between the decrease and increase of active power transmission using VSC-HVDC was investigated to better understand the voltage stability improvement. According to the research, reducing DC power enables the VSC-HVDC to support the voltage when the power supply is disrupted and when the VSC-HVDC link is under heavy load. Since the disturbance lowers the voltage at the bus, reactive power injection into the bus is required to raise the voltage because the VSC cannot generate reactive power when it is severely loaded. It was demonstrated that the voltage at the bus increases when reactive power is injected into the bus simultaneously. It was concluded that if the VSC-HVDC link is heavily loaded and a power system disturbance occurs, a decrease in DC power still allows the VSC-HVDC to support the AC voltage [153].

A further instance of the impact of HVDC on stability was investigated using PV and transient analysis [153]. The investigation was carried out when the network was only a high voltage alternate current (HVAC) and a hybrid of VSC-HVDC and LCC-HVDC. The maximum loading point (MPL) and the voltage magnitude were used to determine the impact of the hybrid network. The maximum loading point with HVAC was 3168.25 MW, with the highest voltage magnitude on bus 12 (0.94321 pu), and two buses (7 & 5) had the lowest voltage magnitude of 0.8028 pu. With LCC- HVDC, the MPL was 3234.37 MW for all buses (active power), with the same bus (bus 12) having the highest voltage magnitude of 0.9532 pu and bus 7 with the lowest voltage profile of 0.8572 pu. When VSC-HVDC was connected, the MLP was 3226.11 MW, bus 12 had a voltage magnitude of 0.9415 pu, and bus 7 possessed the lowest voltage profile with 0.8069 pu. The response of the speed and rotor angle of the network was carried out under a transient fault situation; the investigation shows that VSC-HVDC reduced the system oscillation better than the HVAC and LCC-HVDC with a speed of 1.001 pu, and a steady state operation was achieved 7 seconds after perturbation. It also reduced the first swing oscillation from 1.001pu to 0.9997 before reaching a steady state of operation about 8 seconds after perturbation. The HVAC system was the least damped of the three cases, with a speed of 1.0 pu at rest but increasing to 1.002 pu more than the rest before settling in about 10 seconds. This investigation demonstrated that the VSC-HVDC improved the voltage and transient stability of the hybrid HVAC-VSC-HVDC system [153].

Both a VSC-HVDC and a conventional AC transmission line were considered for reinforcement in a transmission system that was significantly loaded [154]. The first alternative allowed for more power transfer and enhanced the stability of the power system while lowering the demand for generators to produce reactive power [154]. With a VSC-HVDC link connected between two weak points, the voltage magnitude increased to 0.93 pu, and with the AC transmission line, the voltage magnitude was around 0.85 pu [154].

The impact of the HVDC system on the power system stability was carried out using the application of Location Marginal Price (LMP) [155]. This was used to select and manage the overloaded lines on the IEEE 14-bus network. Five lines were considered for optimal locations based on LMP. HVDC was used to replace each line and determine which would impact the network. Based on the power flow study, the graph of voltage, angular speed, active power (P), and reactive power (Q) was plotted against time (T) for each line when the load flow was executed. The results from the graph reveal that only one out of the replaced HVDCs possessed small perturbation, and the time (T) of stability was less than others (10 seconds). This was when stability was achieved on the network [155].

The motivation for performing a stability study is to develop and propose an effective solution to enhance the stability limits of the Nigerian transmission system. This will increase the system loading and the reactive power margin (RPM). The security margin estimates how much the demand can increase before the system collapse is reached. Consequently, increasing the security margin will reduce the risk of system collapse and allow for future system expansion.

4.3 Stability analysis methodology

4.3.1 Stability analysis of two buses

A review of the stability of a power system with two buses is provided here to review fundamental concepts related to this topic. More detailed background information can be found in [156].

Assuming the transmission line is lossless (R=0), the line impedance is expressed as **Z**= jX, where X is the line reactance. Based on [157] and [158], the equations below are used to determine the maximum power ($\mathbf{P}_{max}$) and the critical voltage ($\boldsymbol{V_{crit}}$) of the system, respectively.

$$P_{max} = \frac{1}{2} * \frac{V^2}{X}\left(\frac{1}{Cos\emptyset_2} - tan\,\emptyset_2\right) \quad (MW) \tag{4.1}$$

$$V_{crit} = \frac{1}{\sqrt{2} \times \sqrt{1 + sin\emptyset_2}} \qquad (pu) \tag{4.2}$$

where P_{max} (MW) is the maximum power, V_1 (pu) is the sending end voltage at the initial condition, and $\emptyset_2$ (rad) is the angle between voltage and current. V_{crit} (pu) is the critical voltage. Equation 4.1 is typically called the maximum system load or loadability limit. If the load is increased beyond the loadability limit, the voltages will decline uncontrollably [159]. Therefore, voltage stability analysis is essential to determine the system's critical voltage point and the collapse margin. These parameters will be determined using the PV and QV curves described in the next section. But $Cos\,\emptyset$ = power factor (p.f) of the circuit. Therefore, the power factor and the phase angle are determined using equations 4.3 and 4.4 respectively:

$$\text{p.f} = \text{Cos}\,\emptyset_2 = \frac{\text{P}_2}{\text{Q}_2} \tag{4.3}$$

$$\tan\emptyset_2 = \frac{Q_2}{P_2} \tag{4.4}$$

3.2 Numerical example and simulation results

From a two-bus system, the sending end voltage is 330 kV with the active and reactive power of 170.9 MW and 98.8 MVAR, respectively, at the receiving end. The reactance of the line is 0.331 Ω, and the line length is 218 km. The maximum power and the critical voltage are calculated below.

The phase difference $\emptyset_2$ is determined using equation 4.4, as shown below:

$$\tan \emptyset_2 = \frac{98.8}{170.9} = 0.5547 \tag{4.5}$$

$$\emptyset_2 = 29.02° \tag{4.6}$$

Therefore, the maximum power, which can be transferred to the receiving end, and the critical voltage can be calculated from equations 4.1 and 4.2:

$$P_{max} = \frac{1}{2} * \frac{330^2}{72.158}\left(\frac{1}{0.8745} - 0.5547\right) = 444.31 \text{ MW} \tag{4.8}$$

$$V_{crit} = \frac{1}{\sqrt{2} \times \sqrt{1 + 0.4851}} = 0.5802 \text{ pu} \tag{4.9}$$

The voltage obtained when the maximum power is reached is the critical voltage (0.5802 pu), corresponding to the maximum load point (444.31 MW). An increase above this value leads to system collapse. Consequently, voltage stability is crucial for determining the critical voltage point and collapse margin, which can be determined using the PV curve.

The transmission line was assumed to be lossless, with a resistance of 0.001 Ω/km and a reactance of 0.331 Ω/km. The two-bus system was solved using PowerFactory (PF), and the load flow stopped converging at 444.30 MW. As the load increases, the voltage decreases until a critical voltage of 0.5827 pu is reached [158]. The comparison result from the manual calculation and PF calculation is given in Table 4.1. The comparisons aim to verify that the simulation model is appropriately implemented and provides reliable results.

Table 4.1: Result comparing manual calculation and PF results.

	P_{max} (MW)	V_{crit} (pu)
Manual calculation	444.31	0.5802
PowerFactory result	444.30	0.5827

4.3.3 PV and QV curves

After building the network model, as explained in Section 4.3.4, PV and QV calculations were executed. The adopted power-voltage (PV) and reactive voltage (QV) curves were used to determine the weak buses on the Nigerian Power Network. The calculation was executed using the data provided by the Nigeria Energy System Operator (NESO). The data provided by the NESO for the stability study includes the active power (P) in megawatts (MW) for each load and generator. Generation and demand data were provided for each month of 2019 (January to December).

Based on the data provided by NESO, a load flow analysis was carried out to ensure system stability, as described in Chapter 2. Once the initial load flow had been computed, the PV and QV curves were obtained by gradually increasing the loads' active and reactive power demands. It is worth noting that active power demands were changed by keeping the reactive power demands fixed when computing the PV curves.

Conversely, reactive power values were modified when the active power was fixed and the QV curve was computed. After changing the load conditions, the load flow analysis was repeated for each load level. The new steady-state conditions are calculated based on the updated load conditions, including voltages and power flows. The corresponding voltage magnitudes and active power values are recorded as the load flow analysis is repeated for different load levels.

A graph yields the P-V curve, with voltage magnitude on the Y-axis and active power on the X-axis, by plotting voltage values against active power levels. The resulting curve depicts how the system voltage varies with changes in active power demand. A similar process generates the QV curve, with reactive power values plotted on the X-axis and voltage magnitudes plotted on the Y-axis. PV and QV curves were plotted at each busbar [158].

4.3.4 Network model and HVDC model

To carry out the static stability analysis, a model of the Nigerian transmission 330 kV network of Figure 2.1 was used using the electrical and stability data provided by the NESO. The stability data, such as the reactive power for each load and generator, was calculated (Appendix A.0.1 and Appendix A.0.2).

An HVDC model Figure 3.1 was added to the transmission system model for the weak buses identified by the PV and QV studies. The model of an HVDC was built separately to be integrated into the Nigerian transmission system. The model used for the voltage stability

analysis was adopted from Chapter 3. The adopted model is described in more detail in Chapter 3. The impact of HVDC on system stability was assessed using the control modes described in Chapter 3.

4.4 Stability results

4.4.1 Static voltage stability analysis of the Nigerian transmission system

The first case study used the summer scenario, with no HVDC connected to the network. This case was used to identify the system's weak bus(es). The same analysis was repeated for the winter scenario. Following the identification of the weak bus, an HVDC was connected to the system, and the impact of the HVDC on stability was examined.

4.4.2 PV analysis - Base case results

The PV analysis was carried out by increasing the real power (MW) transfer from the generators to the loads, as described in (section 4.3.3). The PV curves obtained for six busbars (Gombe, Jos, Kaduna, Kano, Makurdi, and Yola) are shown in Figure 4.1. These busbars were chosen because they are the ones that reach the nose point or critical point first, as seen in Table 4.2. For the summer scenario, the initial network demand is 4654 MW. The load flow stops converging when demand reaches the critical value of 5399 MW: at this condition, all six buses show a voltage magnitude below 0.95 pu (below the statutory voltage limit).

When the network demand is 5399 MW, Yola (the red dashed line) is identified as the critical bus, reaching the nose point at a voltage magnitude of 0.66 pu. This result can be explained by observing that Yola lacks voltage regulation equipment and is located at the end of a radial feeder. Gombe (the purple dashed line), too, reaches the nose point at 0.69 pu. Other buses (Jos, Kaduna, Kano, and Makurdi) also have voltage drops of 0.81 pu, 0.94 pu, 0.90 pu, and 0.92 pu, respectively, when the load increases. These values are summarised in Table 4.2. Kaduna is the bus with the highest critical voltage for both the summer case (0.94 pu) and the winter case (0.97 pu). The lowest critical voltage during summer and winter are observed at Yola, with values of 0.66 pu and 0.64 pu, respectively. Based on the PV analysis, it is concluded that Yola and Gombe are the two weakest busbars as both reach the nose point earlier than Jos, Kaduna, Kano, and Makurdi.

The critical demand during the winter scenario is 5223 MW, and the Yola and Gombe buses are the weakest, with 0.64 pu and 0.68 pu, respectively. Jos, Kano, and Makurdi buses have voltage drops of 0.86 pu, 0.93 pu, and 0.92 pu, respectively. These results are included in

Table 4.2. Table 4.2. indicates that, in general, the voltage levels are higher in the winter due to lower load levels than in summer. Therefore, the summer scenario will be considered the one that provides the most conservative results for stability analysis.

Table 4.2: Voltage magnitude for the weak buses.

	Summer			Winter		
Bus	**Load flow voltage (pu)**	**PV (pu)**	**QV (pu)**	**Load flow voltage (pu)**	**PV (pu)**	**QV (pu)**
Gombe	0.91	0.69	0.5	0.95	0.68	0.46
Jos	0.92	0.81	0.75	0.99	0.86	0.78
Kaduna	0.96	0.94	0.93	1.00	0.97	0.96
Kano	0.95	0.9	0.91	0.97	0.93	0.93
Makurdi	0.96	0.92	0.92	1.01	0.92	0.89
Yola	0.91	0.66	0.41	0.95	0.64	0.35

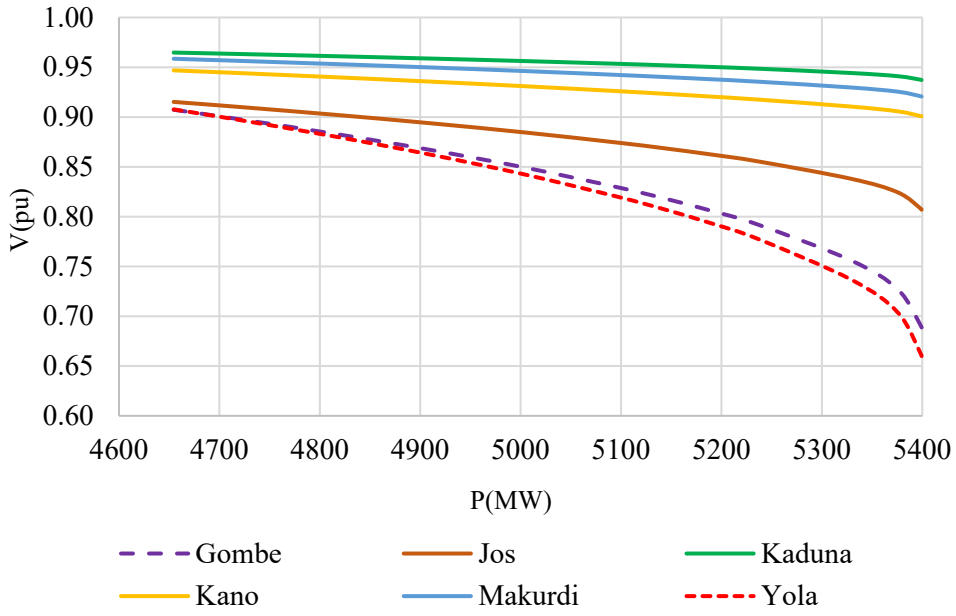

Figure 4.1: PV curve showing the buses that hit the nose point first.

4.4.3 QV analysis - Base case results

The QV analysis was carried out next to evaluate the impact of reactive power variation on voltage stability. Figure 4.2 presents the plot of the critical voltage with the reactive power margin for six buses with a voltage magnitude below 0.95 pu. Notably, these buses are the same as in Figure 4.1; therefore, the two methods lead to the identification of the same weak buses.

Kaduna and Makurdi show 0.84 pu / -619 MVAR and 0.78 pu / -538 MVAR for critical voltage and reactive power, respectively, while Kano and Jos show 0.55 pu / -204 MVAR and 0.76 pu, / -140 MVAR, respectively. Gombe and Yola show 0.66 pu / -54 MVAR and 0.61 pu /-42.57 MVAR respectively. In this work, positive reactive power corresponds to capacitive loads, while an inductive element absorbs negative reactive power.

The bus distance from the generator is essential in relation to the capability of the load to absorb reactive power. Kaduna load can absorb high reactive power to maintain the system stability since it is close to the Shiroro generator. Nevertheless, its voltage magnitude is 0.93 pu (Table 4.2), which is still below the statutory voltage limit of 0.95 pu. Makurdi bus shows a similar pattern. The weakest busbar is the point(s) of the lowest reactive power margin.

The results are summarized in Table 4.2, where the six buses with the least voltage magnitude (pu) on the network are shown. Kaduna bus has the highest voltage magnitude in both scenarios, 0.93 pu during the summer and 0.96 pu during the winter. The lowest QV values during summer and winter are observed at Yola, with values of 0.41 per unit and 0.35 per unit, respectively.

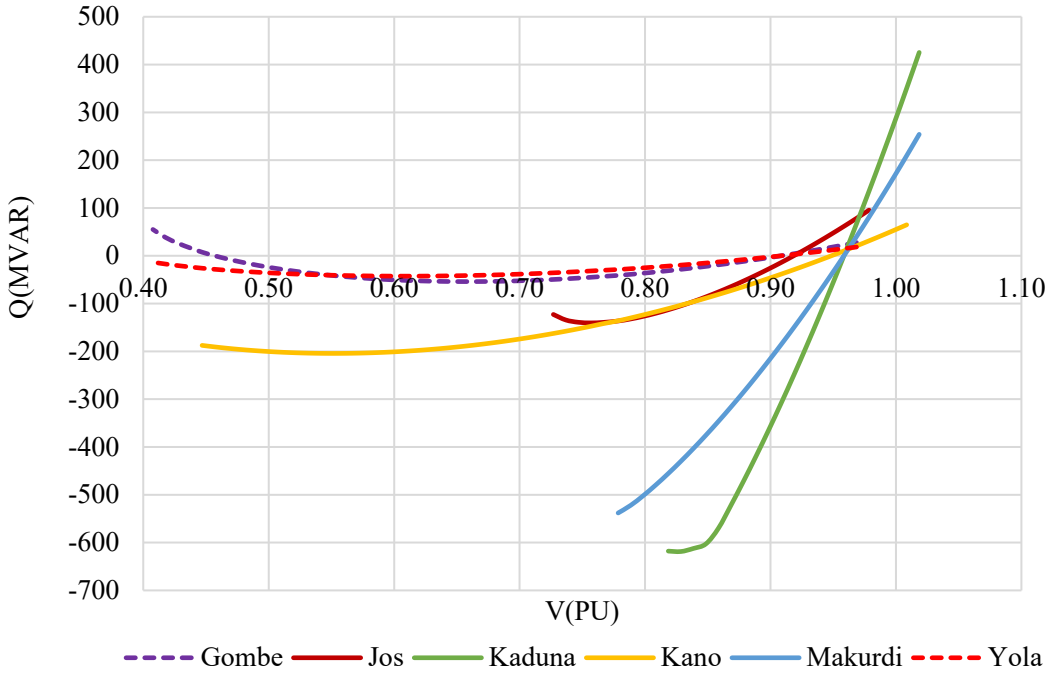

Figure 4.2: QV curves for the weak buses.

Table 4.3: Summary of Load flow/PV and QV result (Base Case).

Base Case	Generator		Load		Losses		Reactor	Critical bus	Critical voltage (pu)
	MW	MVAR	MW	MVAR	MW	MVAR	MVAR		
Load flow	4804	-298	4654	1281	150	-2338	759	-	-
PV	5663	331	5399	1486	264	-1873	725	Yola Gombe	0.66 0.69
QV	4844	109	4654	1281	190	-1890	718	Yola Gombe	0.50 0.41

4.4.4 Active and reactive power analysis

Table 4.3 presents additional results in relation to load flow, PV, and QV analysis for the base case (no HVDC in the network). This table illustrates generated power, load demand, line losses, and reactor output. The sum of active power absorbed by the loads and line losses equals the generated power. The sum of the load reactive power, the line reactive power, and the reactor's output are the same as the generated reactive power.

As a result of load increase during the PV analysis, generated power, load demand, and line losses increased by 18%, 16%, and 76%, respectively. From the QV analysis, the generated power increased slightly by 0.83% and line losses by 27% due to higher current. More reactive power (759 MVAR) is required during the load flow analysis to balance and control the voltage at the bus because the loads are inductive. The static stability study showed that the transmission system's radial feeders are the weakest link because they have a single point of supply. Specifically, both PV and PQ analyses indicate that Yola and Gombe are critical buses, and these two bus bars are now considered for the HVDC connection. In the previous studies, namely, the load flow and reliability study of this network [9], [36], these two buses were identified as having the lowest voltage magnitude and reliability, respectively.

4.5 Impact of HVDC on stability analysis

4.5.1 Impact of HVDC on PV analysis

The impact of HVDC on PV analysis is presented using the same cases as Chapter 3:

- Case 1: the HVDC is connected between Azura and Gombe.
- Case 2: the HVDC is connected between the Azura bus and Yola.

The Azura bus has been chosen as the sending end in both cases because of the presence of a more significant generator and its distance from the loads. The load flow results and PV results are summarized in Table 4.4 (Case 1) and Figure 4.4 (Case 2).

The power generated for Case 1 is 4784 MW, while for Case 2 is 4788 MW. These results are slightly lower than the base case (4804 MW, as shown in Table 4.3). This is partly due to a slight decrease in line power loss when the HVDC is in service (21 MW and 17 MW, respectively, for Cases 1 and 2).

Table 4.4 reveals that the critical demand improved to 8480 MW, while Table 4.5 shows a critical demand of 8329 MW. The increase equals 3081 MW and 2930 MW, respectively, compared to the base case (5399 MW) in Table 4.3. the generated power was improved by 123% compared to the base case. For Case 2, the generated power was enhanced by approximately 119%.

Figure 4.4 shows the PV results for Cases 1 and 2, respectively. Yola's critical voltage improved from 0.66 pu to 0.98 pu for Case 1 and 1 pu for Case 2. Gombe critical 0.91 pu for Case 2. As expected, voltage improves most at the buses connected by the HVDC. For example, in Figure 4.1, the voltage magnitude remains constant (1.00 pu) for the Yola bus throughout the load variation, while the Gombe bus voltage magnitude dropped from 0.99 pu to 0.91 pu as the power increased. Both Figure 4.3 and

Figure 4.4 clearly illustrates the significant increase in system loadability when the HVDC is connected. The outcome load flow when HVDC is connected and PV results are summarized in Table 4.4 and Table ***4.5*** for Cases 1 and 2, respectively. The results above overall indicate that both Case 1 and Case 2 lead to increased system voltage stability.

Table 4.4: Case 1 HVDC connected between Azura-Gombe.

	Generation (MW)	Load (MW)	Losses (MW)	Critical bus	Critical voltage (pu)
Load flow	4784	4654	129	-	-
PV study	10690	8480	2210	Kano	0.72

Table 4.5: Case 2 HVDC connected between Azura-Yola.

	Generation (MW)	Load (MW)	Losses (MW)	Critical bus	Critical voltage (pu)
Load flow	4788	4654	133	-	-
PV study	10475	8329	2146	Kano	0.71

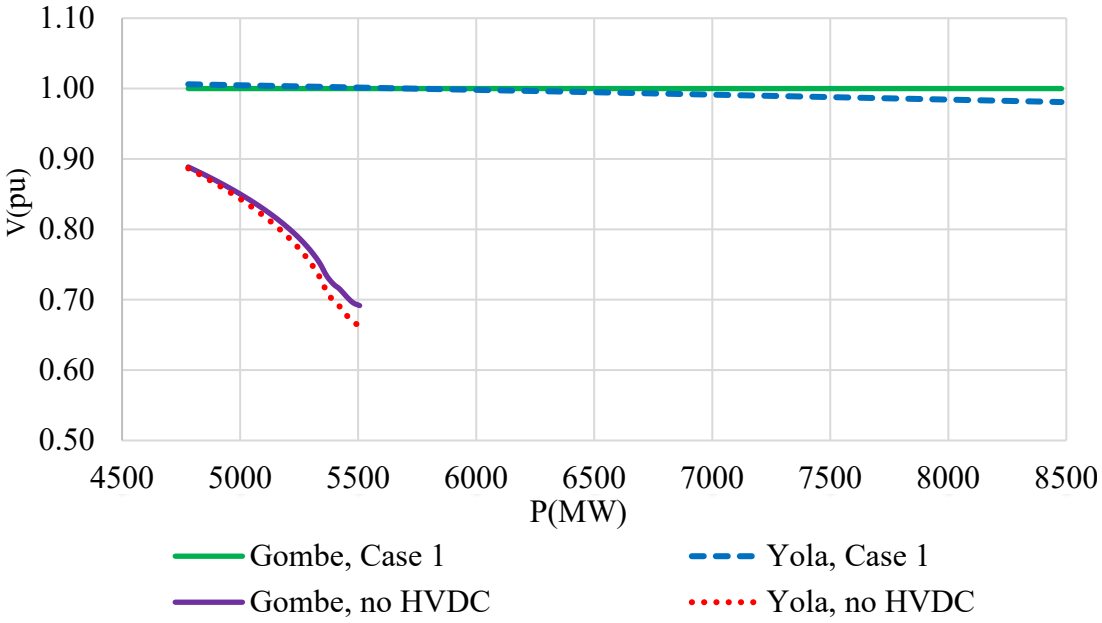

Figure 4.3: PV curves for the base case and for Case 1.

4.5.2 Impact of HVDC on QV analysis

The impact of HVDC on QV analysis is presented in this section for the two cases considered above. Figure 4.5 shows the results for Case 1 and Case 2. The Yola bus improved from 0.91 pu (red curve) to 1.01 pu (blue curve), while the reactive power margin (RPM) improved from -43 MVAR to -306 MVAR. The critical point did not improve, but it slightly degraded from 0.61 pu to 0.62 pu because power systems' load demand might change during the day and throughout the season (change in load patterns). However, for Case 2, an improvement is experienced on the Gombe bus. The operating point improves from 0.91 pu (purple curve) to 0.99 pu (green curve), while the reactive power margin improves from -54 MVAR to -448 MVAR. The critical point of collapse improved from 0.67 pu to 0.61 pu. This implies that the collapse point is further away, with 0.61 pu, and therefore, the loadability of the bus is increased. The power transmission capacity, load margin, and losses were all improved for both Case 1 and Case 2.

The impact of HVDC on the QV analysis is summarized in Table 4.6 and Table 4.7 for Cases 1 and 2, respectively. It shows that Yola voltage improved from 0.91 pu (base case) to 1.01 pu with a critical point of 0.62 pu. Gombe voltage improved from 0.91 pu (base case) to 0.99 pu with a critical point of 0.61 pu, respectively.

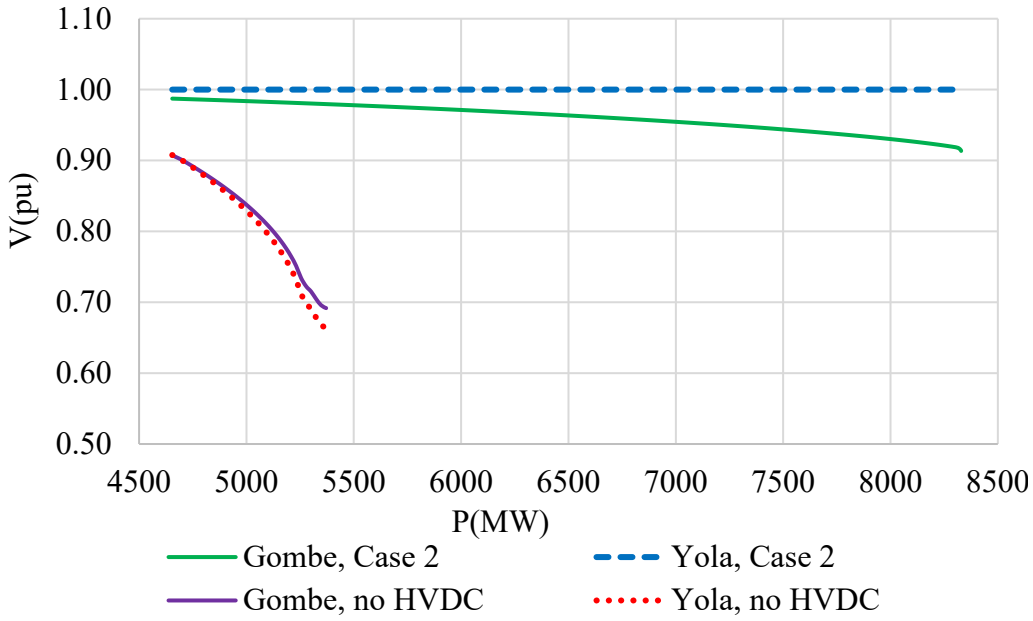

Figure 4.4: PV curves for the base case and for Case 2.

Table 4.6: Case 1 HVDC link on Gombe bus.

	Operating point		Critical point	
Bus	**QV (pu)**	**MVAR**	**QV (pu)**	**MVAR**
Gombe	1	0.02	0	0
Yola	1.01	0	0.62	-306

Table 4.7: Case 2 HVDC link on Yola bus.

	Operating point		critical point	
Bus	**QV (pu)**	**MVAR**	**QV (pu)**	**MVAR**
Gombe	0.99	0	0.61	-448
Yola	1	0.02	0	0

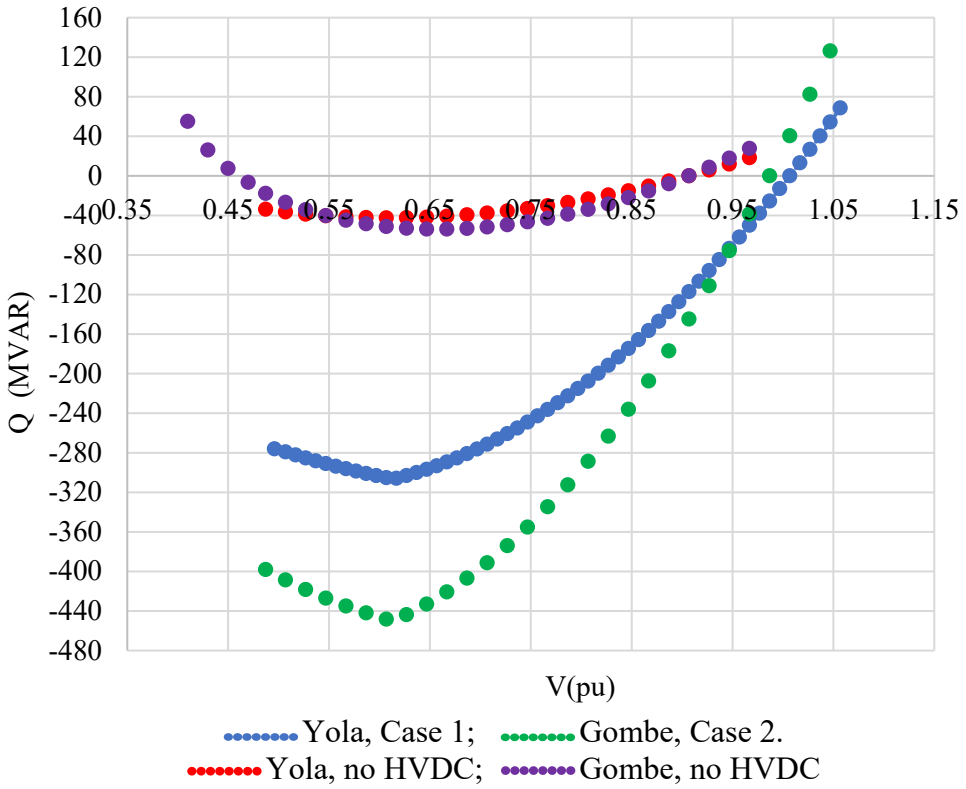

Figure 4.5: VQ curves for the base case, Case 1 and Case 2.

4.6 Impact of HVDC with different control modes

The next step of this analysis investigated the impact of various HVDC control modes on the transmission network. Case 1 results are only presented as they are representative of both cases. The four control modes were defined in Chapter 1 and are summarized below and referred to as follows:

I: $V_{dc}-Q/P-V_{ac}$,

II: $V_{dc}-\text{Cos}\emptyset_2/P-V_{ac}$,

III: $V_{dc}-\text{Cos}\emptyset_2/P-Q$,

IV: $V_{dc}-Q/P-Q$.

4.6.1 Load flow results with different control modes

The load flow analysis was performed for each control mode, and the results are recorded in Table 4.8. The generated power was slightly lower for all different control modes, and this remained constant between 4787- 4788 MW compared to when there was no HVDC on the network (4804 MW). The power generated with I and II is the same, resulting in the same

losses. The losses on these modes (I and II) are lower than those without HVDC. Similarly, control modes III and IV have the same generated power (4787 MW) and losses.

Yola and Gombe have bus voltages of 0.91 pu without HVDC, while with HVDC, the bus voltages for the two buses remain comparatively steady, around 0.99 -1.03 pu for the control modes (I, II, III, and IV). This suggests an improvement in voltage stability. In general, power and losses for the four control modes are very similar; therefore, it can be concluded that the controller did not significantly affect the load flow analysis results.

Table 4.8: Load flow result with each control mode (HVDC connected).

		Generation		losses		Bus Voltage	
	Control mode	MW	MV AR	MW	MVAR	Yola (pu)	Gombe (pu)
-	Without HVDC	4804	-298	150	-2338	0.91	0.91
I	*Vdc−Q/P−Vac*	4788	-497	133	-2560	1.00	0.99
II	*Vdc*−Cos$\emptyset_2$/*P*−*Vac*	4788	-497	133	-2560	1.00	0.99
III	*Vdc*−Cos$\emptyset_2$/*P*−*Q*	4787	-517	132	-2574	1.03	1.01
IV	*Vdc−Q/P−Q*	4787	-517	132	-2574	1.03	1.01

The voltage magnitude across the network was measured with each control mode, and Table 4.9 summarizes the improved voltage. Bus voltages at buses like Gombe, Jos, and Yola rise from 0.91 pu in the base case (without HVDC) to a statutory voltage limit, which shows an improvement in voltage stability. Therefore, HVDC implementation significantly improves bus voltages, bringing them closer to the statutory voltage limit, ranging from 0.96 pu to 1.03 pu (Appendix A.0.3).

Table 4.9: Load flow results summarised improved voltage for different control modes.

Bus	Load flow Without HVDC (pu)	I (pu)	II (pu)	III (pu)	IV (pu)
Gombe	0.91	0.99	0.99	1.01	1.01
Jos	0.91	0.96	0.96	0.97	0.97
Makurdi	0.96	0.98	0.98	0.98	0.98
Yola	0.91	1.00	1.00	1.03	1.03

4.6.2 PV and QV result with different control modes

Table 4.10 shows the PV and QV analysis results for different control modes. The generation output remains constant across all modes, with a value of 10475 MW for control modes I and II and 8298 MW for control modes III and IV. Therefore, a much higher system loadability can be achieved with control modes I and II, which means that critical demand can be increased.

It was observed, however, that no significant changes to the QV calculation resulted from using any of the control modes compared to the base case. This is because, during the QV calculation, the generator power is constant. In contrast, the reactive power is adjusted, and the active power flow is unaffected by the reactive power flow, which oversees voltage management and stability. The generated power was 4784 MW and -556 MVAR with all control modes, and the losses were 129 MW and -2594 MVAR, supplying the same load of 4654 MW and 1281 MVAR. The critical bus for the QV calculation remains the same as that of the PV calculation (Kano and Yola), while the critical voltage is shown in Table 4.10.

Utilizing different control modes improved the analysis of PV and QV. It was observed that control modes I and II resulted in an increase of 2930 MW in the critical demand with Kano as the critical bus. This indicates a higher power demand than in the base case. Furthermore, the critical voltage for both PV and QV improved, reaching 0.73 pu and 0.55 pu, respectively. This suggests an overall improvement in the system's performance.

Similarly, control modes III and IV increased the critical demand by 1963 MW compared to the base case and improved critical voltage for both PV and QV analysis, with 0.68 pu and 0.54 pu, respectively, at the Yola bus. The critical voltage for both PV and QV slightly improved, indicating a better voltage condition than the base case. The PV and QV analysis points to changes in critical demand and enhancements in voltage performance (higher critical voltage) in the control modes.

TABLE 4.10: PV and QV analysis results with different control modes - Case 1.

		PV		QV
Control mode	**Critical bus**	**Critical demand (MW)**	**Critical voltage (pu)**	**Critical voltage (pu)**
Without HVDC	Yola	5399	0.66	0.41
I	Kano	8329	0.73	0.55
II	Kano	8329	0.73	0.55
III	Yola	7362	0.68	0.54
IV	Yola	7362	0.68	0.54

4.7 Converter rating

In this section, different converter ratings were tested on the network. Case 2 was sufficiently studied because of the length of the DC line (1025 km) and the improvement of the voltage stability (0.71 pu) of the particular case. The considered rated power includes 400 MVA, 500 MVA, and 800 MVA with 5% losses of the converter-rated power. The load flow and PV analysis of the network were calculated. The effect of converter rating was noticed on the generators and the system losses, as seen in Table 4.11. The converter rating did not affect the voltage during the load flow calculation. However, during the PV calculation, a few bus voltages dropped (as the load increased, bus voltages dropped). At Akangba, Ayede, Ikeja-West, Kano, Oke-Aro, and Sakete buses, with converter ratings of 400 MVA, the voltage dropped is higher than with converter ratings of 500 MVA and 800 MVA, as shown in Table 4.12.

The study revealed that as the converter rating rises from 400 MVA to 800 MVA in the load flow analysis, the power losses decline while the generation and load values are mostly constant. Similar trends are visible in the PV Analysis. The power losses diminish, and the generation and load values remain steady as the converter rating rises. The PV data demonstrate that the voltage magnitude at various bus stations can be affected by the presence of HVDC systems with differing ratings. The effect varies according to the HVDC rating.

Overall, decreasing power losses in the system is achieved by raising the converter rating. This shows that electricity transmission efficiency can be increased by using higher-rated converters.

Table 4.11: Result with different converter ratings.

	Load flow			**PV Analysis**		
Power rating (MVA)	Generation (MW)	Load (MW)	Losses (MW)	Generation (MW)	Load (MW)	Losses (MW)
400	4790	4654	135	10487	8329	2158
500	4789	4654	134	10475	8329	2147
800	4784	4654	130	10469	8330	2140

Table 4.12: PV calculation (Voltage drop result for each converter rating).

	No HVDC	400 MVA	500 MVA	800 MVA
Bus	V(pu)	V(pu)	V(pu)	V(pu)
Aja	0.96	0.92	0.96	0.96
Akangba	0.96	0.67	0.96	0.96
Alagbon	0.96	0.91	0.96	0.96
Ayede	0.96	0.67	0.96	0.96
Gombe	0.91	0.91	0.99	0.99
Ikeja West	0.96	0.67	0.96	0.96
Jos	0.92	0.85	0.96	0.96
Kano	0.95	0.73	0.96	0.96
Katampe	0.96	0.90	0.97	0.97
Makurdi	0.96	0.89	0.98	0.98
Oke-Aro	0.95	0.59	0.95	0.95
Olorunsogo	0.97	0.78	0.97	0.97
Osogbo	0.98	0.85	0.98	0.98
Sakete	0.95	0.62	0.95	0.95

4.8 Discussion

The weak bus is often placed electrically and physically farthest from the generator in a radial transmission system, with a generator supplying several loads along the transmission line and with insufficient reactive power. This was identified from both PV and QV analyses performed on the Nigerian transmission network. The identified weak buses on the network are Gombe, Jos, Kaduna, Kano, Makurdi, and Yola, which are located far from the generator, with the buses hitting the nose point first and with low reactive power margin assessed from the PV and QV curve respectively (section 4.4.2)

The weakest buses were identified in terms of voltage magnitude and voltage critical point, which determined the best location for HVDC. Gombe and Yola were the points considered for testing the best HVDC location on the network because they have the lowest critical voltage. During the PV analysis, Gombe was considered the best location due to the positive outcomes in voltage improvement on the buses from 0.69 pu to 1.00 pu for Gombe bus and 0.66 pu to 0.98 pu for Yola bus with generated power of 10690 MW (Figure 4.3). Furthermore, in the QV analysis, Yola bus was considered the best position for the HVDC location as the marginal reactive power was achieved when the HVDC was connected to the Yola bus from -54 MVAR (purple curve) to -448 MVAR (green curve) with an improvement on the critical voltage from 0.67 pu to 0.61 pu. The operating point improved from 0.91 pu to 0.99 pu on Gombe bus and 1.00 pu on Yola bus (Figure 4.5).

It was also concluded from the impact of the control mode variation that the HVDC control does not have much effect on the load flow analysis but is significant for PV analysis. The effects are felt on the generated power and critical demand where controllers I and II have a higher power generated than controllers III and IV (Table 4.9). The PV analysis also revealed that as the load increases, the voltage drop is higher with controllers I and II than with controllers III and IV (Table 4.10). The study observed that a converter rating of 500 MVA has a higher generating power on the network compared to another converter rating studied on the network, while controller I (*Vdc-Q*/*P-Vac*) has a higher generating power.

4.9 Conclusion

In this chapter, the stability analysis study was conducted for Nigeria's transmission system, based on data provided by the Nigeria Electricity System Operator - NESO during the summer of 2019 using the PowerFactory (PF) software. An HVDC model was developed and introduced to existing Nigeria High Voltage Alternating Current (HVAC) for investigation. Ongoing research on HVDC is being conducted to address gaps in Nigeria's power system. Through the provided data by the NESO, scenarios were established in the PF environment and analysed accordingly. Stability simulation studies were carried out using PV and QV analysis to determine weak buses on the network.

The two connections, Azura-Gombe (Case 1) and Azura–Yola (Case 2), were chosen to investigate the effect of the HVDC link on system stability with established indices from PV and QV analyses. The findings of the stability studies showed an increased improvement in overall system reliability in both situations. However, based on the QV analysis, the most sensitive bus was determined for the best location of HVDC, and the introduction of an HVDC line between Azura and Yola (referred to as Case 2) revealed better performance, both in terms of voltage profile and the reactive power margin (RPM). The amount of reactive power to be absorbed for the bus to operate at a voltage profile of 0.99 pu for Gombe and 1.00 pu for the Yola bus with an improved critical point of 0.61 pu and reactive marginal point of -448 MVAR was obtained. HVDC appears to be a promising initiative for the Nigerian Power System network to address the challenges of losses and instability experienced by the Nigerian Transmission Grid. The next steps of this work will include an economic analysis.

5 Economic Analysis

5.1 Introduction

In planning a power project, it is essential to find economically viable and technically equal options so that financial resources can be allocated and recovered as efficiently as possible [160]. The economic viability of power projects is crucial in the rapidly changing energy market, necessitating thorough analysis to meet rising energy demands and promote sustainable solutions [161]. By evaluating various options' benefits, drawbacks, and risks, stakeholders make well-informed decisions that will guarantee the effective use of available funds and energy's long-term durability and reliability [162].

As energy becomes an essential input, utilities are under pressure to enhance the quality of their supply. The capacity to meet demand is hampered by ongoing worries about financial stability, operational effectiveness, and long-term viability [163]. Nigeria's growth depends on its ability to produce enough power, which affects industry and promotes economic independence and development [164].

Therefore, an HVDC emerged as a feasible and valuable option with the potential to solve the country's rising electricity consumption [165], [166]. Consequently, there is a need for an economic study to evaluate the HVDC connection and investment. The identification and selection of government investment that will substantially improve the general well-being of consumers and the nation will be aided by economic analysis of HVDC projects [167]. The study is essential to understand the economic implications and potential advantages of having HVDC investments [168]. These investments typically entail financial commitments [163], significantly driven by equipment costs and the construction process [169]. Therefore, an economic study of power systems evaluation and investment is required to make a wise investment decision for power system management [168].

Many businesses choose to protect themselves from outages by purchasing expensive generators and facilities, which raises production costs and causes environmental pollution. Hence, unreliable power supply and outages have a sizeable economic cost and contribute to greenhouse gas (GHG) emissions [21], [165], [166]. However, this also gives more attention

to the economic analysis of HVDC technology for power transmission systems. Therefore, the discussion of financial effects on HVDC links in the HVAC Nigeria transmission network is the focus of this chapter.

Discounted cash flow analysis helps determine the present value of expected future cash flows using a discount rate. Investors widely use this technique to evaluate whether a project's projected future cash flows exceed the initial investment's value. A DCF analysis can be applied to value various assets, and it is commonly used in the investment industry and corporate finance management. The opportunity should be considered if the calculated DCF value exceeds the current investment cost. However, if the calculated value is lower than the cost, it is not an excellent opportunity to pursue. To perform a DCF analysis, an investor must estimate future cash flows and the asset's ending value, such as equipment or other assets [170], [171]. Furthermore, DCF analysis, extending beyond simple cash flow analysis, accounts for the time value of money and the associated risks of project investment. It evaluates project performance through metrics like Net Present Value (NPV), Internal Rate of Return (IRR), and Benefit-Cost (B/C) ratios[172], [173].

The selection of the appropriate method depends on the specific context, objectives, and available data for the economic analysis. However, in this study, the NPV method is considered because it considers the time value of money [174]. The current worth of a project's cash flows at the required rate of return, as compared to the initial investment, is known as net present value (NPV). Practically, NPV is a way to figure out how much money is invested in a project. Evaluating if the predicted financial gains outweigh the present-day investment is necessary. This requires reviewing all anticipated returns from the investment and translating those returns into financial terms [169], [175], [176]. Generally, the net present value (NPV) is calculated by adding the discounted yearly cash flows, which are characterised by discounting future cash flows [172], [177].

The NPV of an investment is the difference between the present value of benefits (cash inflows) and the present value of costs (cash outflows) over the investment's economic life. A viable investment usually has a positive NPV, which means that the present value of benefits exceeds the present value of costs [178]. NPV tool was chosen to carry out this analysis and identify various alternative options for a transmission link. It is used to confirm an investment's long-term financial viability.

This chapter provides some elements for the economic analysis of HVDC links between Azura generating station to Gombe load (Case 1) and the link to Yola (Case 2) load bus in the present Nigeria HVAC transmission network. This economic consideration will have a crucial

role in identifying the worth of investing in this transmission technology as the economic calculation function will be used to analyse the costs and benefits of network expansion using NPV [65], [172], [179].

5.2 Literature review

In-depth research has recently been concentrated on the economic analysis of HVDC networks, and to assess the HVDC technology's financial viability and cost-effectiveness in various power transmission scenarios, researchers have carried out a series of significant analyses. The results in [180] provide crucial information on the price differences between HVAC and HVDC transmission lines. When the transmission line distance is greater than 800 km, it is seen that the substation expenses for AC systems outweigh those for DC systems. In contrast, when an overhead transmission line is longer than 600 km, the cost of the transmission lines for DC systems is cheaper than for AC systems. These findings highlight the cost dynamics, power losses, and voltage drops in both AC and DC systems, emphasising the value of performing cost assessments in high-voltage transmission systems. These observations help us better understand cost factors and offer advice for choosing and implementing transmission technology [180].

The work presented in [181] carried out the techno-economic comparison of HVAC and HVDC for a 4000 MW power station 878 km from the load centres in Pakistan. The authors assessed the economic viability of both transmission networks using the Discounted Cash Flow (DCF) method. A unique Excel/Microsoft-based system was created to examine the effects of numerous input elements on economic comparison. The results showed that compared to HVAC, a VSC-HVDC bipolar transmission system offered a more affordable, effective, and black-start-capable option than HVAC. The VSC-HVDC system's NPV, computed at 2361.7 M$, was lower than that of HVAC, which shows the financial benefits of HVDC for long-distance power transmission [181].

In [40], the study of HVDC links was conducted in New York, where the HVDC project was conducted from upstate New York (Hudson Valley) to southeast New York (Mohawk Valley). It is intended to have a nominal voltage of 400 kV and a rated power flow capacity of 1200 MW. The research revealed that 9.72 M$ reduced consumer payment, and the producer net profit increased by 27.45 M$. It suggests that constructing the HVDC link will benefit generator owners more financially than load customers as the revenue from the transmission

congestion is reduced by 10.89 M$. Hence, the total annual benefit revealed from the economic analysis was 26.28 M$ [40].

The economic assessment of the Low-Frequency AC (LFAC) transmission and HVDC transmission system was carried out for a large offshore wind farm in Korea [182]. A wind farm capacity of 600 MW and 900 MW with distances from 25 km to 100 km from the onshore grid was investigated. The economic analyses of the two separate transmission systems are compared and examined, and the results demonstrate that the LFAC transmission system provides more significant financial benefits than HVDC over distances up to about 60 km for the 600 MW wind farm. It also offers substantial economic benefits for the 900 MW wind farm up to about 110 km [182].

The analysis carried out by [183] compares the cost implication of HVAC, HVDC, gas-insulated transmission Line (GIL), and hybrid HVDC for offshore wind power in Guangdong Province in Eastern China by studying the capital costs, operation and maintenance costs, and loss costs [183]. It was revealed that while the cost of AC-type and GIL transmission technology is generally influenced by expenses linked to the transmission lines and compensation, the capital cost of DC-type transmission technology is mainly influenced by investments in converters. The report also revealed that the capacity of the transmission line and the offshore distance significantly impact capital costs. Compared to the HVAC and HVDC transmission concepts, the GIL electrical transmission concept's economic costs are much higher [183].

The study by [184] proposes a VSC-HVDC transmission link to connect Herat province in the west of Afghanistan, which has potential renewable energy, to Kabul, the country's capital and primary load centre. A techno-economic study of HVDC versus HVAC technology was conducted to assess the feasibility and effectiveness of the proposed transmission system. The project proposes to carry 1000 MW of power at 500 kV voltage through a 640-kilometer stretch. The active power, reactive power, and corona losses were estimated as technical characteristics, and the discounted cash flow (DCF) approach was used to evaluate both systems economically. Technically and financially, HVDC was established as an alternative for bulk power transmission over large distances with lower losses. The findings show that implementing the HVDC transmission project is technically and economically possible and can contribute to the country's energy security and economic stability [184].

Overall, many studies on the economic evaluation of HVDC transmission were retrieved from the literature. These studies offer insightful information about the advantages of HVDC technology and its financial viability. They emphasize how HVDC technology for long-

distance power transmission is affordable, financially viable, and has several other economic benefits.

5.3 Economic analysis methodology

In this chapter, the economic assessments of the HVDC link on the Nigerian network will be carried out using the NPV technique. The economic analysis will be presented for the three cases described in Chapter 3:

- Case 0 (Base Case) - when no HVDC is on the network.
- Case 1- a connection between Azura and Gombe
- Case 2 - a connection between Azura and Yola

In earlier studies, such as the load flow, reliability analysis [9], [36], and stability study, these two buses were recognised as having the lowest voltage magnitude, lowest reliability, and weakest bus, respectively, on the network.

The HVDC model has been described in Chapters 1 and 3. For the economic analysis, data was obtained from NESO, and some assumptions of cost were made based on the works of literature.

The NPV is calculated by summing up all the present values of the projected cash flows. Projects with positive net benefits are seen as viable, and those with higher net present values (NPV) and those with lower NPVs are deemed less profitable. In other words, the project with a higher NPV indicates more incredible expected calculated net benefits from the investment [185], [186]**.** The economic benefit of HVDC installed in the cases (Case 1 and 2) is then evaluated.

The cost of the convert stations is approximately 400 M$, and the overhead lines cost is estimated to be 150 M$ [184]. The economic factors that are impacted by the nation's economy and are subjected to periodic change are considered while evaluating transmission line costs [169]. Thus, an assumption of an 18% interest rate is considered in this work [187] with a technical life expectancy of 40 years, which is estimated according to the previous project that was commissioned [188], [189]. The CfL and EIC for the first year were manually calculated, and the results for CfL, EIC, and NPV were run for 40 years.

To carry out the economic analysis, the investment cost (IC), annual maintenance cost, scrap values (SV), cost for losses (CfL), and expected interruption cost (EIC) are required, and this is discussed in the section below.

5.3.1 Economic analysis

Economic factors like investment, inflation, and interest rates affect the transmission line's life cycle costs; hence, these components must be evaluated [169]. Therefore, a realistic estimate of this investment, including the cost of these components, is necessary. Thus, the data for expenses for the investment were obtained from a literature search [181], [184], [190]. The USD ($) is used in the research because PF adopts this unit. Hence, the Nigerian currency, Naira (#), is converted to $.

To carry out the economic analysis, the investment cost (IC), annual maintenance cost, scrap values (SV), cost for losses (CfL), and expected interruption cost (EIC) are required, and they are discussed below. Mathematically, NPV is calculated as follows:

$$\mathrm{NPV} = \mathrm{TIC} + \mathrm{DAC} \tag{5.1}$$

where TIC is the total investment cost, and DAC is the discounted annual cost.

- Investment cost (IC)

The component and total investment cost (TIC) for VSC-based HVDC transmission systems is shown in Table 5.1. The components are substations/converter stations and overhead transmission lines. The cost of the HVDC equipment is given in equation 5.2.

$$\mathrm{TIC} = \mathrm{CS_c} + \mathrm{OTS_c} \tag{5.2}$$

where CSc and OTSc are the cost of the substation and overhead transmission system (lines and poles), respectively [181]. The data given in Table 5.1 is adapted from some pieces of literature.

- Annual maintenance cost

This is the expense incurred to maintain and keep the installation in the best working condition, estimated at 6 M$ [184].

Table 5.1: Data used for economic analysis.

Total investment cost (TIC)	550 M$
Scrap value	8 M$
Life span	40 years
Interest rate	18%
Energy tariff	0.15 $/kWh

- Scrap values (SV)

This gives the estimated worth of the HVDC equipment when it is no longer productive or economically viable. It was determined using the declined balance method and assuming the deprecation rate of 10% per year [191]. The expression is given in (5.3), and the result is shown in Appendix A.0.4.

Scrap value = Total investment cost – (depreciation rate at the end of the life span of the asset)

$$\text{SV} = \text{TIC} - (10\% \text{ of the asset value for its lifespan}) \tag{5.3}$$

- Cost for losses (CfL)

These are the costs for the losses on the line, which are calculated using (5.4) [65] based on the energy tariff [190].

$$\text{CfL} = \text{Tariff rate (ET)} \times \text{Line losses (Ll)} \times \text{hours in year (Hy)} \tag{5.4}$$

CfL is the cost for losses in $; ET is the energy tariff in $/kWh; Ll is the losses on the line evaluated in Chapter 2 (Table 2.4); Hy is the year's hours.

- Expected interruption cost (EIC)

On a monetary basis, it plays a crucial role in making an optimal investment decision [192]. It represents the projected expenses incurred due to a system's failure, breakdown, or unavailability, and it is measured in $/yr [65]. To evaluate EIC, the following data is required: load point energy not supplied (LPENS) MWh/yr, total fault duration (TFD), which has been calculated in Chapter 3, and the active power (P) of the interrupted load, which was given by the Nigeria Electricity System Operator (NESO). The LPENS and EIC were calculated using equations 5.5 and 5.6 respectively.

$$\text{LPENS} = \text{Total Fault Duration (TFD)} \times \text{Active power (P)} \tag{5.5}$$

$$\text{EIC} = \sum(\text{LPENS} \times \text{ET}) \tag{5.6}$$

5.4 Economic analysis results

The results of the economic analysis are presented and discussed in this section. The manually calculated results for the CfL and EIC for the first year are presented, and the results for CfL, EIC, and NPV were simulated for 40 years.

5.4.1 Manual calculation

This section manually calculated CfL and EIC for the first year using equations 5.4, 5.5, and 5.6, respectively.

- Cost for losses (CfL)

The cost for losses on the network for the first year is calculated, and the calculation requires energy tariff (ET), line losses (Ll) (from Chapter 2), and hours in the year (Hy). This was calculated as shown in equation 5.7 below:

$$\begin{aligned} \text{CfL} = \ & \text{ET} \times \text{Ll x Hy} = 0.15 \times 150 \ \times 8760 \\ = \ & 197.1 \text{ M\$} \end{aligned} \tag{5.7}$$

- Expected interruption cost (EIC)

To calculate the EIC, the load point energy not supplied (LPENS) for each interrupted load is required; the calculation requires the total fault duration (TFD), calculated in Chapter 3, and the active power NESO provided for each interrupted load. The LPENS and total expected interruption cost (TEIC) for Birni-Kebbi were calculated as shown in equations 5.9 and 5.11, respectively below:

$$\text{LPENS}_{\text{Birni}-\text{Kebbi}} = \text{TFD}_{\text{Birni}-\text{Kebbi}} \times \text{Power}_{\text{Birni}-\text{Kebbi}} \tag{5.8}$$

$$\text{LPENS}_{\text{Birni}-\text{Kebbi}} = 17.14 \times 198 = 3394 \quad \text{MWh/y} \tag{5.9}$$

This shows that for the Birnin-Kebbi load, with a total of 132899 customers (chapter 3), the energy not supplied is 3394 MWh/yr. The same was calculated for other buses with interruption, as shown in Table 5.2.

Table 5.2: Total load point energy not supplied (TLPENS).

Loads Interrupted	TFD (h/yr)	Power (MW)	LPENS (MWh/yr)
Birni-Kebbi	17.14	198	3394
Sakete	14.82	226	3349
Yola	3.49	73	225
Gombe	0.5	154	77
Kano	0.1	277	28
		TLPENS	7103

The TEIC on the network for the first year is calculated as shown in equation 5.11 below:

$$\text{TEIC} = \text{TLPENS} \times \text{ET} = 7103 \times 0.15 \ \$/\text{yr} \tag{5.10}$$

$$\text{TEIC} = 1065450 \ \$/\text{yr} = \ 1.07 \ \text{M}\$/\text{yr} \tag{5.11}$$

5.4.2 Simulation results

The simulation result for the network for the 40 years is presented in this section. The summary of the economic analysis result of the network is given in Table 5.3 - Table 5.5; the cases are evaluated based on the CfL, EIC, and NPV across 40 years.

Table 5.3: Summary of the economic analysis result (Case 0).

Investment (K$)	0
Annual cost (K$)	0
Depreciation Value (K$)	0
CfL(M$)	8028
EIC (M$)	44

Table 5.4: Summary of the economic analysis result (Case 1).

Investment (M$)	521
Annual cost (M$)	37
Depreciation Value (K$)	8.99
CfL(M$)	1116
EIC (M$)	6.9
NPV (M$)	1681

Table 5.5: Summary of the economic analysis result (Case 2).

Investment (M$)	521
Annual cost (M$)	37
Depreciation Value (K$)	8.99
CfL (M$)	1146
EIC (M$)	6.7
NPV (M$)	1711

Since there is no investment of an HVDC in Case 0, the result for CfL and EIC was only recorded for 40 years (Table 5.3). For Cases 1 and 2, the investment value decreases from 550 M$ (Table 5.1) to 521 M$ (Table 5.4) because of factors such as wear and tear and deterioration over a period, inflation rate, and time for money [193]. However, the analysis for Cases 1 and 2 is within the same network; therefore, the investment cost, annual cost, and depreciation value remain constant for the two cases (Table 5.4 and Table 5.5). As a result of the HVDC link on the network, the CfL and EIC values for Cases 1 and 2 were reduced

compared to Case 0. Case 2 has a higher CfL compared to Case 1, amounting to 1146 M$, because the generated power in Case 2 is higher (4788 MW as revealed in the stability analysis in Chapter 4 - Table ***4.5***) than the power generated in Case 1 (4784 MW, Table 4.4), thus resulting in a higher loss of 133 MW in Case 2.

It was also revealed that Case 0 has the highest EIC of 44 M$ because there was no HVDC, while the EIC of Case 2 (6.7 M$) is lower than Case 1 (6.9 M$). It suggested that Case 2 has a potentially lower impact from interruptions. Similarly, because Case 0 has no HVDC investment, there is no NPV value. Case 2 has a higher NPV of 1711 M$ than Case 1 with 1681 M$.

5.4.3 Economic impact

The economic analysis tables, Table 5.3 - Table 5.5, reveal some key findings as they demonstrate how the use of HVDC significantly reduced costs associated with losses. This means that energy losses decrease and efficiency increases using HVDC technology. Due to the marginally higher generated power in Case 2, the cost of losses is marginally higher than in Case 1. The fact that Case 1 and Case 2 perform better than Case 0 shows that HVDC is essential for reducing energy losses.

The EIC represents the estimated financial impact of interruptions. The EIC has significantly decreased because of adopting HVDC technology, and the cost of losses has also been reduced. This shows that HVDC improves the system's stability and reliability, reducing downtime and related economic losses. From the NPV results, Case 2 NPV is more significant than Case 1, which indicates that Case 2 produces a better net benefit over its lifespan of 40 years, and it is economically viable, resulting in better financial returns than Case 1.

5.4.4 Socioeconomic impact

The results provide a basis for conducting a socioeconomic analysis by considering the factors of net present value (NPV), cost for losses, and expected interruption cost. The socioeconomic impact of Case 0 substantial loss costs is significant. These losses will put a financial strain on businesses, raise consumer electricity bills, and cause interruptions in the energy supply. Using HVDC increases economic effectiveness, improves reliability, and may even result in a more efficient and dependable energy supply by significantly lowering loss-related costs.

The socioeconomic effects include increased electricity transmission sector performance, decreased financial losses, and increased energy efficiency. High EIC in Case 0

can have adverse socio-economic consequences. Frequent interruptions can disrupt industries, impact productivity, and cause inconvenience to consumers. The lower EIC in Cases 1 and 2 indicate improved reliability, reduced disruptions, and enhanced socio-economic stability. Lower predicted interruption costs are a sign of improved system reliability and stability. With the HVDC link on Case 2, the projects perform better and are more resilient, which would lead to fewer disruptions.

The higher NPV values in Case 2 compared to Case 1 point to better economic consequences. It demonstrates that Case 2 is more likely to produce investment profits, with Case 2 offering a higher net benefit, suggesting a greater possibility for economic returns and benefits throughout the 40-year lifespan. It is an economically viable investment, potentially leading to socioeconomic growth, job creation, and increased access to reliable energy. The result of the socioeconomic impact is out of the scope of this work; however, it may be a subject of future work.

5.5 Conclusion

In this chapter, an economic analysis study was conducted to connect HVDC to Nigeria's transmission network based on a reliability and stability analysis study. The analysis was carried out to connect the HVDC at two locations identified as weak buses, Azura-Gombe (Case 1) and Azura-Yola (Case 2). The HVDC technology improves the effectiveness and reliability of the power transmission networks, reducing energy losses and producing financial benefits in both Cases. However, the highest NPV is seen in Case 2, which, in turn, indicates higher economic performance compared to Case 1. This made Case 2 preferred over Case 1. The analysis carried out in this chapter was limited in scope due to the lack of data. Therefore, more extensive investigations will be required for a thorough assessment.

6 Summary of contributions and recommendations for future work

6.1 Conclusion

The research analysed the Nigeria 330 kV transmission system using the Nigeria Electricity System Operator (NESO) data. The study identified Gombe and Yola buses as the weakest buses on the network. As a result, they suffer from voltage deviation, low reliability, and weak conditions.

Adopting HVDC technology enhanced the system's reliability, stability, and economic performance. Two different HVDC interconnections were studied. The HVDC link between Azura and Yola (Case 2) improved performance overall. More specifically, the reliability result indicates that Case 2 provides the best results in both system indices (Table 3.17) and load point indices (Table 3.19). Regarding stability analysis, Case 2 is also preferred to Case 1 because it increased the network's performance regarding voltage profile and RPM (Table 4.7). Furthermore, with the economic analysis, the highest NPV is seen in Case 2 (Table 5.5), which, in turn, indicates higher financial performance compared to Case 1. The results suggest that HVDC technology can improve efficiency, loadablity, and reliability, and reduce energy losses, leading to favourable financial outcomes for the Nigerian transmission network.

6.2 Research contributions

This research has investigated High voltage direct current (HVDC) use within the Nigerian transmission system, considering technical and economic evaluation. The following is a summary of this research's contributions and accomplishments.

1. Load flow: The Nigerian transmission network was modelled considering two scenarios, summer (the rainy season) and winter (the dry season). The studies of these two scenarios allow for verifying and confirming the accuracy of load flow analysis techniques and models.

The model was established, and the model was ensured it matched the load flow results, and areas affected by voltage violations were identified.

2. HVDC model: an HVDC model with different control modes was built for different power system studies. Reliability data was included, and various control modes were defined.
3. Reliability study: The network's reliability was evaluated using the SAIDI, SAIFI, CAIDI, and ASAI methods in both summer and winter scenarios, which utilized different reliability metrics. The reliability research offered information about how well the transmission network performed, suggesting potential areas to enhance the system's reliability and reduce outages. Two locations (Case 1: Azura-Gombe and Case 2: Azura-Yola) were identified to test the impact of HVDC connections on system reliability. The results showed that both cases significantly improved overall system reliability regarding system and load indices.
4. The voltage stability analysis provided insights into the weak busbars in the Nigerian 330 kV network and highlighted the need for measures to improve voltage stability. Based on the base case results, which included load flow, PV, and QV analyses without HVDC connection, Gombe and Yola were identified as the critical buses. The loadability of the network increased dramatically by 123% in Case 1 and 119% in Case 2 when HVDC was introduced to the network. Also, the RPM improved from -43 MVAR to -306 MVAR in Case 1, while Case 2 improved from -54 MVAR to -448 MVAR, and the critical point improved from 0.67 pu to 0.61 pu. This implies that the collapse point is further away with 0.61 pu, increasing the loadability.
5. According to an economic study, HVDC technology benefits the Nigerian transmission system. Case 2 has the highest net benefit during the 40-year lifespan. Costs are decreased, system stability and reliability are increased, and a greater possibility of financial gain exists. In addition, the socioeconomic effects of HVDC deployment may support consumer and enterprise prosperity by improving economic growth and stability.

6.3 Recommendations for future work

There are a few recommendations for future research based on the findings of this work:

- In this research, a conventional point-to-point HVDC system that has only two converter stations was used. The benefits of building multi-terminal HVDC systems and their sustainability from an economic viewpoint can be carried out as part of future work.

- Further research could focus on using HVDC technology to integrate renewable energy sources into Nigeria's power system. Research how HVDC can help smoothly integrate large-scale renewable energy projects, like solar and wind farms, into the transmission network.
- Additional economic studies can be carried out as future work to investigate how HVDC developments might affect local business prospects, job growth, and overall economic expansion. This is to comprehend the more significant effect of HVDC development on communities, industry, and economic development.

References

[1] "2023 Population and Housing Census Strategy and Implementation Plan," Abuja, 2022. [Online]. Available: https://www.dosm.gov.my/v1/index.php?r=column/cone&menu_id=bDA2VkxRSU40STcxdkZ4OGJ0c1ZVdz09

[2] "Annual abstract of statistics 2019," Abuja, 2019. [Online]. Available: www.nigerianstat.gov.ng

[3] B. Bilquin and A. Delivorias, "Nigeria: Situation ahead of 2023 general election," 2023. [Online]. Available: http://www.europarl.europa.eu/thinktank

[4] C. C. Ibebuchi and I. O. Abu, "Rainfall variability patterns in Nigeria during the rainy season," *Sci. Rep.*, vol. 13, no. 1, pp. 1–12, 2023, doi: 10.1038/s41598-023-34970-7.

[5] N. Yusuf, D. Okoh, I. Musa, S. Adedoja, and R. Said, "A Study of the Surface Air Temperature Variations in Nigeria," *Open Atmos. Sci. J.*, vol. 11, no. 1, pp. 54–70, 2017, doi: 10.2174/1874282301711010054.

[6] I. B. Abaje and E. O. Oladipo, "Recent Changes in the Temperature and Rainfall Conditions Over Kaduna State, Nigeria," *Ghana J. Geogr.*, vol. 11, no. 2, pp. 127–157, 2019.

[7] B. A. Badejo, N. O. Ogunseye, and O. G. Olasunkanmi, "An evaluation of rural electrification in Nigeria: A study of Ibogun community, Ogun state," *Interdiscip. ...*, vol. 15, no. August, pp. 8–17, 2020, [Online]. Available: https://ph02.tci-thaijo.org/index.php/jtir/article/view/241088%0A

[8] O. G. Olasunkanmi, O. O. Olaluwoye, P. O. Alao, and M. O. Osifeko, "Synergy of Effective Power Sector and Town Planning," *FuLafia J. Sci. Technol.*, vol. 4, no. 2, pp. 38–42, 2018, doi: 10.13140/RG.2.2.11038.89925.

[9] O. G. Olasunkanmi, W. O. Apena, A. R. Barron, A. O. White, and G. Todeschini, "Impact of a HVDC Link on the Reliability of the Bulk Nigerian Transmission Network," *Energies*, vol. 15, no. 24, p. 9631, Dec. 2022, doi: 10.3390/en15249631.

[10] L. Aikins and C. Kwaku Amuzuvi, "Power System Stability Improvement of Ghana's Generation and Transmission System Using FACTS Devices," *J. Electr. Electron. Eng.*, vol. 8, no. 2, p. 47, 2020, doi: 10.11648/j.jeee.20200802.12.

[11] Y. N. Chanchangi, F. Adu, A. Ghosh, S. Sundaram, and T. K. Mallick, "Nigeria's

energy review: Focusing on solar energy potential and penetration," *Environ. Dev. Sustain.*, 2022, doi: 10.1007/s10668-022-02308-4.

[12] B. Nkwoh, "Electricity Power Systems and Renewable Energy," International Trade Administration U.S. Department of Commerce. [Online]. Available: https://www.trade.gov/country-commercial-guides/electricity-power-systems-and-renewable-energy#:~:text=Nigeria generates most of its,capacity of about 12%2C522 MW.

[13] USAID, "Power Africa in Nigeria," 2020. Accessed: Jun. 15, 2021. [Online]. Available: https://www.usaid.gov/powerafrica/nigeria

[14] R. Charlotte, B. S. Muhammad, M. A. Chiamaka, and N. E. Chysom, "Nigeria Electricity sector," *energypedia*. Open Africa Power Fellowship Programme, 2021. [Online]. Available: https://energypedia.info/wiki/Nigeria_Electricity_Sector

[15] O. Akinsoji, "The Nigerian power sector investment opportunities and guidelines," 2016.

[16] IEA, "Electricity 2024 Analysis and Forecast to 2026," pp. 3–11, 2024, [Online]. Available: https://www.iea.org/reports/electricity-2024

[17] NERC, "Transmission." Accessed: Mar. 08, 2023. [Online]. Available: https://nerc.gov.ng/index.php/home/nesi/404-transmission

[18] O. O. Akinbobola, "Examining the Legal Compatibility and Regulation of Distributed Ledger Technology in Facilitating Decentralized Energy in Nigeria," University of Calgary, 2022. [Online]. Available: https://prism.ucalgary.ca.

[19] O. G. Olasunkanmi, A. O. Oyodeji, and A. A. Okubanjo, "Fault analysis and prediction of power distribution networks on 11kV Feeders: A case study of Eleweeran and Poly Road 11kV Feeders, Abeokuta," vol. 8, no. 1, pp. 37–48, 2020, [Online]. Available: www.journals.manas.edu.k

[20] A. Adewale, A. Chibuzor, S. Segun, and O. Nike, "A Guide to the Nigerian Power Sector," KPMG Professional Services, Nigeria, 2016. [Online]. Available: kpmg.com/ng

[21] O. G. Olasunkanmi, C. N. Nwaokocha, and W. O. Apena, "Analysis of energy generation spectrum and management in a private power plant in Ogun state, Nigeria," *Ann. Fac. Eng. Hunedoara– Int. J. Eng.*, no. 19, pp. 207–212, 2021.

[22] K. Ogunyale, "Nigeria's Power Generation Drops By 990MW," twentyten. Accessed: Mar. 13, 2024. [Online]. Available: https://twentytendaily.com/nigerias-power-generation-drops-by-990mw/

[23] A. Abdulkareem, A. Adesanya, A. F. Agbetuyi, and A. S. Alayande, “Novel approach to determine unbalanced current circuit on Nigerian 330kV transmission grid for reliability and security enhancement,” *Heliyon*, vol. 7, no. 7, p. e07563, 2021, doi: 10.1016/j.heliyon.2021.e07563.

[24] N. V. Emodi and S. D. Yusuf, “Improving electricity access in Nigeria: Obstacles and the way forward,” *Int. J. Energy Econ. Policy*, vol. 5, no. 1, pp. 335–351, 2015.

[25] J. Augutis, R. Krikstolaitis, R. Alzbutas, V. Matuzas, and E. Uspuras, “Reliability analysis of the electricity transmission system in Lithuania,” *Manag. Inf. Syst.*, vol. 9, pp. 573–580, 2004.

[26] O. G. Olasunkanmi, M. R. Adu, and W. O. Apena, “Enhancing Nigeria’s Power Grid Performance through a Hybrid Transmission Network,” *Niger. J. Technol. Res.*, vol. 14, no. 2, pp. 10–17, 2019, doi: https://dx.doi.org/10.4314/njtr.v14i2.2.

[27] C. O. Ojukwu and C. Odumegwu, “TECHNICAL LOSSES MITIGATION IN 330 KV NIGERIA TRANSMISSION NETWORK SYSTEMS,” no. 12, pp. 1076–1098, 2020.

[28] J. Vanishree and V. Ramesh, “Voltage profile improvement in power systems - A review,” in *2014 International Conference on Advances in Electrical Engineering, ICAEE 2014*, Vellore, India: IEEE, 2014, pp. 1–4. doi: 10.1109/ICAEE.2014.6838533.

[29] S. Garip, Ş. Özdemir, and N. Altın, “Power system reliability assessment - A review on analysis and evaluation methods,” *J. Energy Syst.*, vol. 6, no. 3, pp. 401–419, 2022, doi: 10.30521/jes.1099618.

[30] T. T. Wondie and T. G. Tella, “Voltage Stability Assessments and Their Improvement Using Optimal Placed Static Synchronous Compensator (STATCOM),” *J. Electr. Comput. Eng.*, vol. 2022, p. 12, 2022, doi: 10.1155/2022/2071454.

[31] O. M. Bamigbola, M. M. Ali, and K. O. Awodele, “Predictive models of current, voltage, and power losses on electric transmission lines,” *J. Appl. Math.*, vol. 2014, pp. 1–5, 2014, doi: 10.1155/2014/146937.

[32] A. Abdulkareem, T. E. Somefun, C. O. A. Awosope, and O. Olabenjo, “Power system analysis and integration of the proposed Nigerian 750-kV power line to the grid reliability,” *SN Appl. Sci.*, vol. 3, no. 12, 2021, doi: 10.1007/s42452-021-04847-3.

[33] Federal Ministry of Finance Budget and National Planning, “National Development Plan 2021-2025,” Nigeria, 2021.

[34] O. G. Olasunkanmi, P. O. Alao, F. Onaifo, M. O. Osifeko, and J. O. Sholabi, “Reliability assessment of a gas generating station in Ogun State, Nigeria,” *J. Appl. Sci. Environ. Manag.*, vol. 22, no. 6, p. 1005, 2018, doi: 10.4314/jasem.v22i6.27.

[35] N. A. A. Samaan, “Reliability Assessment of Electric Power Systems Using Genetic Algorithms,” Texas A&M University, Texas, 2004. Accessed: Feb. 18, 2021. [Online]. Available: https://core.ac.uk/download/pdf/147123137.pdf

[36] O. G. Olasunkanmi, Z. Deng, and G. Todeschini, “Load flow analysis of the Nigerian transmission grid using DIgSILENT PowerFactory,” in *2021 56th International Universities Power Engineering Conference (UPEC)*, Middlesbrough: IEEE, 2021, pp. 8–13. doi: https://doi.org/10.1109/UPEC50034.2021.9548253.

[37] Nationalgrid, “High Voltage Direct Current ELECTRICITY- technical information,” London. [Online]. Available: www.nationalgrid.com

[38] C. J. Pillay, M. Kabeya, and I. E. Davidson, “Transmission systems: HVAC vs HVDC,” in *Proceedings of the International Conference on Industrial Engineering and Operations Management*, 2020, pp. 2061–2077.

[39] O. O. Akinte, T. S. Aina, and O. O. Akinte, “HVAC VS HVDC Power System: Contemporary Development In HVAC And HVDC Power Transmission System,” *Int. J. Sci. Technol. Res.*, vol. 10, no. 06, pp. 252–261, 2021, [Online]. Available: www.ijstr.org

[40] S. Wang, J. Zhu, L. Trinh, and J. Pan, “Economic assessment of HVDC project in deregulated energy markets,” *3rd Int. Conf. Deregul. Restruct. Power Technol. DRPT 2008*, pp. 18–23, 2008, doi: 10.1109/DRPT.2008.4523373.

[41] A. Nishioka, F. Alvarez, and T. Omori, “Global Rise of HVDC and Its Background,” 2020.

[42] V. G. Csutar, S. Kallikuppa, and L. Charles, “Introduction to HVDC Architecture and Solutions for Control and Protection,” Texas, 2022.

[43] A. Rehman, M. A. Koondhar, Z. Ali, M. Jamali, and R. A. El-Sehiemy, “Critical Issues of Optimal Reactive Power Compensation Based on an HVAC Transmission System for an Offshore Wind Farm,” *Sustain.*, vol. 15, no. 19, 2023, doi: 10.3390/su151914175.

[44] V. G. Csutar, S. Kallikuppa, and L. Charles, “Introduction to HVDC Architecture and Solutions for Control and Protection,” 2021.

[45] N. R. Watson and J. D. Watson, “An overview of HVDC technology,” *Energies*, vol. 13, no. 17, 2020, doi: 10.3390/en13174342.

[46] M. Gul, N. Tai, W. Huang, M. H. Nadeem, M. Ahmad, and M. Yu, “Technical and economic assessment of VSC-HVDC transmission model: A case study of South-Western region in Pakistan,” *Electron.*, vol. 8, no. 11, 2019, doi:

10.3390/electronics8111305.

[47] nationalgrid, “Interconnectors.” Accessed: Mar. 19, 2024. [Online]. Available: https://www.nationalgrid.com/national-grid-ventures/interconnectors-connecting-cleaner-future

[48] T. Magg, M. Manchen, E. Krige, J. Wasborg, and J. Sundin, “Connecting networks with VSC HVDC in Africa: Caprivi Link Interconnector,” in *IEEE PES PowerAfrica 2012 Conference and Exposition Johannesburg, South Africa*, 2012.

[49] O. Heyman, L. Weimers, and M. Bohl, “HVDC – A key solution in future transmission systems,” 2011.

[50] I. E. Davidson, O. E. Oni, A. Aluko, and E. Buraimoh, “Enhancing the Performance of Eskom’s Cahora Bassa HVDC Scheme and Harmonic Distortion Minimization of LCC-HVDC Scheme Using the VSC-HVDC Link,” *Energies*, vol. 15, no. 11, 2022, doi: 10.3390/en15114008.

[51] NERC, “Nigerian Electricity Regulatory Commission Regulation for Mini-Grids 2016,” 2016. Accessed: Jun. 05, 2021. [Online]. Available: https://nerc.gov.ng/index.php/home/nesi/403-generation

[52] M. A. Jimoh and B. Raji, “Electric Grid Reliability: An Assessment of the Nigerian Power System Failures, Causes and Mitigations,” *Covenant J. Eng. Technol.*, vol. 7, no. 1, pp. 17–20, 2023.

[53] Transmission Company of Nigeria, “Grid maps.” Accessed: Mar. 10, 2024. [Online]. Available: https://www.tcn.org.ng/page_repository.php

[54] “The Nigeria Electricity System Operator.” Accessed: Jun. 05, 2021. [Online]. Available: https://www.nsong.org/Default

[55] D. Elmakias, *New Computational Methods in Power System Reliability*, 1st ed., vol. 111, no. 12. in Studies in Computational Intelligence, vol. 111. Berlin, Heidelberg: Springer Berlin Heidelberg, 2008. doi: 10.1007/978-3-540-77812-7.

[56] A. Ajayi, C. Anyanechi, S. Sowande, Marie, -, and T. Phido, “A Guide to the Nigerian Power Sector,” *KPMG Niger.*, no. December, pp. 1–27, 2013, [Online]. Available: http://www.kpmg.com/Africa/en/IssuesAndInsights/Articles-Publications/Documents/Guide to the Nigerian Power Sector.pdf

[57] Nigerian Electricity Regulatory Commission (NERC), “The Grid Code for the Nigeria Electricity Transmission Index version II,” in *Grid Code*, 2010, pp. 47–49. Accessed: May 30, 2021. [Online]. Available: https://www.abujaelectricity.com

[58] DigSILENT GmbH, “POWERFACTORY APPLICATIONS.” [Online]. Available:

https://www.digsilent.de/en/powerfactory.html

[59] DigSILENT GmbH, “DIgSILENT PowerFactory Simulation and Analysis Software.” Accessed: Mar. 28, 2024. [Online]. Available: https://www.digsilent.me/dme/node/887

[60] M. P. Bahrman and B. K. Johnson, “The ABCs of HVDC Transmission Technologies: An overview of High Voltage Direct Current Systems and Applications,” *IEEE Power & Energy Magazine*, vol. 5, no. 2, p. 245, Mar. 2007.

[61] X. Yang and H. Zhang, “Active Power Shifting Strategy for the Bipolar Active Power Shifting Strategy for the Bipolar VSC-MTDC,” in *IOP Conf. Series: Earth and Environmental Science 223 (2019) 012042*, IOP Publishing, 2019. doi: 10.1088/1755-1315/223/1/012042.

[62] M. P. Bahrman, J. G. Johansson, and B. a Nilsson, “Voltage Source Converter Transmission Technologies - The Right fit for the application,” *Power Eng. Soc. Gen. Meet.*, pp. 1–8, 2003.

[63] A. Kierad, “Load flow (power flow) - step-by-step, theory and calculation.” Accessed: Feb. 13, 2021. [Online]. Available: https://electrisim.com/load-flow-power-flow.html

[64] O. A. Afolabi, W. H. Ali, P. Cofie, J. Fuller, P. Obiomon, and E. S. Kolawole, “Analysis of the Load Flow Problem in Power System Planning Studies,” *Energy Power Eng.*, vol. 7, no. September, pp. 509–523, 2015, doi: http://dx.doi.org/10.4236/epe.2015.710048.

[65] DIgSILENT, *PowerFactory 2020 User Manual*, 2020th ed. Germany: DIgSILENT GmbH Heinrich-Hertz-Straße 9, 2020.

[66] D. P. Kothari and I. J. Nagrath, *Modern Power Systems*, Third. New Delhi: Tata McGraw Hill Education Private Limited, 2009.

[67] Y. M. S. Hlaing and A. Z. Ya, “Performance Analysis on Transmission Line for Improvement of Load Flow,” *Adv. Mater. Res.*, vol. 433–440, no. January 2012, pp. 7208–7212, 2012, doi: 10.4028/www.scientific.net/AMR.433-440.7208.

[68] “Load Flow or Power Flow Analysis | Electrical4U,” *Https://Www.Electrical4U.Com/*. Accessed: Mar. 02, 2023. [Online]. Available: https://carelabz.com/load-flow-analysis/

[69] S. Dey and T. Bhattacharya, “Monopolar operation of Modular Multilevel DC-DC Converter Based Hybrid Bipolar HVDC Links,” *2021 IEEE Texas Power Energy Conf. TPEC 2021*, 2021, doi: 10.1109/TPEC51183.2021.9384953.

[70] S. AG, “High Voltage Direct Current Transmission – Proven Technology for Power Exchange,” Germany, 2016. doi: 10.4018/978-1-5225-0884-7.les6.

[71] “Load Flow or Power Flow Analysis | Electrical4U,” *https://www.electrical4u.com/*,

Accessed: Feb. 13, 2021. [Online]. Available: https://www.electrical4u.com/load-flow-or-power-flow-analysis/

[72] A. Dubey, "Load Flow of Analysis Power Systems.," *Int. J. Sci. Eng. Res.*, vol. 7, no. 5, pp. 79–84, 2016.

[73] M. Albadi, "Power Flow Analysis," in *Computational Models in Engineering*, Konstantin Volkov, Ed., United Kingdom: IntechOpen, 2020, pp. 2–22. doi: 10.5772/intechopen.83374.

[74] B. Radović, M. Müller-Mienack, and C. Hewicker, "A Regulator ' S Guide To the Use of Load Flow Study Tools for a Regulator ' S Guide To the Use of Load Flow Study Tools for Transmission," USA, 2020. [Online]. Available: https://pubs.naruc.org/pub.cfm?id=93118741-155D-0A36-314D-7D52BF2F62C1

[75] S. S. Al-Hajri and I. O. Habiballah, "Review of Solution Techniques for Load Flow Studies," *Int. J. Eng. Res. Technol. www.ijert.org*, vol. 11, no. 12, pp. 49–52, 2022, [Online]. Available: www.ijert.org

[76] A. Vijayvargia, S. Jain, S. Meena, V. Gupta, and M. Lalwani, "Comparison between Different Load Flow Methodologies by Analyzing Various Bus Systems," *Int. J. Electr. Eng.*, vol. 9, no. 2, pp. 127–138, 2016, [Online]. Available: http://www.irphouse.com

[77] L. Powell, *Power System Load Flow Analysis*, 1st ed., vol. 1, no. 1. McGraw-Hill Education, 2005.

[78] I. Samuel, J. Katende, S. A. Daramola, and A. Awelewa, "Review of System Collapse Incidences on the 330-kV Nigerian National Grid," *Int. J. Eng. Sci. Invent.*, vol. 3, no. 4, pp. 55–59, 2014, [Online]. Available: www.ijesi.org55%7C

[79] F. Osazee Agbontaen, J. Osarumwense Egwaile, and I. K. Okakwu, "Power Flow Analysis of the Enhanced Proposed 330kV Transmission Network of the Nigeria Grid," *Mehran Univ. Res. J. Eng. Technol.*, vol. 38, no. 4, pp. 875–884, Oct. 2019, doi: 10.22581/muet1982.1904.02.

[80] U. C. Ogbuefi and T. C. Madueme, "A Power Flow Analysis of the Nigerian 330 kV Electric Power System.," *IOSR J. Electr. Electron. Eng.*, vol. 10, no. 1, pp. 46–57, 2015, doi: 10.9790/1676-10114657.

[81] B. E. Ibekwe, H. N. Nwobodo, and C. . Mgbachi, "Load Flow Studies on Nigeria 330KV National Grid System, Using Newton-Raphson's Method," *Int. Res. J. Microbiol.*, vol. 1, no. 4, pp. 39–52, 2014, doi: 10.14303/irjm.2014.022.

[82] S. A. Salgar and C. Mallareddy, "Load Flow Analysis for a 220Kv Line – Case

Study," *Int. J. Innov. Eng. Res. Technol. [IJIERT]*, vol. 2, no. 5, pp. 1–12, 2015.

[83] M. Ghiasi, "A Detailed Study for Load Flow Analysis in Distributed Power System," *Int. J. Ind. Electron. Control Optim. .© 2018 IECO…*, vol. 1, no. 2, pp. 153–161, 2018, doi: 10.22111/IECO.2018.24423.1027.

[84] M. V. Amritha and J. S. Savier, "Load Flow Analysis of Islanded Droop Regulated Microgrids," in *Proceedings of 2020 IEEE International Conference on Power, Instrumentation, Control and Computing, PICC 2020*, 2020, pp. 5–10. doi: 10.1109/PICC51425.2020.9362492.

[85] G. Anders and V. Alfredo, *Innovations in Power Systems Reliability*. New York: Springer Series in Reliability Engineering, 2011. doi: 10.1007/978-0-85729-088-5.

[86] K. V. Ajit, A. Srividya, and R. K. Durga, *Reliability and Safety Engineering*, Second., vol. 0, no. 9789811300882. New York: Springer London Heidelberg, 2018. doi: 10.1007/978-1-4471-6269-8.

[87] I. S. Qamber, *Power Systems Control and Reliability*. Canada: Apple Academic Press, Inc., 2020. [Online]. Available: www.appleacademicpress.com

[88] R. Allan, "Power system reliability assessment - A conceptual and historical review," *Reliab. Eng. Syst. Saf.*, vol. 46, no. 1, pp. 3–13, Jan. 1994, doi: 10.1016/0951-8320(94)90043-4.

[89] M. Ghiasi, N. Ghadimi, and E. Ahmadinia, "An Analytical Methodology for Reliability Assessment and Failure Analysis in Distributed Power System," *SN Appl. Sci.*, vol. 1, no. 1, pp. 1–44, Nov. 2018, doi: 10.1007/s42452-018-0049-0.

[90] J. Ayaburi, M. Bazilian, J. Kincer, and T. Moss, "Measuring 'Reasonably Reliable' access to electricity services," *Electr. J.*, vol. 33, no. 7, pp. 1–7, Aug. 2020, doi: 10.1016/j.tej.2020.106828.

[91] "IEEE Guide for Electric Power Distribution Reliability Indices," New York, Mar. 2012. Accessed: Sep. 10, 2021. [Online]. Available: https://ieeexplore.ieee.org/stamp/stamp.jsp?tp=&arnumber=6209381

[92] J. D. Kueck, J. K. Brendan, N. O. Philip, and C. M. Lawrence, "Measurement Practices for Reliability and Power Quality," 2004. Accessed: Feb. 20, 2021. [Online]. Available: https://info.ornl.gov/sites/publications/Files/Pub57467.pdf

[93] CEER (Council of European Energy Regulators), "6th CEER benchmarking report on the quality of electricity and gas supply," Brussels, Aug. 2016. Accessed: Mar. 05, 2021. [Online]. Available: http://webfileservice.nve.no/API/PublishedFiles/Download/201506197/2126667

[94] “5th CEER Benchmarking Report on Quality of Electricity Supply 2011,” Brussels, 2011.

[95] “Reliability and quality of supply of electricity to customers in NSW,” New South Wales, Jul. 2005.

[96] A. R. Khanorkar and N. Kinhekar, “Development of reliability assessment framework for extra high voltage transmission network in India and application on Maharashtra,” in *Proceedings - 2018 International Conference on Smart Electric Drives and Power System, ICSEDPS 2018*, IEEE, 2018, pp. 198–203. doi: 10.1109/ICSEDPS.2018.8536027.

[97] O. H. Abdalla *et al.*, “Key Performance Indicators of a Transmission System,” *Proc. 5th GCC Cigre Int. Conf.*, no. January, pp. 19–21, 2009.

[98] “SAIDI & SAIFI | kplc.co.ke.” Accessed: Aug. 30, 2021. [Online]. Available: https://kplc.co.ke/content/item/794/saidi---saifi

[99] Nationalgrid, “Managing Electricity Transmission Network Reliability Contents,” 2019.

[100] NationalgridESO, “National Electricity Transmission System Performance Report,” 2019.

[101] S. E. El-Arab and H. Zarzoura, “Reliability Evaluation for the Egyptian Transmission and Sub-Transmission Networks,” *PowerTech 2007*, pp. 1723–1725, 2007.

[102] J. N. Nweke, A. G. Gusau, and L. M. Isah, “Reliability and protection in distribution power system considering customer-based indices,” *Niger. J. Technol.*, vol. 39, no. 4, pp. 1198–1205, 2020, doi: 10.4314/njt.v39i4.28.

[103] G. Rouse and J. Kelly, “Electricity Reliability: Problems, Progress, and Policy Solutions,” 2011. [Online]. Available: http://www.galvinpower.org/sites/default/files/Electricity_Reliability_031611.pdf

[104] R. Billinton and R. N. Allan, *Reliability evaluation of engineering systems: concepts and techniques*, 2nd ed., vol. 5, no. 1. New York: Plenum Press, New York, 1992. doi: DOI 10.1007/978-1-4899-0685-4.

[105] C. Dechsiri, “Introduction to Stochastic Models and Markov Chains,” University of Groningen, 2004. [Online]. Available: http://www.rug.nl/research/portal

[106] A. Gibb, M. St-Jacques, G. Nourry, and M. Johnson, “A Comparison of Deterministic vs Stochastic Simulation Models for Assessing Adaptive Information Management Techniques over Disadvantaged Tactical Communication Networks,” *7th ICCRTS*, no. April 2002, pp. 1–16, 2002, [Online]. Available:

http://dodccrp.org/events/7th_ICCRTS/Tracks/pdf/076.PDF

[107] Faculty and Institute of Actuaries, “Description of Stochastic Models,” 1997. doi: 10.1016/b978-1-4831-9727-2.50016-8.

[108] F. Li, “Stochastic Methods For Optimization and Machine Learning,” 2005.

[109] P. Gajendrakar, “Stochastic Modeling.” Accessed: Mar. 04, 2024. [Online]. Available: https://www.wallstreetmojo.com/stochastic-modeling/

[110] G. L. Aschidamini, G. A. da Cruz1, M. Resener, R. C. Leborgne, and L. A. Pereira1, “A Framework for Reliability Assessment in Expansion Planning of Power Distribution Systems,” *Energies 2022*, vol. 15, no. 14:5073, pp. 1–24, 2022, doi: https://doi.org/10.3390/en15145073.

[111] S. O Okozi, “Reliability Assessment of Nigerian Power Systems Case Study of 330kv Transmission Lines in Benin Sub–Region,” *Int. J. Eng. Res.*, vol. V7, no. 03, pp. 399–405, 2018, doi: 10.17577/ijertv7is030181.

[112] J. Van der Merwe, “Simplified approach for the reliability estimation of large transmission and sub-transmission systems,” 2014.

[113] R. Billinton and S. Kumar, “A Comparative Study of System Versus Load Point Indices for Bulk Power Systems,” *IEEE Power Eng. Rev.*, vol. PWRS-1, no. 3, p. 41, 1986, doi: 10.1109/MPER.1986.5527791.

[114] P. U. Okorie, U. O. Aliyu, B. Jimoh, and S. M. Sani, “Reliability Indices of Electric Distribution Network System Assessment,” *Quest Journals J. Electron. Commun. Eng. Res.*, vol. 3, no. 1, pp. 1–6, 2015, [Online]. Available: www.questjournals.org

[115] Safegrid, “How to Improve SAIDI with Safegrid.” Accessed: Mar. 23, 2024. [Online]. Available: https://safegrid.io/how-safegrid-can-help-improve-saidi/

[116] J. Teixeira, “IEEE 1366-Reliability Indices,” Boston, Feb. 2019.

[117] A. A. Akintola and C. O. A. Awosope, “Reliability Analysis of Secondary Distribution System in Nigeria: A Case Study of Ayetoro 1 Substation, Lagos State,” *Int. J. Eng. Sci.*, vol. 06, no. 07, pp. 13–21, Jul. 2017, doi: 10.9790/1813-0607011321.

[118] A. Alassi, S. Bañales, O. Ellabban, G. Adam, and C. MacIver, “HVDC Transmission: Technology Review, Market Trends and Future Outlook,” *Renew. Sustain. Energy Rev.*, vol. 112, pp. 530–554, 2019, doi: 10.1016/j.rser.2019.04.062.

[119] H. F. Latorre., “Modeling and Control of VSC-HVDC Transmissions,” Royal Institute of Technology, 2011.

[120] D. M. Mohan, B. Singh, and B. K. Panigrahi, “Analysis, design and control of two-level voltage source converters for HVDC systems,” *J. Power Electron.*, vol. 8, no. 3,

pp. 248–258, 2008.

[121] DIgSILENT GmbH, *Technical Reference PWM Converter*. Germany: DIgSILENT GmbH Heinrich-Hertz-Straße 9, 2020.

[122] N. Flourentzou, S. Member, V. G. Agelidis, S. Member, and G. D. Demetriades, "VSC-Based HVDC Power Transmission Systems : An Overview," *IEEE Trans. POWER Electron.*, vol. 24, no. 3, pp. 592–602, 2009.

[123] A. Font, S. Ilhan, H. Ismailoglu, F. E. Cortes, and A. Ozdemir, "Design and technical analysis of 500-600 kV HVDC transmission system for Turkey," *2017 10th International Conference on Electrical and Electronics Engineering, ELECO 2017*, vol. 2018-Janua. pp. 201–205, 2018.

[124] "Converter," *Wartsila*. Accessed: Jan. 24, 2022. [Online]. Available: https://www.wartsila.com/encyclopedia/term/converter

[125] K. Linden, B. Jacobson, M. H. . Bollen, and J. Lundquist, "Reliability study methodology for HVDC grids," *Power*, pp. 1–10, 2010.

[126] X. Qin, P. Zeng, Q. Zhou, Q. Dai, and J. Chen, "Study on the development and reliability of HVDC transmission systems in China," in *2016 IEEE International Conference on Power System Technology, POWERCON 2016*, IEEE, 2016. doi: 10.1109/POWERCON.2016.7753862.

[127] Akinloye B O, P. O. Oshevire, and A. M. Epemu, "Evaluation Of System Collapse Incidences On The Nigeria Power System," 2016. [Online]. Available: www.jmest.org

[128] U. Department of Energy, "Reliability Improvements from the Application of Distribution Automation Technologies - Initial Results," Dec. 2012. [Online]. Available: www.smartgrid.gov.

[129] E. Saadati and A. Mirzaei, "Voltage Stability Indices: Taxonomy, Formulation and Calculation algorithm," *Int. J. Sci. Eng. Innov. Res.*, vol. 8, pp. 1–6, 2016.

[130] B. Ismail, N. I. A. Wahab, M. L. Othman, M. A. M. Radzi, K. N. Vijayakumar, and M. N. M. Naain, "New Line Voltage Stability Index (BVSI) for Voltage Stability Assessment in Power System: The Comparative Studies," *IEEE Access*, vol. 10, pp. 103906–103931, 2022, doi: 10.1109/ACCESS.2022.3204792.

[131] R. Verayiah and A. Mohamed, "Comparison of weak load bus detection using LQP_LT index with PV and QV analysis of PSS/E," *Indones. J. Electr. Eng. Comput. Sci.*, vol. 12, no. 2, pp. 577–584, 2018, doi: 10.11591/ijeecs.v12.i2.pp577-584.

[132] O. G. Olasunkanmi, A. R. Barron, A. Orbaek White, and G. Todeschini, "Evaluation of a HVDC Interconnection to Improve the Voltage Stability of the Nigerian

Transmission Network," *J. Electron. Electr. Eng.*, 2024, doi: 10.37256/jeee.3120243799.

[133] B. A. Badejo, O. G. Olasunkanmi, and N. O. Ogunseye, "Investigating Electricity Consumption in Ogun State, Nigeria," *J. Eng. Stud. Res.*, vol. 26, no. 1, pp. 7–18, 2020, doi: 10.29081/jesr.v26i1.344.

[134] C. Subramani, S. S. Dash, V. Kumar, and H. Kiran, "Implementation of line stability index for contingency analysis and screening in power systems," *J. Comput. Sci.*, vol. 8, no. 4, pp. 585–590, 2012, doi: 10.3844/jcssp.2012.585.590.

[135] S. Ratra, R. Tiwari, and K. R. Niazi, "Voltage stability assessment in power systems using line voltage stability index," *Comput. Electr. Eng.*, vol. 70, pp. 199–211, 2018, doi: 10.1016/j.compeleceng.2017.12.046.

[136] N. Hatziargyriou *et al.*, "Definition and Classification of Power System Stability - Revisited & Extended," *IEEE Trans. Power Syst.*, vol. 36, no. 4, pp. 3271–3281, 2021, doi: 10.1109/TPWRS.2020.3041774.

[137] P. Kundur *et al.*, "Definition and classification of power system stability," *IEEE Trans. Power Syst.*, vol. 19, no. 2, pp. 1387–1401, 2004, doi: 10.1109/TPWRS.2004.825981.

[138] Mehmet B. Keskin, "Continuation Power Flow and Voltage Stability in Power Systems," Middle East Technical University, 2007. [Online]. Available: http://digilib.unila.ac.id/11478/16/16. BAB II.pdf

[139] S. K. Mazumder and E. Pilo De La Fuente, "Stability Analysis of Micropower Network," *IEEE J. Emerg. Sel. Top. Power Electron.*, vol. 4, no. 4, pp. 1299–1309, 2016, doi: 10.1109/JESTPE.2016.2592938.

[140] A. S. Ravi, A. Dwivedi, and B. Sharma, "Voltage Stability Analysis," *Int. J. Sci. Eng. Res.*, vol. 4, no. 6, pp. 1572–1583, 2013.

[141] C. Reis and F. P. Maciel Barbosa, "A comparison of voltage stability indices," in *Proceedings of the Mediterranean Electrotechnical Conference - MELECON*, 2006, pp. 1007–1010. doi: 10.1109/melcon.2006.1653269.

[142] O. Mogaka, R. Orenge, and J. Ndirangu, "Static Voltage Stability Assessment of the Kenyan Power Network," *J. Electr. Comput. Eng.*, pp. 1–16, 2021, doi: 10.1155/2021/5079607.

[143] X. Li, Z. Li, L. Guan, X. Wu, Y. Mei, and J. Li, "Study on the Corresponding Relationship Between Critical Points of P-V Curve and V-Q Curve of Simple Thevenin Equivalent System," in *2020 IEEE 1st China International Youth Conference on Electrical Engineering*, Wuhan, China, 2020, pp. 1–7. doi:

10.1109/CIYCEE49808.2020.9332740.

[144] L. Zhang and H. Lennart, “Power System Reliability and Transfer Capability Improvement by VSC- HVDC (HVDC Light ©),” *CIGRE Reg. Meet.*, pp. 1–7, 2007.

[145] M. Haro-Larrode, “Variable Reactance Criteria to Mitigate Voltage Deviations in Power Transformers in Light- and Over-Load Conditions,” *Machines*, vol. 11, no. 8, 2023, doi: 10.3390/machines11080797.

[146] Western Power Distribution, “Project NETWORK EQUILIBRIUM: Voltage Limits Assessment Discussion Paper,” 2016.

[147] Energy Networks Association, “Voltage Measurements for Assessment of Compliance with Statutory Voltage Limits,” no. 1, pp. 1–9, 2017.

[148] E. D. Aguero, J. C. Cepeda, and D. G. Colome, “FACTS models for stability studies in DIgSILENT Power Factory,” in *2014 IEEE PES Transmission and Distribution Conference and Exposition, PES T and D-LA 2014 - Conference Proceedings*, Medellin, Colombia: IEEE, 2014. doi: 10.1109/TDC-LA.2014.6955182.

[149] N. Manjul and M. S. Rawat, “PV/QV Curve based Optimal Placement of Static Var System in Power Network using DigSilent Power Factory,” in *8th IEEE Power India International Conference*, Kurukshetra, India: IEEE, 2018, pp. 1–6. doi: 10.1109/POWERI.2018.8704441.

[150] F. Aydin and B. Gumus, “Determining Optimal SVC Location for Voltage Stability Using Multi-Criteria Decision Making Based Solution: Analytic Hierarchy Process (AHP) Approach,” *IEEE Access*, vol. 9, pp. 143166–143180, 2021, doi: 10.1109/ACCESS.2021.3121196.

[151] S. B. Dandawate and S. L. Shaikh, “Analysis of Effect on Transient Stability of Interconnected Power System by Introduction of HVDC Link.,” *Int. J. Eng. Res. Appl.*, vol. 3, no. 3, pp. 1383–1387, 2013.

[152] M. Kirik, “VSC-HVDC for Long-Term Voltage Stability Improvement,” Royal Institute of Technology (KTH), 2009.

[153] L. C. Azimoh, K. Folly, S. P. Chowdhury, S. Chowdhury, and A. Haddad, “Investigation of voltage and transient stability of HVAC network in hybrid with VSC-HVDC and HVDC link,” in *45th International Universities Power Engineering Conference UPEC2010*, Cardiff, Wales: IEEE, 2010, pp. 23–28.

[154] H. F. Latorre and M. Ghandhari, “Improvement of power system stability by using a VSC-HVdc,” *Int. J. Electr. Power Energy Syst.*, vol. 33, no. 2, pp. 332–339, 2011, doi: 10.1016/j.ijepes.2010.08.030.

[155] A. A. Raouf, E. K. Salah, and A. M. Mohamed, “Impact of HVDC System on Power System Stability,” *Int. J. Sci. Eng. Res.*, vol. 7, no. 6, pp. 1157–1163, 2016, doi: 10.1109/TCSI.2011.2169744.

[156] B. Venkata Ramana, K. V. S. R. Murthy, P. Upendra Kumar, and V. R. Kumar, “A Two Bus Equivalent Method for Determination of Steady State Voltage Stability Limit of a Power System,” *Int. J. Comput. Eng. Res.*, vol. 2, no. 2, pp. 428–434, 2012.

[157] T. He, S. Kolluri, S. Mandal, F. Galvan, and P. Rastgoufard, “Identification of weak locations in bulk transmission systems using voltage stability margin index,” *2004 Int. Conf. Probabilistic Methods Appl. to Power Syst.*, pp. 878–882, 2004, doi: 10.1007/0-387-23471-3_3.

[158] V. Ajjarapu, *Computational Technique for Voltage Stability Assessment and Control*. USA: Springer, 2006.

[159] P. Kundur *et al.*, “Definitions and classification of Power System Stability,” *IEEE/CICRE Jt. Task Force Stab.*, vol. 19, no. 3, pp. 1387–1401, 2004, doi: 10.1109/TPWRS.2004.825981.

[160] Working Group 14.20, “Economic assessment of HVDC links,” *cigre*, no. June, 2001.

[161] M. J. B. Kabeyi and O. A. Olanrewaju, “Sustainable Energy Transition for Renewable and Low Carbon Grid Electricity Generation and Supply,” *Front. Energy Res.*, vol. 9, no. March, pp. 1–45, 2022, doi: 10.3389/fenrg.2021.743114.

[162] National Infrastructure Commission, “The Second National Infrastructure Assessment,” no. October, 2023.

[163] I. Ali, “Economic Analysis of Investment in Power Systems,” 1991. [Online]. Available: https://www.adb.org/publications/economic-analysis-investment-power-systems

[164] B. Haliru, “Analysis of the Economic and Technical Determinants of Electricity Supply in Nigeria,” *SSRN Electron. J.*, pp. 1–29, 2023, doi: 10.2139/ssrn.4475052.

[165] N. R. Watson and J. D. Watson, “An overview of HVDC technology,” *Energies*, vol. 13, no. 17, pp. 1–35, 2020, doi: 10.3390/en13174342.

[166] M. Aissaoui, M. N. Tandjaoui, C. Benachaiba, and B. Abdellaoui, “Future of HVDC power transmission in Africa,” in *3rd World Conference on Innovation and Computer Sciences 2013*, AWERProcedia Information Technology & Computer Science, 2013, pp. 950–956. [Online]. Available: www.awer-center.org/pitcs

[167] Asian Development Bank, “Key Areas of Economic Analysis of Projects,” Asia, 2004. doi: 10.1201/9781003151364-4.

[168] J. C. Bhojwani, “Economic operation of Electric power system,” Kansa, 1963.

[169] S. K. Teegala and S. K. Singal, “Economic analysis of power transmission lines using interval mathematics,” *J. Electr. Eng. Technol.*, vol. 10, no. 4, pp. 1471–1479, 2015, doi: 10.5370/JEET.2015.10.4.1471.

[170] J. FERNANDO, “Discounted Cash Flow (DCF) Explained With Formula and Examples,” Investopedia. Accessed: Mar. 01, 2024. [Online]. Available: https://www.investopedia.com/terms/d/dcf.asp#:~:text=Discounted cash flow (DCF) refers,will generate in the future.

[171] CFI Team, “What is Discounted Cash Flow (DCF)?,” CFI. Accessed: Mar. 01, 2024. [Online]. Available: https://corporatefinanceinstitute.com/resources/valuation/discounted-cash-flow-dcf/

[172] J. L. Herbohn and S. R. Harrison, “Introduction to Discounted Cash Flow Analysis and Financial Functions in Excel,” *Socio-economic Res. methods For. A Train. Man.*, vol. 1000, no. January 2002, pp. 109–118, 2002, [Online]. Available: https://espace.library.uq.edu.au/view/UQ:8138/n11__introduction.pdf

[173] “How to calculate a project economic value.” Accessed: Jun. 21, 2023. [Online]. Available: https://www.floridatechonline.com/blog/business/how-to-calculate-a-projects-economic-value/

[174] M. Stahl, “Net Present Value (NPV),” 2012. doi: 10.4135/9781412950602.n533.

[175] A. Gallo, “A Refresher on Net Present Value,” Harvard Bussiness Review. Accessed: Mar. 02, 2024. [Online]. Available: https://hbr.org/2014/11/a-refresher-on-net-present-value

[176] “What is net present value (NPV) in project management,” Wrike. Accessed: Mar. 02, 2024. [Online]. Available: https://www.wrike.com/project-management-guide/faq/what-is-net-present-value-npv-in-project-management/

[177] E. Weiss and S. Majkuthova, “Discounted Cash Flow (DCF) Assessment Method and its use in Assessment of a Producer Company,” *Mod. Methods Valuat.*, vol. 45, no. 1, pp. 169–179, 2020, doi: 10.4324/9780080971179-20.

[178] European Network of Transmission System Operators for Electricity (ENTSOE), “4th ENTSO-E Guideline for Cost Benefit Analysis of Grid Development Projects,” 2022.

[179] DigSILENT GmbH, “Economic Analysis tools,” 2023. [Online]. Available: https://www.digsilent.de/en/economic-analysis-tools.html

[180] M. T. Alam, J. Rahaman, and F. D. Dhali, “Technical Comparison of Modern HVAC and HVDC Transmission System Along with Cost Analysis,” *J. Control Instrum.*

Eng., vol. 8, no. 1, pp. 10–19, 2022, doi: 10.46610/jcie.2022.v08i01.002.

[181] A. Raza, A. Shakeel, H. T. ul Hassan, M. Jamil, and S. O. Gillani, "Economic Analysis for HVDC Transmission System in Pakistan," *Int. J. Control Autom.*, vol. 10, no. 11, pp. 29–38, 2017, doi: 10.14257/ijca.2017.10.11.03.

[182] T. Park, N. Kwak, C. Moon, S. Cha, and S. Kwon, "Economic Assessments of LFAC and HVDC Transmissions for Large Offshore Wind Farms," *KEPCO J. Electr. Power Energy*, vol. 1, no. 1, pp. 73–77, 2015, doi: 10.18770/kepco.2015.01.01.073.

[183] Q. Jiang, B. Li, and T. Liu, "Tech-Economic Assessment of Power Transmission Options for Large-Scale Offshore Wind Farms in China," *Processes*, vol. 10, no. 5, 2022.

[184] G. A. Ludin *et al.*, "Technical and Economic Analysis of an HVDC Transmission System for Renewable Energy Connection in Afghanistan," *Sustain.*, vol. 14, no. 3, 2022, doi: 10.3390/su14031468.

[185] R. R. Ha, "Methodology: Cost-benefit analysis," 2019. doi: 10.1016/B978-0-12-809633-8.20776-0.

[186] Cam Merritt, "How to Evaluate Two Projects by Evaluating the Net Present Value," yourbusiness.azcentral.com. Accessed: Jul. 13, 2023. [Online]. Available: https://www.sapling.com/how-to-evaluate-two-projects-by-evaluating-the-net-present-value.html

[187] "Central Bank of Nigeria." Accessed: Jun. 14, 2023. [Online]. Available: https://www.cbn.gov.ng/rates/mnymktind.asp#_

[188] M. Guqilherme, M. Cleberson, K. Hans-Joachim, B. Hans, E. Jansson, and U. Elgqvist, "Life cycle service for HVDC systems," *CIGRE Sess. B4-119*, 2018, [Online]. Available: http://www.cigre.org

[189] "Hitachi Energy." Accessed: Jun. 14, 2023. [Online]. Available: https://www.hitachienergy.com/uk-ie/en/about-us/customer-success-stories/skagerrak

[190] IBEDC, "Service Based Tariff (SBT)," Ibadan Electricity Distribution Company PLC. [Online]. Available: https://ibedc.com/uploads/tariff/SERVICE_BASED_TARIFF_2023.pdf

[191] "Scrap Value Depreciation Formula and Example Using It." Accessed: Jun. 14, 2023. [Online]. Available: https://www.investopedia.com/terms/s/scrap-value.asp#:~:text=Key Takeaways,Scrap value is the worth of a physical asset's individual,%2C or break-up value.

[192] S. N. A. A. Majid, N. A. Salim, H. Mohamad, and Z. M. Yasin, "Assessment of

expected customer interruption cost due to power system contingency by sensitivity analysis," *PECon 2020 - 2020 IEEE Int. Conf. Power Energy*, pp. 171–175, 2021, doi: 10.1109/PECon48942.2020.9314386.

[193] B. Tomasetti, "Depreciation." Accessed: Aug. 16, 2023. [Online]. Available: https://www.carboncollective.co/sustainable-invest

Appendix A

Appendix A.0.1: Active, Reactive and Apparent power of each load.

Load	Power Factor	SUMMER P (MW)	SUMMER Q (MVAR)	SUMMER S(MVA)	WINTER P (MW)	WINTER Q (MVAR)	WINTER S (MVA)
Aja	0.8	162.7	121	202.76	123.41	0	123.41
Alagbon	0.91	162	75	178.52	135.03	50	143.99
Alaoji	0.97	414.7	100.46	426.69	330.6	230.76	403.17
Ayede	0.99	208	24.74	209.47	230	57.34	237.04
Bernin Kebbi	1.00	198	2.76	198.02	187	76.78	202.15
Benin T. S	0.74	132.9	120.8	179.6	170.9	94.79	195.43
Ganmo	1.00	80.00	0	80.00	122	12.22	122.61
Gombe	0.98	154	30.00	156.89	116	100.19	153.28
Ikeja West	0.98	1135	200.41	1152.56	1102	701	1305.86
Jebba-T. S	1.00	14.00	1.41	14.07	21.00	7.01	22.14
Jos	0.79	80.00	62.98	101.81	54	39.96	67.18
Kaduna	1.00	176	0	176	102	0	102
Kano	1.00	277	0	277	199	0	199
Katampe	0.96	465	130	482.83	381.1	86.98	390.9
Makurdi	0.78	161.96	130.69	208.11	135.23	0	135.23
New Haven	0.99	100	15.47	101.19	170	155.25	230.22
Onitsha	0.93	141.5	55.88	152.13	168	101.67	196.37
Osogbo	0.86	167	100.84	195.09	162.6	113.05	198.04
Sakete	0.99	226	30.11	228	54.00	25.41	59.68
Sapele	0.8	64.1	47.77	79.94	74.4	8.73	74.91
Shiroro	.001	61.6	5.01	61.8	88.00	10.30	88.57
Yola	0.94	73.00	26.00	77.49	42.00	31.50	52.5
Lekki	1.00	-	-	-	135.03	0	135.03
Total		4654.46	1281.33	4939.97	4303.3	1902.94	4838.71

Appendix A.0.2: Reactive power for generator.

Generator	P(MW)	Power Factor	∅	tan ∅	Q(MVAR)
Afam	363.00	1.00	0.01	0.01	3.17
Azura	290.00	0.89	0.46	0.50	144.95
Delta	338.00	0.94	0.35	0.37	124.99
Egbin	626.29	0.96	0.27	0.28	175.06
Geregu	566.00	0.97	0.25	0.26	144.41
Ibom	103.50	0.62	0.90	1.25	129.82
Ihovbor	108.00	0.96	0.29	0.30	32.14
Jebba G. S	346.00	0.94	0.34	0.36	122.97
Kanji G. S	280.00	0.96	0.27	0.28	77.04
Odukpani	315.70	0.88	0.49	0.53	168.65
Olorunsogo	341.60	1.00	0.08	0.08	27.32
Omaku	58.30	0.96	0.28	0.29	16.79
Omotosho	314.40	1.00	0.06	0.06	18.51
Paras Energy	64.10	0.98	0.21	0.21	13.67
River	152.00	1.00	0.00	0.00	0.00
Sapele	159.30	0.85	0.56	0.63	100.35
Shiroro	313.00	0.76	0.71	0.85	266.62
Trans Amadi	65.20	0.99	0.16	0.16	10.19

Appendix A.0.3: Load flow results for the improved voltage for different control modes.

Bus	Without HVDC	I (PU	II (pu)	III (pu)	IV (pu)
Adiabor	1.00	1.00	1.00	1.00	1.00
Afam	1.02	1.02	1.02	1.02	1.02
Aja	0.96	0.96	0.96	0.96	0.96
Ajaokuta	1.00	1.00	1.00	1.00	1.00
Akangba	0.96	0.96	0.96	0.96	0.96
Aladja	1.03	1.03	1.03	1.03	1.03
Alagbon	0.96	0.96	0.96	0.96	0.96
Alaoji	1.01	1.01	1.01	1.01	1.01
Asaba	1.01	1.01	1.01	1.01	1.01
Ayede	0.97	0.97	0.97	0.97	0.97
Azura	1.01	1.01	1.01	1.01	1.01
Birni-Kebbi	1.02	1.02	1.02	1.02	1.02
Benin G. S	1.01	1.01	1.01	1.01	1.01
Delta	1.04	1.04	1.04	1.04	1.04
Egbin	1.01	1.01	1.01	1.01	1.01
Ganmo	0.99	0.99	0.99	0.99	0.99
Geregu	1.00	1.00	1.00	1.00	1.00
Gombe	0.91	0.99	0.99	1.01	1.01
Gwagwalada	0.99	0.99	0.99	0.99	0.99
Ibom	1.00	1.00	1.00	1.00	1.00
Ihovbor	1.00	1.00	1.00	1.00	1.00
Ikeja west	0.96	0.96	0.96	0.96	0.96
Ikot-Epene	1.01	1.01	1.01	1.01	1.01
Jebba G. S	1.00	1.00	1.00	1.00	1.00
Jebba- T. S	1.00	1.00	1.00	1.00	1.00
Jos	0.91	0.96	0.96	0.97	0.97
Kaduna	0.96	0.97	0.97	0.98	0.98
Kanji G. S	1.01	1.01	1.01	1.01	1.01
Kanji T. S	1.01	1.01	1.01	1.01	1.01
Kano	0.95	0.96	0.96	0.96	0.96
Katampe	0.96	0.97	0.97	0.97	0.97
Lekki	0.96	0.96	0.96	0.96	0.96
Lokoja	1.00	1.00	1.00	1.00	1.00
Makurdi	0.96	0.98	0.98	0.98	0.98
Molai	0.00	0.00	0.00	0.00	0.00
New-Haven	0.99	1.00	1.00	1.00	1.00
Odukpani	1.00	1.00	1.00	1.00	1.00
Oke-aro	0.95	0.95	0.95	0.95	0.95
Okpai	0.00	0.00	0.00	0.00	0.00
Olorunsogo	0.97	0.97	0.97	0.97	0.97
Omoku	1.02	1.02	1.02	1.02	1.02
Omotosho	1.03	1.03	1.03	1.03	1.03

Onitsha	1.00	1.00	1.00	1.00	1.00
Osogbo	0.98	0.98	0.98	0.98	0.98
Paras Energy	1.01	1.01	1.01	1.01	1.01
River	1.02	1.02	1.02	1.02	1.02
Sakete	0.95	0.95	0.95	0.95	0.95
Sapele	1.00	1.00	1.00	1.00	1.00
Shiroro	1.01	1.01	1.01	1.01	1.01
Trans Amadi	1.02	1.02	1.02	1.02	1.02
Ugwuaji	0.99	1.00	1.00	1.00	1.00
Yola	0.91	1.00	1.00	1.03	1.03

Appendix A.0.4: Scrap value calculation.

Year	Investment cost	depreciation rate at 10%
1	550000	55000
2	495000	49500
3	445500	44550
4	400950	40095
5	360855	36085.5
6	324769.5	32476.95
7	292292.55	29229.255
8	263063.295	26306.3295
9	236756.9655	23675.69655
10	213081.269	21308.1269
11	191773.1421	19177.31421
12	172595.8278	17259.58278
13	155336.2451	15533.62451
14	139802.6206	13980.26206
15	125822.3585	12582.23585
16	113240.1227	11324.01227
17	101916.1104	10191.61104
18	91724.49935	9172.449935
19	82552.04941	8255.204941
20	74296.84447	7429.684447
21	66867.16002	6686.716002
22	60180.44402	6018.044402
23	54162.39962	5416.239962
24	48746.15966	4874.615966
25	43871.54369	4387.154369
26	39484.38932	3948.438932
27	35535.95039	3553.595039
28	31982.35535	3198.235535
29	28784.11982	2878.411982
30	25905.70783	2590.570783
31	23315.13705	2331.513705
32	20983.62335	2098.362335
33	18885.26101	1888.526101
34	16996.73491	1699.673491
35	15297.06142	1529.706142
36	13767.35528	1376.735528
37	12390.61975	1239.061975
38	11151.55777	1115.155777
39	10036.402	1003.6402
40	9032.761798	903.2761798
	Depreciation rate total	541870.5144
Scrap value		(Investment cost – Depreciation rate total) = 8129. Approximately 8000